1.   Introduction

Phosphoric acid is widely used as a chemical intermediate. In the chemical field phosphoric acid is used to produce materials such as detergents, water treatment chemicals, leavening agents and animal feed supplements. Phosphoric acid is however mainly used in the fertiliser field where it serves as an intermediate between phosphate ore and major end products such as ammonium phosphate, triple superphosphates, liquid mixed fertilisers, high-analysis solid mixed fertilisers and some types of nitric phosphates (Slack, 1968a).

The final uses of phosphoric acid usually depend on the purity of the acid and this in turn is influenced by the way in which it was produced. Phosphoric acid can be produced in two main ways (Slack, 1968a):

- Wet processes involving the reaction of sulphuric acid with naturally occurring phosphate rock.

- Furnace processes in which phosphorous is first produced by the reduction of phosphate rock followed by oxidation and hydration to give phosphoric acid

Fedmis Pty (Ltd) situated in Palaborwa, South Africa produces phosphoric acid using the wet process production process. For this study, two main areas of concern in the wet process phosphoric acid production were investigated. The first area is the formation of sludge in the system due to impurities that reduces the grade of the acid produced, thereby lowering the selling price. The second area is the crystallisation of the gypsum that influences filtration and thereby affects plant productivity. . These are two different studies focusing on two different steps in the process that will be discussed separately in Chapter 3, *X-compound and Related Studies* and in Chapter 4, *Gypsum*.

Due to the complexity of the system, experiments were mainly done using chemically pure reagents on laboratory scale to control the variables.

2.   Background Study

2.1   The History of the Wet-Process Phosphoric Acid Process

The first commercially produced phosphoric acid for the fertiliser industry was in Germany between 1870 and 1872 and for a short period in the United States beginning in 1890 (Slack, 1968a; Hudson and Dolan, 1982).

There were about 12 companies in 1900 in Europe making wet-process phosphoric acid for use in concentrated superphosphates. Unfortunately ore had to be imported from the United States and this made the operations uneconomical and wet-process phosphoric acid production declined for several years (Slack, 1968a).

The Stauffer Chemical Company (United States) is considered to be the pioneer in the production of wet-process phosphoric acid. It developed a process in 1897 for acidulating bones from the Chicago stockyards to make acid for use in the manufacture of calcium phosphate leavening agents. In 1912, the process was converted to using phosphate rock and a food grade acid was produced. Up to this time, all phosphoric acid was produced using batch processes. The Dorr Company introduced the first continuous process in 1915 (Slack, 1968a).

During 1932, research was done on producing phosphoric acid by precipitating calcium sulphate hemihydrate, rather than the usual method of forming calcium sulphate dihydrate. By following this route phosphoric acid of 40 % - 50 % P_2O_5 can directly be produced where as the dihydrate process produces acid of ~27 % P_2O_5 (Becker, 1989). Filtration problems prevented the commercialisation of this method (Slack, 1968a).

In the late 1940's and early 1950's, Davison Chemical investigated a process of producing a 50 % - 54 % P_2O_5 product in which calcium sulphate anhydrite was formed, but this was never commercialised (Slack, 1968a).

This investigation focuses on the dihydrate process used by Fedmis.

2.2   The Dihydrate Process

The wet-process phosphoric acid production is usually described as the reaction of naturally occurring phosphate rock with sulphuric acid to produce phosphoric acid and a calcium sulphate that is removed through filtration. In the dihydrate process this calcium sulphate by-product is $CaSO_4.2H_2O$ (gypsum). In fact, the phosphate rock does not dissolve very well in sulphuric acid alone and in practice the dissolution takes place in the presence of a large excess of phosphoric acid (Anon, 1997).

The sulphuric acid present in the solution must be able to react effectively with the phosphate contained in the rock so that little remains unreacted. The calcium sulphate that is produced should be of a crystal structure that would aid filtration and would give minimum P_2O_5 losses. This usually means forming crystals that are of uniform size and shape that are not too small (Anon, 1997). To form these crystals, stable reaction conditions need to be maintained so that the sulphuric acid can react with the phosphate rock efficiently. The stability of the reaction is very important and is maintained by controlling the temperature and the acid strength (% P_2O_5).

In the dihydrate process the temperature is controlled at 80^oC and the acid concentration at 27 % P_2O_5. The production of phosphoric acid and calcium sulphate dihydrate can be explained by three parallel and simultaneous reactions (Becker, 1989).

- Dispersion of sulphuric acid in the reaction medium

    $$H_2SO_{4(aq)} \rightarrow 2H^+_{(aq)} + SO_4^{2-}_{(aq)}$$
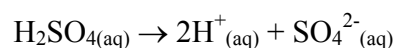
    This reaction is instantaneous when the sulphuric acid is dispersed within the slurry.

- The attack of phosphate rock particles by H^+ ions

    $$nH^+_{(aq)} + Ca_3(PO_4)_{2(s)} \rightarrow 2H_3PO_{4(aq)} + (n-6)H^+_{(aq)} + 3Ca^{2+}_{(aq)}$$

    This reaction is slower. As the rock phosphate is introduced into the reaction medium, the particles are dispersed and impregnated by phosphoric acid. Hydrogen ions from the acid medium then attack the tri-calcium phosphate to liberate P_2O_5 into solution.

- Ca^{2+} ions encounter SO_4^{2-} and precipitate as gypsum crystallites

$$Ca^{2+}_{(aq)} + SO_4^{2-}_{(aq)} \rightarrow CaSO_4.2H_2O\downarrow$$
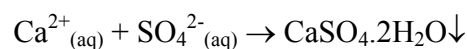
Once the Ca^{2+} ions diffuse from the solid into the liquid phase, they react with the SO_4^{2-} in solution and form crystals. This is the slowest of the three reactions.

A simplified overall reaction equation for the dihydrate process can then be given as follows:

$$Ca_3(PO_4)_{2(s)} + 3H_2SO_{4(aq)} + 6H_2O \rightarrow 2H_3PO_{4(aq)} + 3CaSO_4.2H_2O\downarrow$$
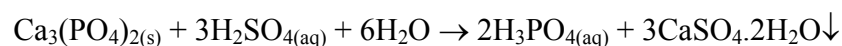
When a sufficient degree of crystallisation has been achieved, the crystals are separated by filtration. More detail on the formation of gypsum and the parameters affecting crystallisation will be presented in Chapter 4, *Gypsum*.

As stated earlier, the acid produced has a concentration of 27 % P_2O_5 and needs to be concentrated in order to make it an acceptable feed material for the final fertiliser product. Depending on the fertiliser to be produced, phosphoric acid is usually concentrated to 40 % - 55 % P_2O_5.

2.3   Impurities in the Production of Phosphoric Acid

Phosphate rock that is used for the production of phosphoric acid contains varying amounts of impurities that end up in the acid. Consumers will inevitably have to cope with the problems caused by their presence. Most impurities are not easily removed. To produce pure phosphoric acid from crude wet process acid, sophisticated pre-purification followed by solvent extraction processes are used. In the production of acid for fertiliser use, only sludge is removed for clarification purposes so that most of the impurities remain solubilised within the acid.

The wet-process phosphoric acid impurities can be classified into three categories namely process impurities, common impurities and trace elements originating from the phosphate ore (Becker, 1989).

Process impurities originate from the reagents used in the production of phosphoric acid namely sulphuric acid and process water (Becker, 1989). As sulphuric acid is used in excess, not all is consumed and thus some sulphuric acid remains in the acid. The excess sulphates do not usually cause any problems in the use of the final acid product. Sodium chloride is the main impurity in the process water. Although there is already sodium in the rock, any excess amount causes additional sodium hexafluorosilicate to precipitate. This leads to more sludge generation that needs to be removed through filtration (Becker, 1989). The chlorides can cause problems due to their corrosive behaviour.

Common impurities in the phosphate rock are aluminium (Al^{3+}), iron (Fe^{3+}), magnesium (Mg^{2+}), calcium (Ca^{2+}), potassium (K^+), strontium, chlorides (Cl^-) and fluoride (F^-).

Iron (Fe^{3+}) and aluminium (Al^{3+}) are often considered to belong to the same impurity category. Studies (Becker, 1989) have shown that the disadvantages of aluminium impurities are that it increases the acid density and viscosity. Aluminium can precipitate from 30 % - 40 % P_2O_5 acid solutions as ralstonite ($AlF_6MgNa.6H_2O$) or together with iron as the so-called x-compound (($Fe,Al)_3KH_{14}(PO_4)_8.4H_2O$) in 50 % - 54 % P_2O_5 (Becker, 1989). If the Fe^{3+} is reduced to Fe^{2+} the precipitation of iron x-compound can be restrained, but the reduced form is highly unstable in open air storage (Becker, 1989).

Aluminium does have some advantages in the improvement of gypsum crystal quality with regard to filtration rates in the right concentration ranges (Glazyrina, Savinkova and Grinevich, 1981). Unfortunately, the presence of F^- and Al^{3+} increases the solubility of gypsum compared to pure phosphoric acid solutions (Glazyrina, Savinkova and Grinevich, 1981). It also acts as a corrosion inhibitor by forming noncorrosive AlF_6^{2-} complexes, which effectively removes the corrosive fluoride ions (Becker, 1989; Schorr and Lin, 1997). Some fluoride is however, lost by volatilisation of the HF and SiF_4 decomposition products of fluorosilic acid (Van der Sluis, Schrijver, Baak and Van Rosmalen, 1988).

Budz, Jones and Mullin (1986) found that the addition of aluminium caused agglomeration of gypsum crystals. The crystals also appeared larger and more plate-like than crystals formed from pure acid. On the other hand, Jun, JianHua and YunXiang (1997) found that the crystal morphology was unaffected by the presence of aluminium alone, but in the presence of fluoride changes were seen and sphere shaped aggregates instead of elongated needles formed.

Hasson; Addai-Mensah and Metcalfe (1990) studied the effect of impurities on the filterability of the produced gypsum slurry with regard to iron and aluminium. They found that iron and aluminium exert similar effects at the same molar concentration. At low concentrations, the impurities reduce the specific resistance of the filter cake and increase the average size of the produced gypsum. At high impurity concentrations, the specific resistance of the filter cake is increased and the average crystal size is decreased. These results explain the conflicting reports in the literature relating to the influence of iron and aluminium on the filterability of the gypsum slurry as different results are achieved at different impurity concentrations (Hasson *et al*, 1990)

Precipitation of x-compound has been considered as a strategy to remove aluminium and iron impurities. However, this causes extensive P_2O_5 losses. Apart from solvent purification processes, there is no economical way of eliminating aluminium from the system so that it is easier to try and use it as an advantage (Becker, 1989).

Magnesium is an undesirable impurity because of its influence on viscosity and the formation of insoluble compounds in many finished products such as $MgNH_4PO_4$ when phosphoric acid is ammoniated. According to a study done by Rinaudo and Franchini-Angela (1989), curved gypsum crystals formed from the solutions enriched with magnesium and cadmium. Allied Chemical Corporation (Becker, 1989) has taken out a patent for complex precipitation of a compound containing Al_2O_3, MgO, F, and P_2O_5. Unfortunately well-defined ratios of the components are required. Removal of magnesium through solid ion exchangers has also been investigated.

Purification of wet-process phosphoric acid with dibutyl ether has been investigated with good results for metallic impurities such as iron, aluminium and magnesium and sulphates, but proved

unsuitable for fluoride removal (Marcilla, Ruiz, Campos and Asensio - Part I and II, 1989). Solvent extraction with methyl isobutyl ketone seems to have the best selectivity for sulphates. It showed intermediate behaviour between those of isoamyl alcohol and ethers with regard to metallic impurities (Feki and Ayedi, 1998). This is however not commercially viable for the removal of impurities in the production of phosphoric acid for fertiliser use.

The calcium content of the produced acid is a function of the sulphate level left in the acid. As the acid is cooled, the solubility is lowered and $CaSO_4.2H_2O$ precipitates. This can be removed through filtration.

Although the x-compound only contains 4 % potassium, the latter is a key ingredient of this precipitate. Even small amounts of potassium can cause sludge formation. It can also precipitate as potassium hexafluorosilicates (K_2SiF_6) that often forms scale on filter or cooling pipes. Studies were done to remove potassium from the system, but have not shown any positive results (Becker, 1989). X-compound will be discussed in detail in Chapter 3, *X-compound and related studies*.

Strontium is partially precipitated as strontium sulphate in the wet-process acidulation system. Strontium sulphate tends to form fouling deposits in heat exchanger pipes. The presence of as little as 0,1 % strontium in the phosphate ore is sufficient to cause these problems (Becker, 1989).

Chlorides are generally soluble and are thus found in the acid. They pose a corrosion problem but their removal from weak acids is difficult and uneconomical (Becker, 1989; Schorr and Lin, 1997). If the corrosion problem becomes too great, chlorides should be removed from the rock rather than from the acid. Alternatively corrosion resistant metals should be used. This again, is very expensive.

Common trace elements in the phosphate ore are arsenic, cadmium, mercury, uranium, copper, zinc and lead.

The arsenic concentration in the phosphate rock ranges between 3 ppm - 15 ppm. For fertiliser use it is not necessary to remove the arsenic from the acid. For phosphates used in the animal food industry, the concentration must be reduced. This can be done with H_2S treatment forming insoluble S_3As_2 and S_5As_2. The precipitate can be removed using filtration (Becker, 1989).

Cadmium content varies considerably in phosphate rock. Cadmium is the cause of a painful bone disease. Consequently, the World Health Organisation has recommended a cadmium consumption limit of 57 µg and 70 µg per day per capita. Northern Europe has banished cadmium from fertiliser. The removal of cadmium from phosphoric acid has been achieved successfully. It co-crystallises within the calcium sulphate crystal structure (Becker, 1989).

Cadmium extraction from phosphoric acid with diorganyldithiophosphinic acids had satisfactory results (Tjioee, Durville and Von Rosmalen -Part I and II, 1989). Extracting cadmium by using amines in phosphoric and nitric acid mixtures poses some problems.   Increase in amine concentrations leads to acid losses owing to co-extraction of phosphoric acid (Stenström, 1989). Removal of cadmium using anion exchange has also been investigated. Iodide appears to be the most effective (Tjioe, Weij, Wesselingh and Von Rosmalen, 1988).

Mercury is a very toxic element, but is not really a problem in the phosphoric acid as it remains with the gypsum as an insoluble mercury sulphide. HgS_2 is a very stable compound (Becker, 1989). The copper and zinc does not pose any problem and the lead is found insoluble with the calcium sulphate solid phase.

Uranium has been recovered from phosphoric acid since 1970 after energy prices skyrocketed (Becker, 1989). Investigations have been done on the extraction of uranium from wet-process phosphoric acid using a liquid phosphine oxide synergist (Rickelton, 1988) and kerosene solutions of nonylphenyl phosphoric acids and hexylphenyl phosphoric acids (Górecki, Górecka and Sielicki, 1989). Both these methods showed good results.

The effects that impurities have on the production process of phosphoric acid have been explained, but what effect do they have after the production step? The gypsum formed in the

production contains large amounts of phosphates and some of the impurities that originated from the rock.

This is reason for concern as it could have negative environmental impact as gypsum is usually accumulated on large heaps that are exposed to environmental conditions such as rain and wind. These impurities can enter and affect the environment through the following pathways (Martin, Bolivar, Respaldiza, Garcia-Tenorio & Da Silva, 1995):

- Dissolution/leaching: The impurities such as heavy metals and natural radionuclides can reach the ground water supply through leaching and can then be transported to other surroundings.
- Atmospheric transport: Wind erosion of gypsum heaps is not uncommon.
- Direct transport by water: Dispersion of gypsum by a moving body of water. This could have serious consequences for the aquatic life as this could poison the water system.

The only way that the negative effect of gypsum could be neutralised is through the transformation of it into a saleable product. It can be used as plaster and plaster-derived products, cement retarder, soil conditioner (with purification) and use in the paper industry (Becker, 1989). Unfortunately, the supply of gypsum is much greater than the demand so that accumulation is inevitable.

3.   X-Compound and Related Studies

3.1   Introduction

Sludge formation is an increasing problem in the phosphoric acid industry as it reduces the grade of the acid produced, thus reducing the acid's selling price. A major component of this acid sludge is known as x-compound, $(Fe,Al)_3KH_{14}(PO_4)_8.4H_2O$. The rest of the sludge contains mostly gypsum and hexafluorosilicates.

The purpose of this investigation of the x-compound was to determine what effects the different ionic impurities have on its precipitation and to determine if these effects could be used to control the sludge formation. Due to the complexity of the system and the wide variety of impurities involved (as discussed in Chapter 2.3, *Impurities in the Production of Phosphoric Acid*), only the major impurities were considered in this study. These impurities included potassium (K^+), sodium (Na^+), magnesium (Mg^{2+}), aluminium (Al^{3+}) and iron (Fe^{3+}).

For the experiments investigating the effect of impurities, chemically pure reagents were used on laboratory scale. For the silica experiments, commercially available samples were used.

3.2   Background Study

The increasing presence of soluble ionic impurities in the phosphate rock, such as potassium (K^+), sodium (Na^+), magnesium (Mg^{2+}), aluminium (Al^{3+}) and iron (Fe^{3+}), influences the viscosity and density of the produced phosphoric acid, and promotes the formation of sludge as explained previously. Furthermore, as the acid cools during filtration it becomes supersaturated resulting in the precipitation of more gypsum and also alkali hexafluorosilicates such as Na_2SiF_6 and K_2SiF_6.

During the concentration process precipitation of other compounds also occurs. One of these compounds is $(Fe,Al)_3KH_{14}(PO_4)_8.4H_2O$, known as x-compound, which accounts for a major fraction of most acid sludge. This compound can be found in acid concentrations between 42 %

to 58 % P_2O_5 (Becker, 1989; Frazier and Kim, 1989). The precipitate not only causes problems during the storage and transportation of the acid, but also results in major P_2O_5 losses owing to the high phosphate content of the complex (72.18 %).

It is known that the nucleation process of this x-compound is very slow, delaying the precipitation process and making it difficult to remove the precipitate before transportation of the merchant grade acid (Becker, 1989). The potassium ions released from potassium hexafluorosilicates will react with aluminium or iron in highly viscous mediums and continue to precipitate up to 14 days after production (Becker, 1989).

Frazier, Waerstad, Kim and Crim (1989) studied the different phases in a system containing iron, potassium and phosphates.   They found that these three components at different acid concentrations could form nine different compounds that are shown in Figure 1
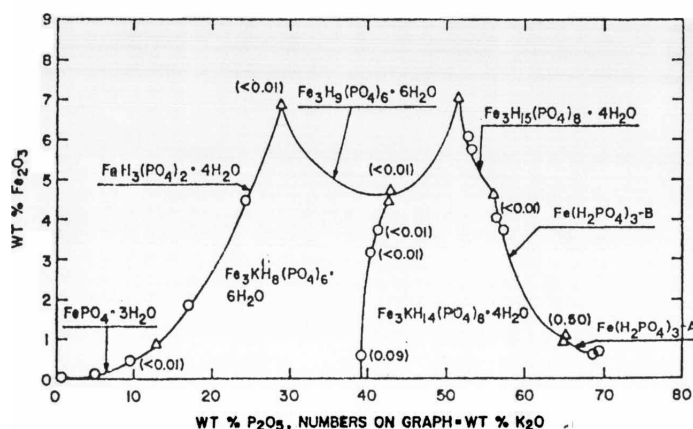
Figure 1: System Fe_2O_3-K_2O-P_2O_5-H_2O at 25 ^{o}C (Frazier *et al*, 1989)

The final acid produced by Fedmis contains 54 % P_2O_5. In this range $Fe_3KH_{14}(PO_4)_8.4H_2O$ is the stable product. Waerstad and Frazier (1987) investigated the crystal forms for the x-compound. It was found that the precipitates do not possess high degrees of crystallinity. The presence of amorphous material was indicated by the presence of several broad and diffuse reflections in the powder diffraction patterns. The x-compound crystallises as thin, hexagonal plates (Waerstad *et al*, 1987).

A study by Lehr, Frazier and Smith (1966) indicated that the solubility of $(Fe,Al)_3KH_{14}(PO_4)_8.4H_2O$ decreases as the iron content of the acid increases. They also found that elevated temperatures, a high degree of supersaturation, high ratios of iron to aluminium and the presence of other impurities accelerate the precipitation of x-compound. When the aluminium content is high, precipitation is delayed. Interestingly, although fluoride does not enter into the composition of the compound, it accelerates the precipitation. This could be attributed to the complexation of aluminium with fluoride that, in turn, increases the ratio of iron to aluminium (Lehr *et al*, 1966).

Many of the proposed treatment methods to remove x-compound focus on nucleation and growth of the compound through high-shear mixing, rapid cooling, addition of free sulphuric acid and even the addition of sludge as seeding crystals. Unfortunately this means that P_2O_5 losses are inevitable. X-compound has however found value as slow-release fertiliser (Slack, 1968b).

3.3   Experiments Investigating the Impurity Effects on X-Compound Precipitation

3.3.1 Planning and Procedure

For the experiments, different aspects were investigated and will be discussed separately.

Precipitation of the x-compound

The phase diagram presented in Figure 1 (Frazier *et al,* 1989) was used to calculate the amount of ferric and potassium ions, that needs to be dissolved in chemically pure phosphoric acid, in order to precipitate 12.5% x-compound (m/m).

Table 1 contains the amounts of reagents needed for x-compound precipitation. The final concentration of the solution after precipitation has taken place will be 40 % P_2O_5, 0.36 % Fe_2O_3 and 0.09 % K_2O.

Table 1: Reagents needed for x-compound precipitation

Chemicals used	Mass (g)	Composition of Equilibrium Solution after Precipitation
85 % H_3PO_4	169.53	40.00% P_2O_5
85 % KOH	2.24	0.09 % K_2O
97 % $Fe(NO_3)_3.9H_2O$	41.18	0.36 % Fe_2O_3
Water	37.06	-
Total	**250.00**	

Addition of impurity ions

Ferric ions were added as ferric nitrate nonahydrate and potassium as potassium hydroxide. The impurities were added as magnesium nitrate hexahydrate (0.6 % Mg^{2+} as observed in the acid), sodium hydroxide (0.09 % Na^+ as observed in the acid), fluorosilisic acid (7.3 g of 33.5 % solution), x-compound (1.0 g) and gypsum (1.0 g) respectively. The fluorosilisic acid was added to determine if hexafluorosilicates would form rather than x-compound. In one experiment potassium hexafluorosilicate (3.3 g) was added in place of potassium hydroxide as a potassium ion source keeping the stoichiometric ratio constant.

Each experiment was repeated to determine the reproducibility. For most of the experiments, the solutions were stirred for 30 minutes and placed in a water bath at 35°C for one week to ensure that conditions are kept constant. After one week the precipitate was collected through filtration and washed twice using ethanol. One experiment and the repeat were stirred continuously for 24 hours and then placed in the waterbath. This was done to determine the effect of mixing.

The presence of hydrated ferric ions in the acid solutions gives it a pink colour. Precipitation of x-compound can thus be followed, as the pink colour fades. Powder X-Ray Diffraction (XRD) data of solid samples were recorded on a Siemens D501 automated diffractometer equipped with a secondary graphite monochromator, while electron micrographs were recorded on a JEOL JSM-840 scanning electron microscope (SEM).

A Raman study investigating the effect of impurities on nucleation process of the x-compound.
Raman spectroscopy is a well-known method to study PO_4 units in different environments. In this study it was used as a probe to investigate the complex formation between three of the soluble ionic impurities (K^+, Al^{3+} and Fe^{3+}) and phosphoric acid, in order to understand the influence thereof on the nucleation process of the x-compound.

A series of phosphoric acid solutions (5%, 10%, 27%, 39%, and 54% P_2O_5 (m/m)) were prepared by diluting orthophosphoric acid (85% H_3PO_4, analytical reagent) with distilled water.

Stoichiometric quantities of ionic impurities were dissolved in 27%, 39% and 54% P_2O_5 phosphoric acid solutions to yield ion impurity concentrations of 0.1%, 0.5%, and 0.75% (m/m). Ferric ions were added as ferric nitrate nonahydrate and potassium and aluminium ions as their respective hydroxide salts (analytical reagents).

Samples of the acid solutions were placed in glass tubes and the Raman spectra recorded in the macro sample chamber of a Dilor XY Raman instrument. The 514.5nm line of an Ar^+ - ion laser (Coherent Radiation Innova 90) was used as exciting line. Laser power was kept less than 25mW at the sample, with a spectral resolution of $1cm^{-1}$ and acquisition time of 60 seconds. Raman spectra of the solid sample were recorded under the 100x objective of the microprobe of the same instrument.

3.3.2 Results and Discussion

The SEM analysis of all the samples revealed thin, hexagonal plates as shown in Figure 2. This crystal habit is characteristic of x-compound (Waerstad *et al*, 1987). This was confirmed using XRD (Appendix A) that proved that only x-compound was precipitated and that the weighed precipitate of the different experiments could be compared directly.

The conditions and results for each experiment are shown in Table 2 and the average yield obtained is shown in Figure 3. From the table, it is clear that good reproducibility was obtained for all the experiments.
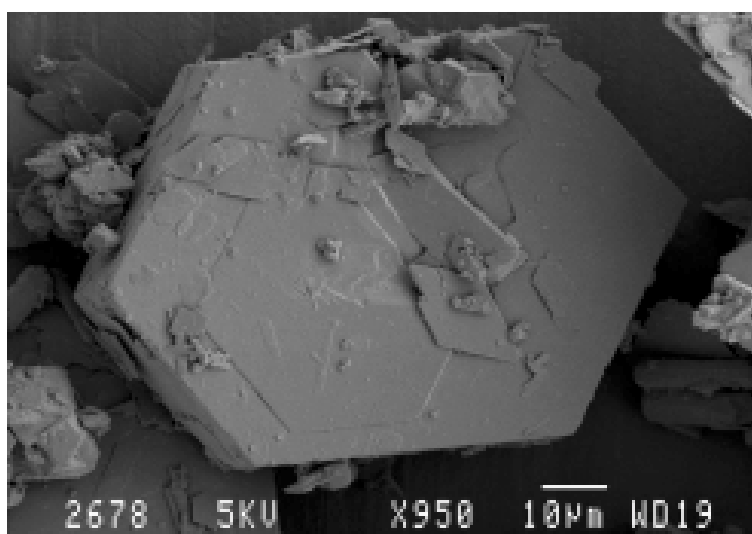
Figure 2: Micrograph of x-compound

Table 2: X-compound experimental conditions and results

Experiment number	Mixing time	Precipitate (g, 1 week)	Yield (%)	KOH	Fe(NO$_3$)$_3$.9H$_2$O	Mg(NO$_3$)$_2$.6H$_2$O	Gypsum	H$_2$SiF$_6$	x-compound	K$_2$SiF$_6$	NaOH
1(a)	30 minutes	28.62	91.58	✓	✓						
1(b)	30 minutes	28.44	91.01	✓	✓						
2(a)	24 hours	31.28	100.10	✓	✓						
2(b)	24 hours	31.27	100.06	✓	✓						
3(a)	30 minutes	30.50	97.60	✓	✓	✓					
3(b)	30 minutes	30.26	96.83	✓	✓	✓					
4(a)	30 minutes	31.11	99.55	✓	✓				✓		
4(b)	30 minutes	31.08	99.46	✓	✓				✓		
5(a)	30 minutes	26.16	83.71	✓	✓		✓				
5(b)	30 minutes	26.25	84.00	✓	✓		✓				
6(a)	30 minutes	27.61	88.35	✓	✓						✓
6(b)	30 minutes	27.30	87.36	✓	✓						✓
7(a)	30 minutes	18.88	60.42		✓					✓	
7(b)	30 minutes	18.69	59.81		✓					✓	
8(a)	30 minutes	24.20	77.44	✓	✓			✓			
8(b)	30 minutes	24.05	76.96	✓	✓			✓			

Comparing the precipitation of x-compound, with only potassium and iron present, agitation for 30 minutes (experiment 1) and agitation for 24 hours (experiment 2) proved that agitation aids the precipitation of x-compound. Through agitation, mass transfer barriers are overcome, bringing ions in constant contact with nucleated crystal surfaces. Crystals thus grow faster as diffusion doesn't first need to occur as with the case where crystals settle to the bottom.
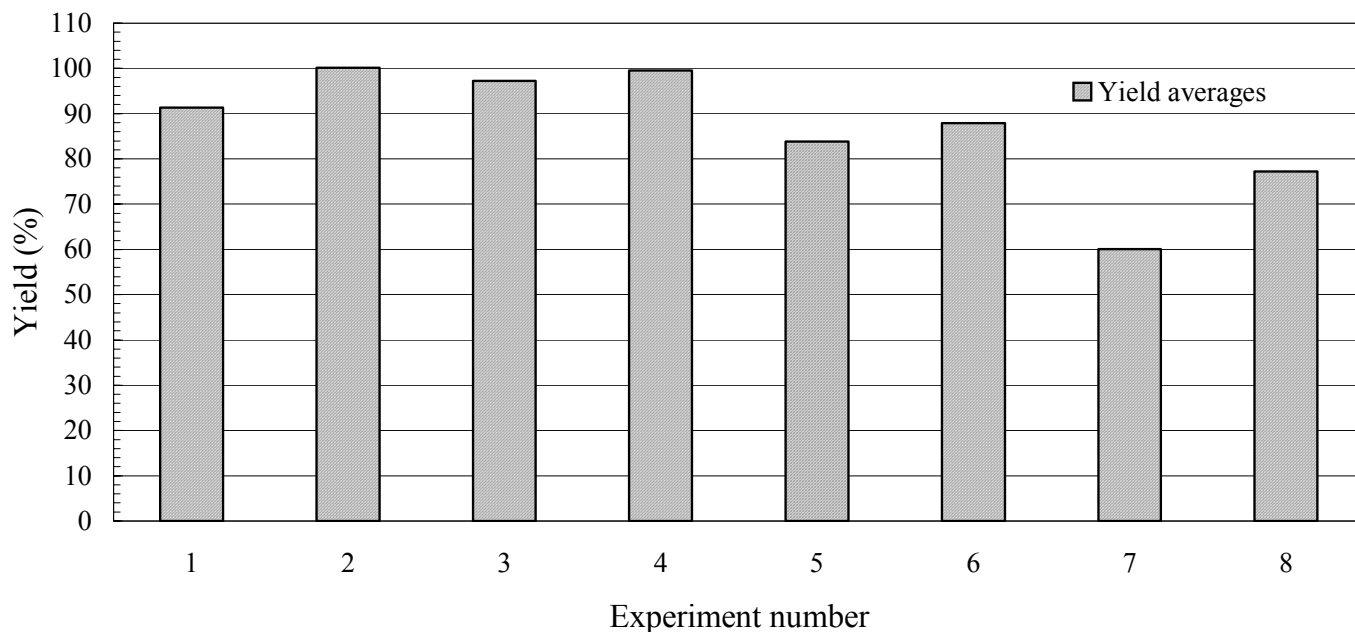
Figure 3: Precipitate yield averages for x-compound experiments after seven days of precipitation at 35 ^{o}C

Mixing or agitating the solution is thus one method that can be used to increase the rate of x-compound precipitation, so that the sludge can be filtered before transportation. Adding magnesium ions (experiment 3) and x-compound as seeding crystals (experiment 4) also increased precipitation to almost maximum yield. Adding gypsum (experiment 5), sodium ions (experiment 6), hexafluorosilicates (experiment 7) and fluorosilisic acid (experiment 8) reduced the yield of precipitated x-compound.

The low pH values of the acid solutions investigated in the Raman study (pH < 1.22), limits the speciation of the acid to $O=P(OH)_3$ and $H_2PO_4^-$, according to the first ionisation reaction:

$$H_3PO_4 + H_2O \rightarrow H_3O^+ + H_2PO_4^- \qquad Ka_1 = 7.5 \times 10^{-3}$$

The dominant specie at high industrial concentrations (shown in Figure 4) is H_3PO_4, but a certain amount of $H_2PO_4^-$ is also present. The $H_2PO_4^-$ specie increases as the acid concentration is lowered.
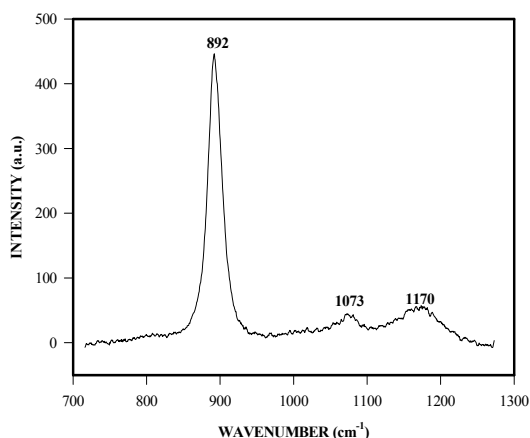
Figure 4: A Raman spectra of 10 % P$_2$O$_5$

The peak at 892 cm^{-1} in the Raman spectrum (See Figure 4) is due to the P-OH stretching and the peak at 1170 cm^{-1} the P=O stretching band in H$_3$PO$_4$. The peak at 1073 cm^{-1} is the O-P-O stretch H$_2$PO$_4^-$ and its intensity provides an indication of the degree of dissociation of the acid.

Figure 5 shows the shift in peak position and the peak intensity for the P-OH stretch band with acid concentration. The peak intensity is proportional to the concentration of the species, and the relative intensities can therefore be used in quantitative analysis studies (Willis, van der Maas and Miller, 1987). Although hydrogen bonds in phosphoric acid solutions are particularly strong, the shift in peak position is not attributed to changes in hydrogen bonding (Tromp, Spieser and Neilson, 1999; Caminiti, Cucca and Atzei, 1985). The shift in peak position is accounted for by the relative concentrations of the H$_3$PO$_4$ and H$_2$PO$_4^-$ molecular species; the contribution of the H$_3$PO$_4$ species increases with increasing P$_2$O$_5$ concentrations (Zwick, Lakhdar-Ghazal and Tocanne, 1989).

Regression lines for both the relative peak positions and intensities, as a function of acid concentration, are presented in Figure 6. It is clear that a better linear fit is obtained with the use of peak positions than with peak intensities, which is a novel way of determining phosphoric acid concentration in a water solution.
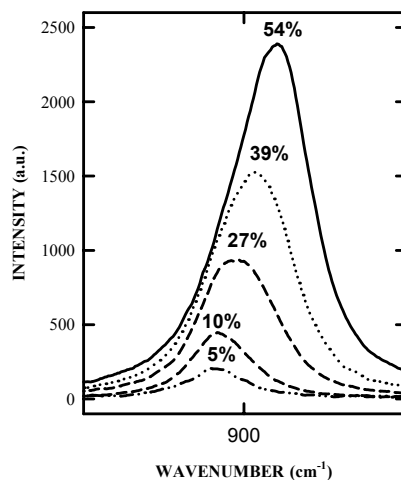
Figure 5: Peak intensity and peak shift for the P-OH stretch band as a function of acid concentration (% P_2O_5)
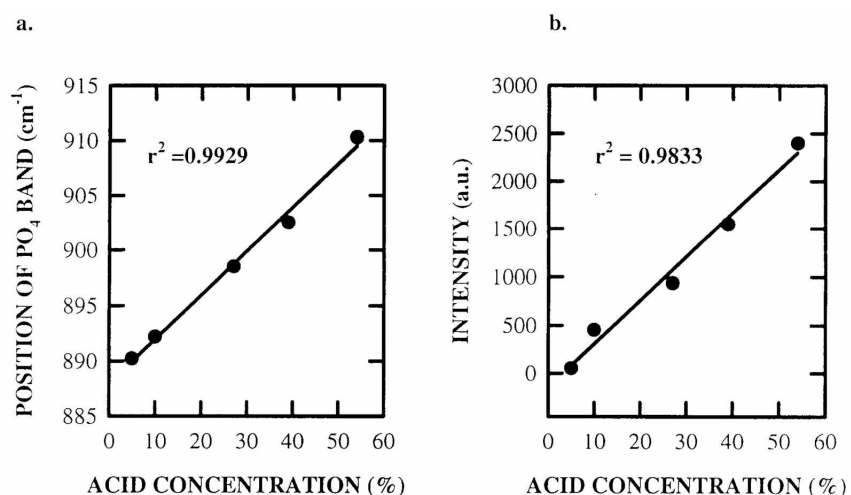

Figure 6: (a) Regression lines of relative peak positions and (b) Intensities as a function of acid concentration (% P_2O_5)

The Raman spectra of phosphoric acid solutions (27 % P_2O_5 and 54 % P_2O_5), with increasing ferric ion concentrations are presented in Figure 7. With the addition of 0.1% ferric ion impurity to the 27 % P_2O_5 acid, a clear decrease in the intensity of the band at 896 cm^{-1} could be observed. A new band also formed at 1048 cm^{-1} attributed to resonance enhancement as the solution containing ferric ions has a distinct pink colour.

The addition of 0.5% and 0.75% ferric ion impurity had the same result but the new peak at 1048 cm^{-1} grew in intensity as the concentration of the impurity increases. It can be seen from the figure that at higher acid concentration (54 % P_2O_5), the new peak is not as prominent. The reduction in the intensity of one band, together with the simultaneous increase in intensity of a new band that is more prominent at lower acid concentrations, suggests complex formation between $H_2PO_4^-$ ions acid and ferric ions.
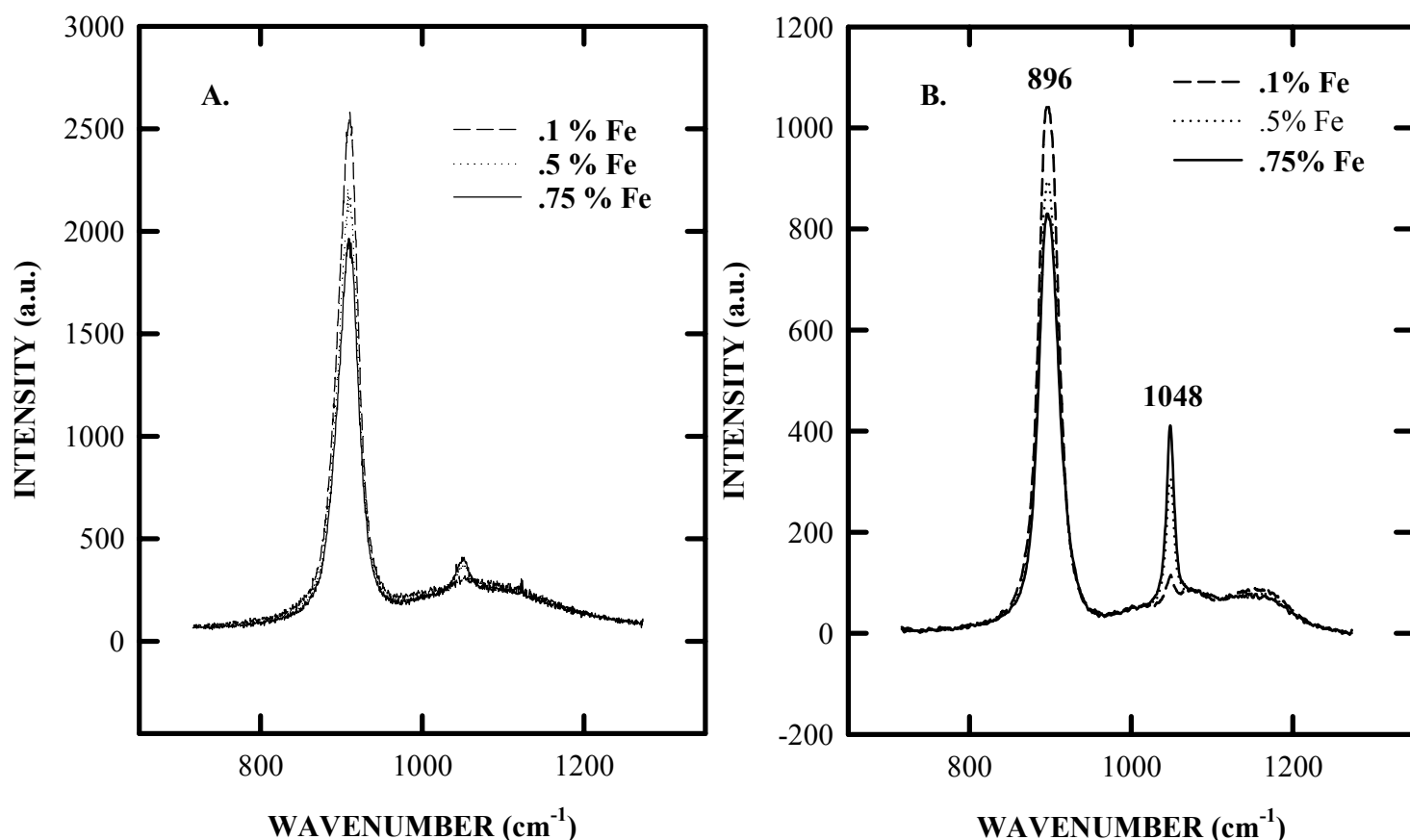
Figure 7: Raman spectra of phosphoric acid solutions A) 27% P_2O_5 and B) 54% P_2O_5 with increasing concentration of ferric ion impurity

It is known that the basic building units in solids persist in solutions (Caminiti, 1982; Magini, 1979). The cation-O-P angles and cation-P distances of complexes in solutions are thus similar to that in the corresponding solid structures (Caminiti, 1982). The new band at 1048 cm^{-1} is therefore assigned to the Fe-O stretch vibration, in accordance with the frequencies for the solid structures found in the literature (Farmer, 1974). The complex stays in solution at the lower 27

% P_2O_5 acids, and no precipitate could be observed even after weeks. This implies that the soluble complex is more stable than the solid x-compound.

Addition of aluminium impurities reduced the intensity of the Raman peak at 896 cm^{-1}. No further effect was noted. It was expected that potassium impurities would not form a complex with the acid at any concentrations and this was confirmed using Raman spectra as no effect was observed.

From these results it can be concluded that at low acid concentrations, more $H_2PO_4^-$ ions are present and that they form complexes with iron and aluminium. As the acid concentration increases, the concentration of $H_2PO_4^-$ ions decreases. The complexes are broken down making the impurities available for reaction and thus precipitation of x-compound can occur.

3.4 The Foskor Rock Impurity and the Fedmis Precipitate and Acid Monitoring Program

3.4.1 Planning and Procedure

Figure 8 is a simplified schematic layout of a wet-process phosphoric acid plant to illustrate where impurities enter the process and where these impurities can possibly be removed through filtration.

Impurities present in the reactor (from rock, sulphuric acid and water) are distributed between the gypsum precipitate and the 27 % P_2O_5 acid. The gypsum precipitate is discarded to heaps after the first filtration step and this is one of two points during the process where impurities are removed. The second point where impurities can be removed is at the pressure filters, after the 39% P_2O_5 concentration step. Impurities that are not removed at one of these points will remain in the merchant grade acid where it can contribute to the formation of sludge through the continuing accumulation of impurities. For a better understanding concerning the concentration and the distribution of the impurities present in the acid produced at the Fedmis plant, a monitoring program was introduced.

The Fedmis monitoring program includes the monitoring of Foskor rock analyses on a daily basis, and the monitoring of the 27 %, 39 % and 54 % P_2O_5 phosphoric acid and precipitate from these acid solutions on a weekly basis. The rock was analysed for the period between 3 September 1999 to 2 August 2000 and the acid with its precipitate was analysed between 16 May 2000 to 29 August 2000. Samples were taken and analysed at the Foskor facilities. Trends observed in these results are of importance in understanding the distribution of impurities in the Fedmis plant.
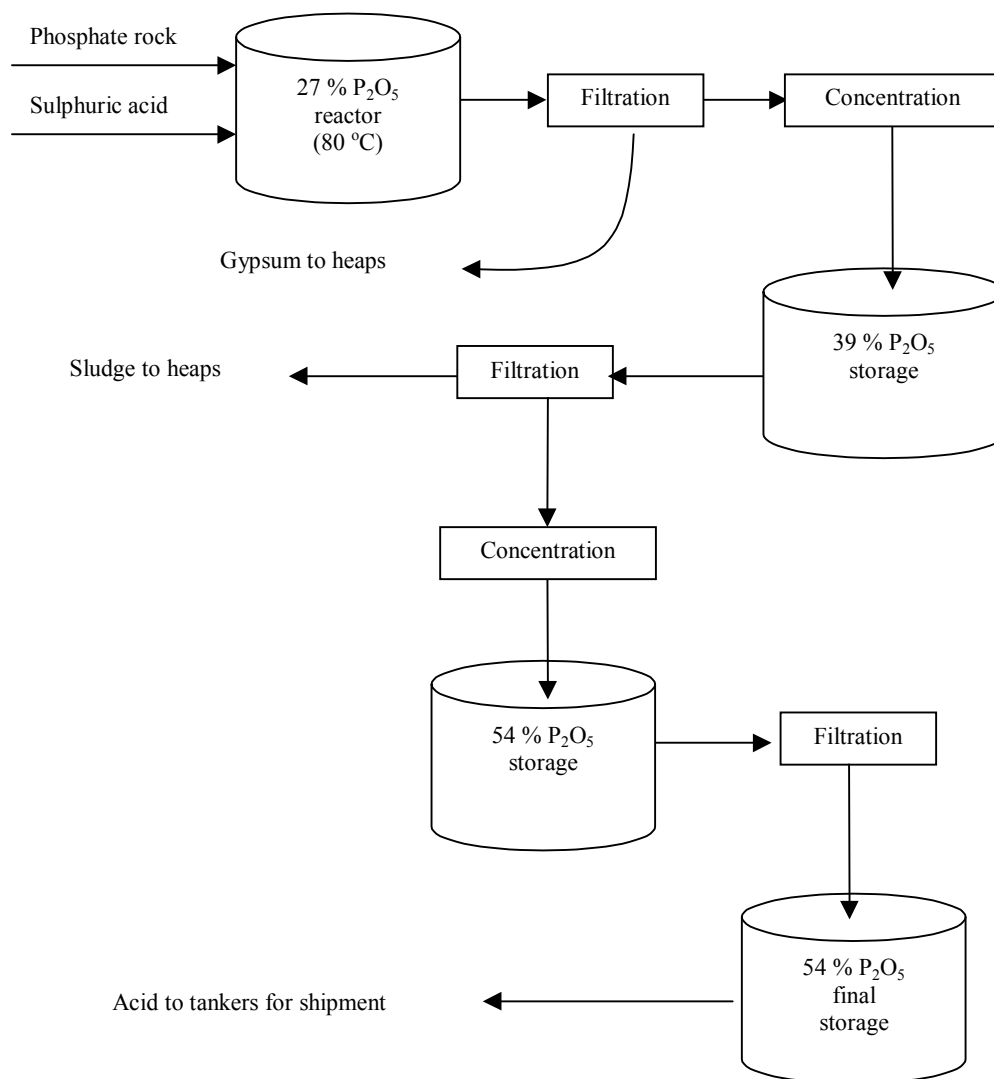
Figure 8: Simplified process layout of a wet-process phosphoric acid plant

3.4.2 Results and Discussion

The composition of phosphate rock send to Fedmis was monitored on a daily basis. Impurity variations for potassium, iron, magnesium, aluminium, chlorine and silica, along with the P_2O_5 content of the rock are presented in Appendix B. All concentrations are expressed as mass percentages of the corresponding oxides with the exception of chlorine, which was expressed as the element.

The impurities present in the rock can however not be compared to the impurity content of the acid for a specific day as it is difficult to say when exactly the specific rock analysed was used by Fedmis. The following was observed in the rock for the time period investigated.

- P_2O_5, SiO_2, MgO, Cl and Al_2O_3 content of the rock is fairly constant
- Fe_2O_3 content seems to be very constant over the last few weeks that were monitored.
- K_2O content of the rock steadily increased

The increasing potassium content in the rock is reason for concern as it could cause increasing sludge formation.

Analyses graphs for the precipitate are shown in Appendix C and for the acid in Appendix D. The concentration of a specific impurity should increase when the acid is concentrated unless it precipitates. The ratio of impurity concentration between 27 % P_2O_5 and 39 % P_2O_5 (0.692) should further also be comparable with the ratio of impurity concentration between 39 % P_2O_5 and 54 % P_2O_5 (0.722) as the acid is only concentrated. A reduction in the relative impurity concentration implies precipitation of the specific impurity. Impurity concentrations in the 39 % P_2O_5 and 54 % P_2O_5 acid and precipitate are further influenced by the addition of defluorination slurry and tanker wash (from time to time) to the 39 % P_2O_5 holding tank.

For each impurity, three acid graphs are presented where all impurities are given in terms of their respective oxides as mass percentages. The first graph represents the relative impurity analysis in the 27 %, 39 % and 54 % P_2O_5 phosphoric acid. The second and third graph represents the 'theoretically expected' concentrations (using the values in the 27% P_2O_5 acid) in comparison with the actual values obtained, for the 39 % P_2O_5 and 54 % P_2O_5 acids respectively. Higher

values (in comparison with the theoretical values) can be attributed to the addition of defluorination slurry and tanker wash that contains x-compound, fluorosilicates and gypsum, while lower values can be attributed to the precipitation of the specific ion.

Analyses of the precipitate from the different acid concentrations show that the major fraction of the precipitate is gypsum. The gypsum concentration is much higher than the other components present. For this reason, gypsum will not be included on the graphs indicating the impurity distributions of the precipitate from the different acid concentrations.

From the precipitation graphs in Appendix C it can be concluded that the precipitate taken from the 27 % P_2O_5 contained concentrations of P_2O_5, varying considerably between 0.08 % and 0.86 % for the time period investigated. For the results and for this study, constant analysis procedures and therefore P_2O_5 contamination was assumed. The varying acid content of the precipitate is thus possibly an indication of the amount of x-compound in the recycled sludge.

The silica content of the precipitate also varies considerably between 0.05 % and 0.68 %. As the silica content of the phosphate rock stayed relatively constant, a possible explanation for this is that the sludge pumped from the 54 % P_2O_5 pressure filters back to the 27% P_2O_5 reactor contained large amounts of K_2SiF_6. The K_2SiF_6 is formed in the defluorination section as the sludge from this process is added on an irregular basis to the 39 % P_2O_5 tank.

The precipitate contained low concentrations of sodium (0.004 % to 0.06 %), aluminium (0.004% to 0.13 %), magnesium (0.001 % to 0.17 %) and iron (0.02 % to 1.00 %). The potassium concentrations were relatively low (0.01 % to 1.2 %) and could be attributed to the addition of sludge from the 54 % P_2O_5 filters that contain K_2SiF_6 and x-compound.

The presence of $CaSO_4.2H_2O$ is not unexpected. Due to the cooling of the acid, the solubility of the gypsum will decrease and precipitation will occur. The high content however is unexpected indicating a poor first filtration step. Figure 9 (27% P_2O_5 precipitate) was compiled taking the averages of the main impurities together with the P_2O_5 content of the precipitate to get a generalised view of the distribution and how it changes to Figure 10 (39% P_2O_5 precipitate) and

Figure 11 (54 % P_2O_5 precipitate). As mentioned earlier, the gypsum will not be indicated on these graphs, as its content is much higher than any of the other components present.
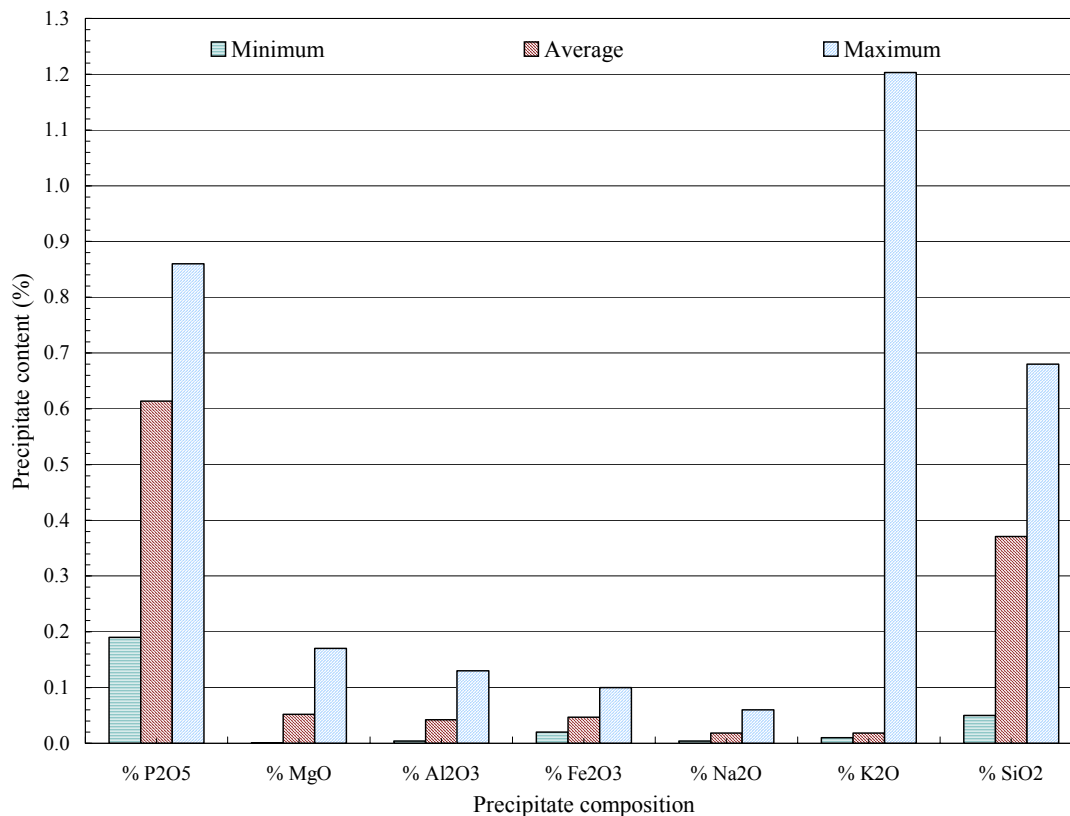

Figure 9: Average impurity concentrations in precipitate obtained from 27 % P_2O_5

The highest impurity concentration can be found in the precipitate taken from 39 % P_2O_5 sample. This is to be expected as the sample is taken before the filtration step where high sludge content is found. Figure 10 show that the precipitate contains more acid (0.33 % P_2O_5 to 2.7 % P_2O_5). This again indicates the varying presence of x-compound in the precipitate with irregular addition of defluorination sludge.

The silica content is higher and even greater variation is observed (0.06 % to 1.94 %) than with the lower acid precipitate. This can be attributed to the defluorination sludge added on an irregular basis. Defluorination sludge contains K_2SiF_6 and acid and is added to recover some of the P_2O_5 lost during defluorination. The addition of defluorination sludge is not sensible as the impurities removed previously are returned to the system.

The potassium (0.11 % to 1.84 %) and the iron (0.03 % to 0.29 %) content were substantially higher than in the 27 % P_2O_5 precipitate and are consistent with x-compound precipitation. The variation can be explained by the addition of K_2SiF_6 and tanker wash that is added on an irregular basis. The final concentrated acid is pumped into tankers and they are washed out to clean them from sludge formation and this sludge is pumped back to the 39 % P_2O_5 tank. This sludge contains mostly x-compound which consists of potassium, iron (or aluminium in the absence of iron) and phosphate.
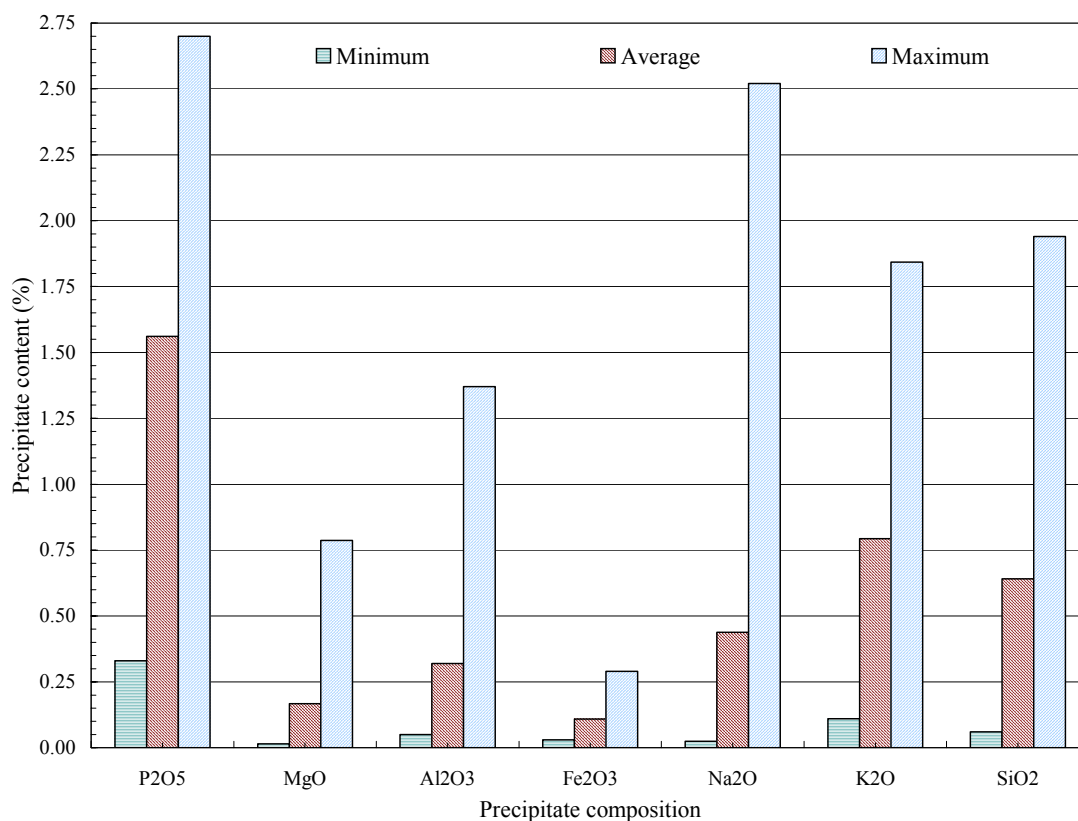
Figure 10: Average impurity concentrations in precipitate obtained from 39 % P_2O_5

The sodium content varies between 0.03 % and 2.52 %. As there is silica in the system from the rock and from the defluorination section, this could be an indication of the formation of sodium hexafluorosilicates that would vary as the silica in the system varies. The magnesium and aluminium is relatively low. Again, the rest of the sample consists of calcium and sulphate.

The precipitate from the 54 % P_2O_5 in Figure 11 showed relatively lower (sodium, potassium and silica) or constant (magnesium, aluminium and iron) impurity concentrations than the 39 % P_2O_5 precipitate although the acid concentration is again higher. This is to be expected as the samples were taken after the 54 % P_2O_5 filters before transportation.
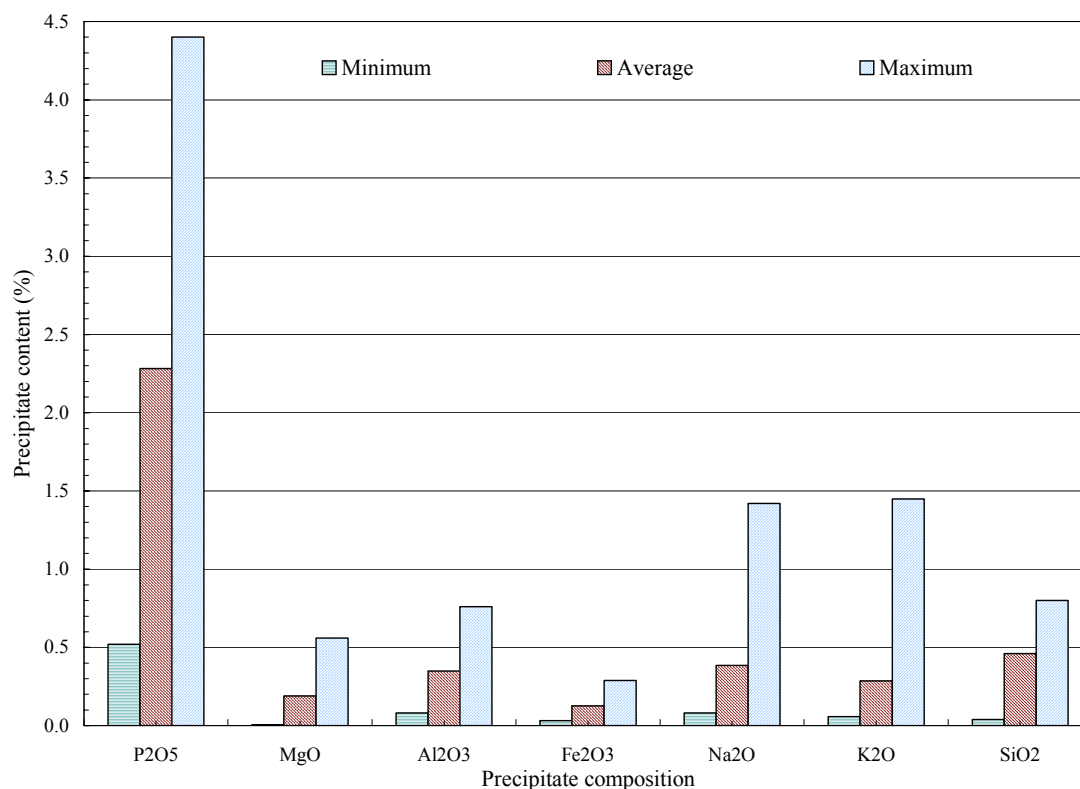

Figure 11: Average impurity concentrations in precipitate obtained from 54 % P_2O_5

The problem of sludge formation continuous to be a problem even after the acid has been loaded for shipment. It is also true that acid viscosity increases with acid concentration. This increases the mass transfer barriers increasing the time it takes for reactions to take place, as these barriers first have to be overcome. It is believed, after the Raman study, that at higher acid concentrations, less $H_2PO_4^-$ ions are present for iron complex formation. The ions thus become more readily available for x-compound formation and due to the movement during transport, mass transfer barriers are overcome. This is a reason for the increased precipitation after the transport of the acid. When the impurities of the acid solutions are discussed it will become clear how much iron and potassium ions are still available in solution for possible x-compound precipitation.

As mentioned earlier, the concentration of a specific impurity should increase when the acid is concentrated unless it precipitates. The ratio of impurity concentration between 27 % P_2O_5 and 39 % P_2O_5 (0.692) should further also be comparable with the ratio of impurity concentration between 39 % P_2O_5 and 54 % P_2O_5 (0.722) as the acid is only concentrated. This will be referred to as the theoretical trend.   A reduction in the relative impurity concentration implies precipitation of the specific impurity. Impurity concentrations in the 39 % P_2O_5 and 54 % P_2O_5 acid and precipitate are further influenced by the addition of the defluorination slurry and tanker wash (from time to time) to the 39 % P_2O_5 holding tank.

The acid graphs (Appendix D) for % MgO and % Al_2O_3 as do not show anything out of the ordinary when the 27 % P_2O_5 is concentrated to 39 % P_2O_5 and then to 54 % P_2O_5. It follows the predicted theoretical trend, which means that magnesium and aluminium did not precipitate.

The Fe_2O_3 concentration is slightly higher than predicted. The iron content of the precipitate and of the acid is increasing with concentration. This indicates that there is an impurity build-up in the system. There is thus iron available in the acid for x-compound precipitation. As the iron is in solution, filtration of the acid before transportation will not solve the problem. The addition of tanker sludge and defluorination sludge to the system only makes problems worse through impurity build-up. The impurities need to be removed.

The potassium content of the 54 % P_2O_5 is much higher than expected due to the addition of defluorination sludge and tanker wash. This explains why with the high concentration of iron in the acid, sludge formation occurs after the last filtration step.

The Na_2O and the SiO_2 is removed through filtration as possible sodium hexafluorosilicates, as the theoretical values are much higher than the actual impurity concentration. In both cases for both impurities, the concentration is lower than the concentration in the 27 % P_2O_5 where it was expected to be higher. The concentration of sodium from the 39 % P_2O_5 to the 54 % P_2O_5 concentration is relatively constant. This could mean that the solubility of sodium is constant with an increase in acid concentration i.e. the sodium is removed through filtration.

3.5 Experiments Investigating the Removal of Potassium through Precipitation as Potassium Hexafluorosilicates and the Effect of Impurities on the Solubility

3.5.1 Planning and Procedure

Potassium and ferric ions are some of the components that take part in the precipitation of the x-compound. One of the methods that can be used to remove ferric ions from a solution is the complexation of the ions with a suitable organic ligand. The very acidic conditions, in combination with the high temperature, makes it very difficult if not impossible, to make use of this method. It was therefore decided to focus on the potassium ions.

Set Point Laboratories did analyses for all the potassium hexafluorosilicate precipitation and impurity experiments.

Precipitation of potassium hexafluorosilicates

As x-compound cannot form in the absence of potassium, in principle the problem of sludge formation could therefore be solved through the selective removal of potassium. A possibility is to try and remove the potassium as insoluble potassium hexafluorosilicates by the addition of reactive silica. The plant already includes a defluorination section implying the presence of sufficient fluoride. The precipitated potassium hexafluorosilicates can then be removed at the pressure filters.

Four different commercially available silica sources from different suppliers were investigated. Different amounts were added to see if an optimum could be found where the maximum amount of potassium could be removed. The silica's investigated were Dicalite, Serina Kaolin, Foskor silica and Aerosil 200. The Aerosil 200 used is a pure amorphous nano-sized silica that is expected to be highly reactive and the other silica sources are commercially available on large scale and contain impurities.

Table 3 contains the basic composition of the samples to which different amounts of silica were added. The solutions were heated for 24 hours at 60 °C and then filtered. The composition and

elemental concentration percentages are given on a mass basis. The amount of potassium added was taken as the average K_2O concentration found in the rock and in the 39% acid and the fluoride was then added in a ratio of 1:3 (stoichiometric quantity).

Table 3: Basic composition of silica experiments

Chemicals used	Mass (g)	Composition Resulting from Dosage Used	Elemental Concentration in the Solution
85 % H_3PO_4	158.40	39.00% P_2O_5	-
85 % KOH	0.42	0.12% K_2O	0.10% K^+
40 % HF	0.96	0.15% HF	0.15% F^-
Water	90.22	-	-

Set Point Laboratories analysed the samples for silica, potassium and fluoride. The solutions were also analysed for aluminium, as it is a component of the different silica sources. It is possible in the formation of x-compound for aluminium to replace iron although this is rare when iron is present in the system. For the analysis, approximately 5 grams of concentrated acid was taken and diluted to a final mass of approximately 100 grams with a known amount of de-ionised water. Without dilution the acid concentrations were too high for Set Point Laboratories to perform the analyses.

Effect of impurities on the solubility of potassium hexafluorosilicates

The effect of impurities namely iron, aluminium, magnesium, fluoride and chloride on the solubility of potassium hexafluorosilicates were investigated. It is essential to know if impurities cause the K_2SiF_6 formed at the defluorination section of the plant to be more soluble. This will cause potassium not to be removed through filtration and will stay in the system. Approximately 5 grams of K_2SiF_6 was added to 39 % P_2O_5 acid solutions with different impurities and different concentrations. 5 Grams were chosen as this was far above the expected amount of K_2SiF_6 that is soluble in 250 grams of 39 % P_2O_5 acid.

The concentrations of impurities selected were taken on the basis of actual impurities in 39 % P_2O_5 produced by the Fedmis plant as discussed in Chapter 3.4, *The Foskor Rock Impurity and the Fedmis Precipitate and Acid Monitoring Program*. The concentrations selected were:

- Fe as Fe_2O_3 - 0.4 %, 0.56 %, 0.65 % and 0.72 %
- Mg as MgO - 1.0 %, 1.2 % and 1.55 %
- Al as Al_2O_3 - 0.12 %, 0.16 % , 0.19 % and 0.21 %
- Cl - 580 ppm, 700 ppm and 820 ppm
- F - 0.31 %, 0.70 % and 1.04 %

Fedmis does not analyse for fluoride, but through their plant experience the values chosen are in the range expected for the fluoride content.   Aluminium, iron and magnesium impurities were introduced to the system as nitrates. Chlorine and fluoride were introduced as hydrochloric acid and hydrofluoric acid respectively.

Solutions were heated in a water bath for 24 hours at 60 °C to ensure that equilibrium was reached. As with the silica experiments, approximately 5 grams of acid solution was diluted up to approximately 100 grams total solution with de-ionised water to make analysis by Set Point Laboratories possible. These solutions were only analysed for potassium.

3.5.2 Results and Discussion

Table 4 contains the results of the potassium hexafluorosilicate precipitation experiments for the different amounts of silica used and their sources.

The initial potassium concentration of the acid solutions was 0.12 % K_2O (0.10 % K^+ or 1000 ppm K^+). In the case of Dicalite, the concentrations increased which means that this silica source contains potassium. Addition of Dicalite and Serina Kaolin led to increases in the aluminium concentration as they contain aluminium. It is however clear that the potassium content was not sufficiently reduced in any of the cases as was expected. One of the possible explanations for this result is the low solubility of the various silica sources in the acid solution. When more silica was added however, the concentration of potassium was not reduced. Another explanation is the formation of other complex ions in the acid solution such as aluminium-fluoride (AlF^{3+})

and silica-phosphate complexes. It can therefore be concluded that none of the silica sources that were investigated will be useful for this application and thus potassium cannot be removed with this method.

Table 4: Silica results

Experiment	Silica source	Mass silica (g)	Acid Solution Composition				
			Al_2O_3 (ppm)	**K (ppm)**	SiO_2 (ppm)	F (ppm)	P_2O_5 (%)
1	Dicalite	1.25	327.79	**1040.38**	969.12	1154.39	39.48
2	Dicalite	2.50	474.73	**1345.05**	901.98	1186.81	38.77
3	Dicalite	3.75	750.63	**1079.04**	797.55	1063.40	38.94
4	Dicalite	5.00	873.30	**1120.45**	659.09	1071.02	38.89
5	Serina Kaolin	1.25	1745.92	**913.75**	620.05	1060.60	38.51
6	Serina Kaolin	2.50	3490.10	**861.39**	638.61	1069.31	38.02
7	Serina Kaolin	3.75	4783.52	**943.91**	383.96	879.91	37.60
8	Serina Kaolin	5.00	6318.04	**996.74**	417.99	964.59	38.42
9	Foskor silica	1.25	33.12	**851.56**	1072.34	1135.42	37.22
10	Foskor silica	2.50	34.77	**831.35**	1254.58	982.50	39.15
11	Foskor silica	3.75	22.33	**848.38**	982.34	1160.95	37.21
12	Foskor silica	5.00	43.45	**900.07**	1055.26	1055.26	37.55
13	Aerosil 200	1.25	3.26	**859.91**	874.74	1037.82	37.66
14	Aerosil 200	2.50	7.68	**832.08**	1040.10	1152.12	37.12
15	Aerosil 200	3.75	6.86	**898.42**	849.42	882.09	38.22
16	Aerosil 200	5.00	4.33	**850.91**	761.34	940.48	37.77

The results of the solubility experiments are shown in Table 5. From the data given in Table 5, there is virtually no change in the concentration of potassium in the acid with an increase in a specific impurity concentration. Only when iron is added, a slight potassium concentration increase from 0.17 % to 0.20 % with increase in the iron concentration is observed. There is however, a difference in the potassium concentration in the acid for the different impurities added. The average potassium concentration in the acid for the different impurities is compared in Figure 12.

Table 5: Results of solubility experiments for different impurities and concentrations

Impurity	% Fe$_2$O$_3$	K in concentrated acid (ppm)	K in concentrated acid (%)
Iron	0.40%	1441.47	0.14%
	0.56%	1486.11	0.15%
	0.65%	1501.68	0.15%
	0.72%	1678.97	0.17%

Impurity	% Al$_2$O$_3$	K in concentrated acid (ppm)	K in concentrated acid (%)
Aluminium	0.12%	1621.04	0.16%
	0.16%	1680.82	0.17%
	0.19%	1743.33	0.17%
	0.21%	1779.25	0.18%

Impurity	% MgO	K in concentrated acid (ppm)	K in concentrated acid (%)
Magnesium	1.00%	1885.71	0.19%
	1.20%	1840.47	0.18%
	1.55%	1851.30	0.19%

Impurity	% Cl	K in concentrated acid (ppm)	K in concentrated acid (%)
Chlorine	0.058%	1388.36	0.14%
	0.070%	1459.39	0.15%
	0.082%	1462.48	0.15%

Impurity	% F	K in concentrated acid (ppm)	K in concentrated acid (%)
Fluorine	0.31%	880.18	0.09%
	0.70%	862.23	0.09%
	1.04%	885.62	0.09%

From Figure 12, it can be seen that the highest potassium concentration in the acid was found when magnesium was added as impurity. It can therefore be concluded that the magnesium causes the potassium hexafluorosilicate to be the most soluble in the acid solution, thereby increasing the concentration of potassium in the solution. Fluoride on the other hand caused the potassium hexafluorosilicates to be the least soluble as it had the lowest potassium concentration in the acid solution. Even this unfortunately is still above the potassium concentration needed

for x-compound formation.   From the monitoring program it was seen that even with concentrations of 0.12% K_2O, sludge formation occurred.   Although fluoride impurities gave potassium values below this, fluoride is one of the impurities that is purposely removed in the defluorination section.   It is thus not viable to add more fluoride to reduce the solubility of K_2SiF_6 in the acid solution.
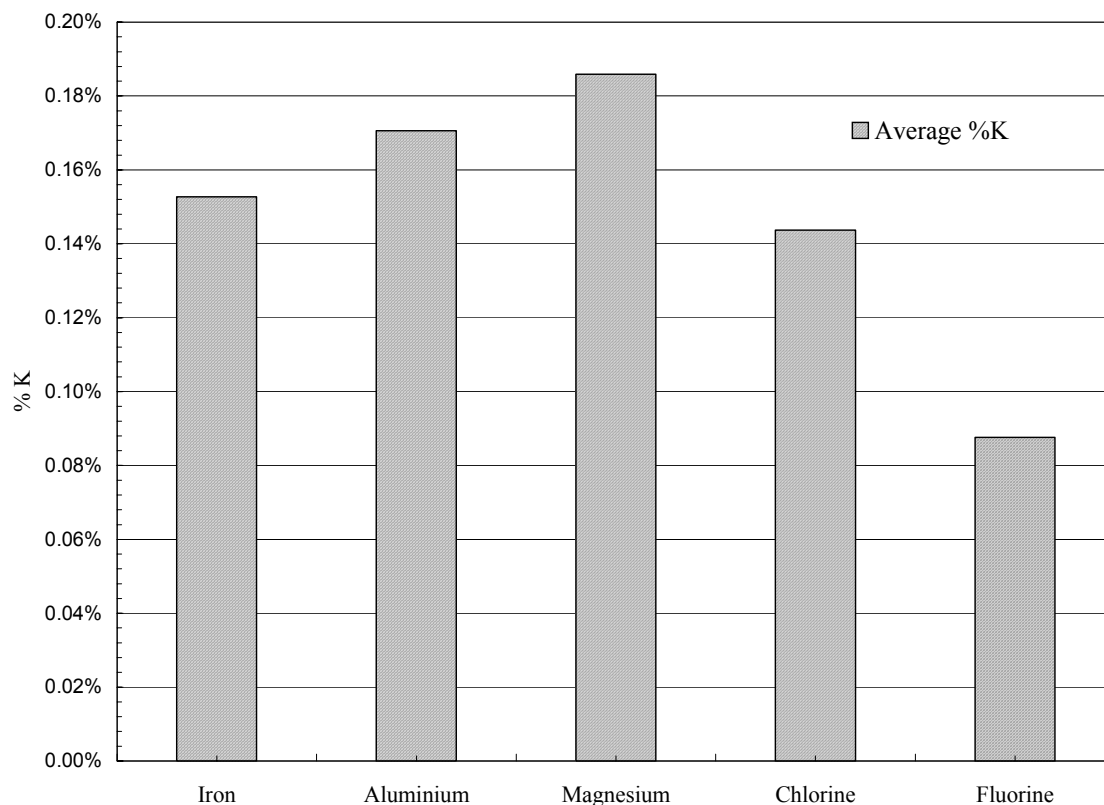
Figure 12: K_2SiF_6 solubility differences with different impurities in 39 % P_2O_5

3.6   Conclusions and Recommendations

Experiments investigating the impurity effects on x-compound precipitation

- It was confirmed using XRD and SEM analyses that mainly x-compound precipitated in all the experiments.   The weighed precipitate of the different experiments that was collected after one week could thus be compared directly.

- From the results it was found that:
  - Agitation increases x-compound precipitation and can be used commercially to increase the precipitation rate to a point where sludge can be removed before transportation.
  - Adding x-compound seeding crystals or magnesium ions also increases the rate of precipitation.
  - Adding gypsum, hexafluorosilicates and fluorosilic acid reduces the rate of precipitation, with sodium ions showing the lowest yield. This reduction is not sufficient to be used commercially as a solution to the sludge problem experienced in wet-process phosphoric acid production.

A Raman study investigating the effect of impurities on nucleation process of the x-compound.

- From the Raman study the following was observed to explain the slow nucleation process of x-compound:
  - In low acid concentrations, more $H_2PO_4^-$ ions are present that forms a complex with iron and aluminium.
  - As the acid concentration increases the concentration of $H_2PO_4^-$ ions decrease as the degree of dissociation of phosphoric acid decreases. The ferric-$H_2PO_4^-$ and aluminium-$H_2PO_4^-$ complexes become less stable and ultimately precipitation of the x-compound is favoured above solvation.
  - Addition of potassium impurities to the solutions had no visible effect on the Raman spectra because it does not complex with the acid.
- A novel way of determining the phosphoric acid concentration is to use the line of the relative peak positions, as a function of acid concentration.

The Foskor rock impurity and the Fedmis precipitate and acid monitoring program

- The Fedmis monitoring program includes the monitoring of Foskor rock analyses on a daily basis, and the monitoring of the 27%, 39% and 54% P_2O_5 phosphoric acid and precipitate from these acid solutions on a weekly basis.

- The rock was analysed for the period between 3 September 1999 to 2 August 2000 and the acid with its precipitate was analysed from 16 May 2000 to 29 August 2000.

- From the monitoring program of the rock it was observed that the:
  - P_2O_5, MgO, Cl_2, SiO_2, Fe_2O_3 and Al_2O_3 content of the rock was fairly constant for the time period investigated.
  - K_2O content of the rock is increasing.

- From the precipitation graphs of the 27 % P_2O_5 acid the following was observed:
  - For the results and for this study a constant analysis procedure was assumed and therefore constant P_2O_5 contamination. The varying acid content of the precipitate is thus possibly an indication of the amount of x-compound in the recycled sludge.
  - The varying silica content of the precipitate could be attributed to the sludge pumped from the 54 % P_2O_5 pressure filters back to the 27% P_2O_5 reactor. It contains large amounts if K_2SiF_6 that was not removed efficiently in the defluorination section
  - The precipitate contained low concentrations of sodium, aluminium, magnesium and iron.
  - The potassium concentrations were relatively low, but varied significantly and, as with the silica, it could be due to the addition of sludge from the 54 % P_2O_5 filters, which contains K_2SiF_6 and x-compound.

- From the precipitation graphs of the 39 % P_2O_5 acid the following was observed:
  - The analysis of the precipitation indicated the highest impurity concentration and is due to the sample being taken before the filtration step where high sludge content is found.
  - The precipitate contains more P_2O_5, which again could be attributed to higher x-compound precipitation consisting of phosphate.
  - The silica content of the precipitate is higher and even greater variation was found. This can be attributed to defluorination sludge containing K_2SiF_6 that is added on an irregular basis.
  - The potassium and the iron content was substantially higher than in the 27 % P_2O_5 precipitate. This shows that more x-compound was precipitated and this could be due to tanker wash added on an irregular basis.
  - The sodium content varied and could be due to silica in the system that could form sodium hexafluorosilicates that would vary as the silica in the system varies.
  - The magnesium and aluminium levels were relatively low.

- From the precipitation graphs of the 54 % P_2O_5 acid the following was observed:
  - The precipitate showed relatively lower (sodium, potassium and silica) or constant (magnesium, aluminium and iron) impurity concentrations than the 39 % P_2O_5 precipitate. This is to be expected as the samples were taken after the 54 % P_2O_5 filters.
  - The P_2O_5 concentration is again higher indicating x-compound precipitation.

- From the acid graphs, the following was observed:
  - Magnesium and aluminium did not precipitate. The three acid graphs for % MgO and Al_2O_3 followed the predicted trend when the 27 % P_2O_5 is concentrated to 39 % P_2O_5 and then to 54 % P_2O_5.
  - The iron concentration is slightly higher than predicted. There is thus an impurity build-up in the system.
  - The sodium is removed through filtration, as the theoretical values are much higher than the actual impurity concentration is the acid.
  - The potassium content of the 54 % P_2O_5 is much higher than expected due to the addition of defluorination sludge and tanker wash.

Precipitation of potassium hexafluorosilicates

- From the silica's investigated namely Dicalite, Serina Kaolin, Foskor silica and Aerosil 200 it can be concluded that none of them will be useful for the removal of potassium through formation of potassium hexafluorosilicates.

- After filtration, there is still enough potassium in the system to cause x-compound formation.

Effect of impurities on the solubility of potassium hexafluorosilicates

- From the data it is clear that there is virtually no change in the concentration of potassium in the acid with an increase in a specific impurity concentration.

- A difference in the potassium concentration in the acid is observed when different impurities are compared with each other.

- The highest potassium concentration in the acid was found when magnesium was added as impurity. It can therefore be concluded that the magnesium causes the potassium hexafluorosilicate to be more soluble in the acid solution.

- Fluoride on the other hand suppressed the solubility of the potassium hexafluorosilicates.

- It is recommended that additional experiments be done using impurity combinations in order to determine what the effect would be using different concentrations. An optimum condition might be found where potassium hexafluorosilicate could be least soluble to remove the maximum amount of potassium from the acid. Using a crystal habit modifier to increase precipitation could also be investigated to find a solution to the problem.

4.   Gypsum

4.1   Introduction

Calcium sulphate dihydrate (gypsum) is obtained as a by-product of various chemical processes such as in the production of sulphuric acid, phosphoric acid, citric acid and organic polymers (Petersen, Kaleta &Kingston, 1995). In the production of wet-process phosphoric acid, filtration is used to separate the acid form the gypsum crystals. It is well established that the quality of the crystals formed affects the filtration rate (Becker, 1989). Large needle-like crystals with a narrow size distribution give the best filtration rates (Becker, 1989).

The effect of various surfactants on the crystallisation of gypsum in phosphoric acid was studied. The purpose of the investigation was to determine whether surfactants could be used to control gypsum crystal quality and thus filtration rate. The investigation was limited to surfactants with sulphate or phosphate hydrophilic groups.   To cancel out variables such as the effect of impurities at different concentrations, the experiments were done on laboratory scale using analytical reagents.

4.2   Background Study

The $CaSO_4$-H_2O system is characterised by five solid phases. Four exist at room temperature namely calcium sulphate dihydrate (gypsum), calcium sulphate hemihydrate, anhydrite III, and anhydrite II. The fifth phase, anhydrite I, only exists above 1180 °C (Wirsching, 1985). The dihydrate process was described earlier in Chapter 2.2, *The Dihydrate Process*" as this is the method Fedmis uses to produce phosphoric acid.

Wet process phosphoric acid is produced by reacting sulphuric acid with naturally occurring phosphate rock. The reaction combines calcium from the phosphate rock with sulphate from sulphuric acid forming calcium sulphate dihydrate as by-product at a reaction temperature of 80 $^{\circ}$C and the produced acid is 27 % P_2O_5. When crystallisation is achieved, the acid is separated form the calcium sulphate dihydrate through filtration.   A saturation limit exists and no

crystallisation will start below this boundary (See Figure 13). The CaO/SO$_4$ diagram shows Ca^{2+} and SO$_4^{2-}$ solubility concentrations lines in 30% P$_2$O$_5$ wet-process phosphoric acid with a calcium sulphate crystal suspension. The concentrations are given in mass percentages for convenience. When additional SO$_4^{2-}$ and Ca^{2+} ions are introduced into a system at equilibrium a state of supersaturation is established. The more of these ions are introduced, the more supersaturated the solution will become. Beyond a certain supersaturation limit spontaneous nucleation will take place. This limit is shown as the super saturation line (SSL) on Figure 13 (Kruger, Focke, Kwela & Fowles, 2001).
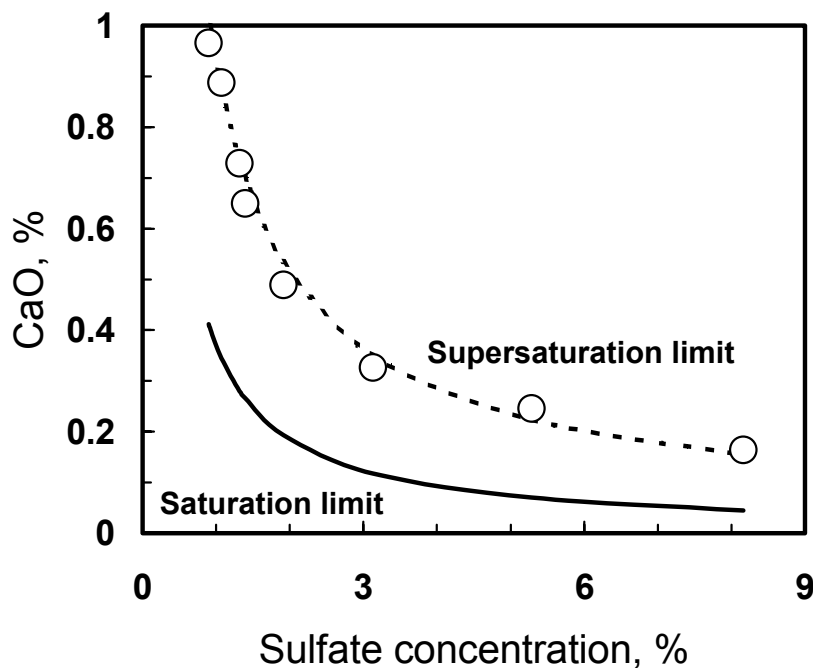
Figure 13: Effect of sulfate concentration on calcium sulfate solubility and apparent supersaturation limit in phosphoric acid (33% P$_2$O$_5$) at 80°C (Kruger *et al*, 2001).

The supersaturation solubility product corresponding to these experimental results in Figure 13 can be mathematically presented as:

$$K_{SSL} = [\%CaO] \times [\%SO_4] \approx 1.30, \text{ in 30\% P}_2\text{O}_5 \text{ phosphoric acid at 75°C (Becker, 1989)}$$

It states that the product of the CaO and SO$_4$ mass percentages must exceed a certain level before spontaneous nucleation will occur.

In the region between the saturation and supersaturation lines, crystal growth without nucleation takes place. Reactants added at levels that exceed the supersaturation limit react spontaneously to form precipitated solids by homogeneous nucleation. The solubility product depends on temperature and phosphoric acid concentration. Solubilities corresponding to saturation and supersaturation lines increases with a rise in temperature.

Several investigators have studied the crystal growth of gypsum. Smith and Sweett (1971) found that the crystallisation of gypsum from aqueous solutions at 30 ^{o}C was heterogeneous (only calcium sulphate dihydrate precipitated) and that the growth rate was proportional to the crystal surface area. Aggregation, crystal fracture and secondary nuclei also influence the growth rate of gypsum (Klima & Nancollas). Rosmalen, Daudey and Marchee (1981) have concluded that the growth mechanism of gypsum can be explained by a combined spiral growth and layer growth mechanism. Gypsum forms layers parallel to the (010) face, originating from screw dislocations.

According to Hünger and Henning (1988), the crystallisation process can be influenced by the differences between the concentrations of the reaction solutions, temperature fluctuations and the addition of other salts.

Studies have also been done investigating the effect of impurities on gypsum crystal growth (Brandse, Rosmalen & Brouwer, 1977). Increasing sodium chloride concentrations increases the crystallisation rate of gypsum. These experiments were done in supersaturated solutions both in pure water and in the presence of sodium chloride (Brandse, Rosmalen & Brouwer, 1977). Witkamp, van der Eerden and Rosmalen (1990) investigated the growth kinetics of gypsum over a wide range of ionic strengths in the presence of sodium nitrate. They found that the growth rate increased with electrolyte concentration and with temperature. It was also found that the presence of sodium ions causes twinning of gypsum crystals (Rinaudo, Robert & Lefaucheux, 1985).

Rinaudo and Franchini-Angela (1989), investigated the effect of sodium and magnesium and their combinations. They found that the presence of sodium causes deformed and twinned crystals whereas magnesium causes curved crystals to form. Aluminium enhances the degree of agglomeration, but reduces the overall growth and nucleation rates (Budz, Jones & Mullin, 1985).

Many current technologies require crystallisation strategies that provide control over the structure and size of inorganic crystals like gypsum. Additives of both organic and inorganic nature play a role in the crystallisation process (Öner, Dogan & Öner, 1998). Additives like surfactants can be used (Öner *et al*, 1998).

The term surfactant is a contraction of surface-active agent (Lynn & Bory, 1995). Since 1950, surfactant has become universally accepted to describe organic substances having certain characteristics in structure and properties. Surfactants are generally characterised by the following features (Lynn *et al*, 1995).

- Amphiphilic structure: Surfactants molecules are composed of groups of opposing solubility tendencies, typically an oil-soluble hydrocarbon chain (hydrophobic) and a water-soluble (hydrophilic) ionic group.
- Solubility: A surfactant is soluble in at least one phase of a liquid system.
- Adsorption at interfaces: At equilibrium, the concentration of a surfactant solute at a phase interface is greater than its concentration in the bulk of the solution.
- Orientation at interfaces: Surfactant molecules and ions form oriented monolayers at phase interfaces.
- Micelle formation: Surfactants form aggregates of molecules or ions called micelles when the concentration of the surfactant solute in the bulk of the solution exceeds a limiting value, the so-called critical micelle concentration. This is a fundamental characteristic of each solute-solvent system.
- Functional properties: Surfactant solutions exhibit combinations of cleaning (detergency), foaming, wetting, emulsifying, solubilising and dispersing properties.

Since surfactants mainly act in aqueous systems, they are mostly classified according to the chemical structure of their hydrophilic groups (Kosswig, 1994). The hydrophilic groups may be ionic (anionic or cationic) or nonionic, and their chemical structure can vary widely (Kosswig, 1994).

Additives such as surfactants can alter the crystallisation process in several ways. They may alter the concentration of ions at the growth face of the crystal, influencing the rate at which they deposit on the growing plane as well as selectively absorbing on crystal faces, blocking growth on one face while permitting growth on another face (Smith & Alexander, 1970). This results in crystals that differ in shape and size from the typical crystal. They can alter the surface properties of the crystals, which leads to changes in nucleation, growth and thereby to changes in the shape of crystals as well as in their agglomeration or dispersion behaviour (Öner *et al*, 1998). Overall, surfactants can be used to control reagent reactivity, crystal size distributions, crystal porosity and crystal properties as was found with the investigation of the influence of surface modifiers on the structure of precipitated calcium carbonate (Agnihotri, Mahuli, Chauk & Fan, 1999).

Previous studies sought to reduce or prevent the crystallisation of calcium sulphate from supersaturated solutions (Smith & Alexander, 1970). McCartney and Alexander (1958) have examined the effect of a number of polyelectrolytes on the growth rate of calcium sulphate dihydrate. They found that polymers containing carboxyl groups such as carboxymethyl cellulose, aliginic acid, polymethacrylic acid and polyacrylic acid were the most active inhibitors, while polyacrylamide had little effect and polycationic additives had no effect at all (Smith & Alexander, 1970).

Liu and Nancollas (1973) have studied the precipitation of gypsum in the presence of trace amounts of polyphosphates and phosphonates. It was reported that trace amounts of phosphonates could stabilise supersaturated calcium sulphate solutions and lengthen the induction time before the onset of crystallisation.

Öner, *et al* have prepared and studied a range of acrylic acid and methacrylic acid polymers with different architectures to explore their relative effectiveness in inhibiting crystal growth of calcium sulphate dihydrate.   They found the effectiveness of growth inhibition of polymethacrylic acids to be homopolymer>block copolymer>random copolymer.   They also found that the introduction of a hydrophobic methyl group into a polymer molecule has a negative influence on its inhibiting performance. High molecular weight PAA and PMAA were less effective for inhibiting crystal growth. In the case of copolymers, increase in effectiveness was found with increase in molecular weight in the range of 2000-18 000.

Al-Sabbagh, Widua and Offermann (1996) conducted gypsum crystal growth experiments and found that partially esterified citric acid is an effective habit modifier. The crystals changed from a needle-like to a stumpy shape. Addition of silicone oil caused crystal agglomeration and increased the filtration time.

4.3   Experiments for the Production of Calcium Sulphate Dihydrate without Surfactants

4.3.1 Apparatus

Two different methods were used in the production of calcium sulphate dihydrate. From Method A, satisfactory results were not produced and therefore the experimental set-up was changed to Method B. The reason for this will be discussed in the detail in the following section. The experimental set-up of Method A and Method B are illustrated in Figure 14 and Figure 15 respectively.
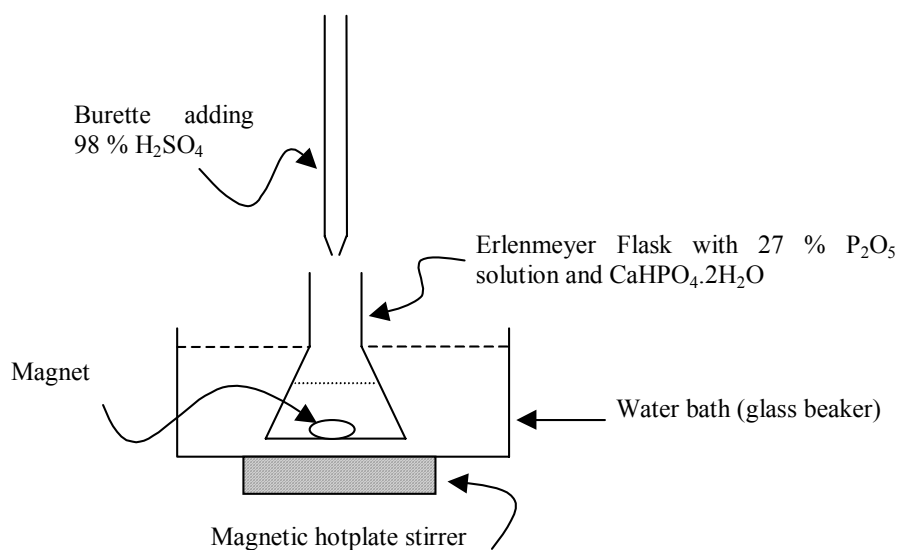
Figure 14: Experimental set-up used for Method A

Powder X-Ray Diffraction (XRD) data of solid samples were recorded on a Siemens D501 automated diffractometer equipped with a secondary graphite monochromator, while electron micrographs were recorded on a JEOL JSM-840 scanning electron microscope (SEM).
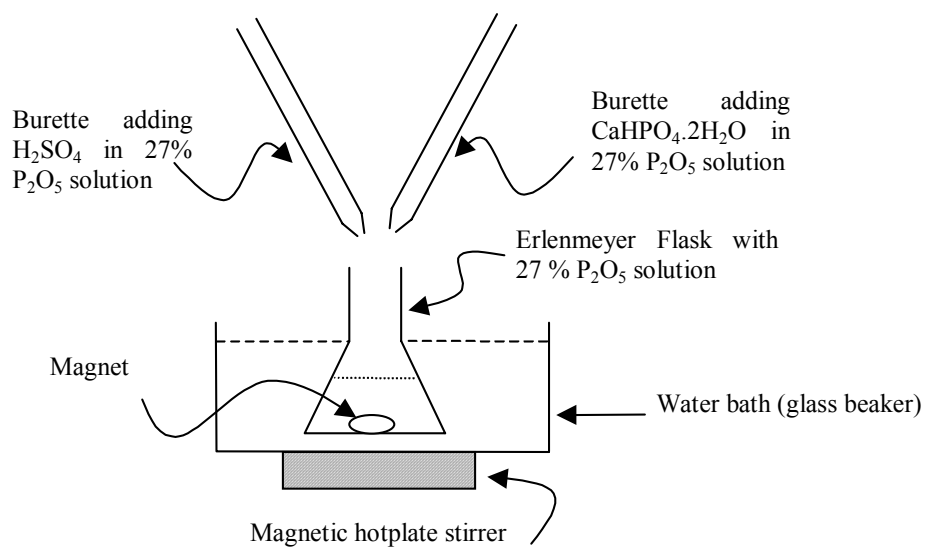
Figure 15: Experimental set-up used for Method B

4.3.2 Planning and Procedure

A soluble calcium phosphate needed to be used for the experiments so that the calcium ions and sulphate ions from the sulphuric acid could react to form calcium sulphate dihydrate. The calcium phosphate chosen was $CaHPO_4.2H_2O$ (99% pure). 85 % Analytical grade phosphoric acid (H_3PO_4) was used, with 98% analytical grade sulphuric acid (H_2SO_4). Distilled water was used for dilution purposes.

With Method A, for each experiment 250 g solutions were made containing 27% P_2O_5 (37.28% H_3PO_4), in which different amounts of $CaHPO_4.2H_2O$ was dissolved. The solutions were placed in a 2.5 litre glass beaker filled with water and placed on a magnetic hotplate stirrer. The temperature was controlled at 80°C. The Erlenmeyer flasks with the different solutions were clamped in the water bath as close as possible to the hotplate so that the magnet in the sample could stir the solution continuously. When the desired temperature was reached, sulphuric acid was slowly added with a burette to this solution until spontaneous nucleation occurred. This point indicated that the super saturation limit was reached and this method was used to draw up a supersaturation diagram (Figure 16) for 80 ^{o}C as discussed in Chapter 4.3.3, *Results and Discussion*.

This diagram was needed for the surfactant experiments. It is important to have an idea of how much sulphuric acid needs to be added to the solution to precipitate gypsum so that experimental parameters can be kept constant. Adding surfactant might change the supersaturation diagram and in this way some variables are eliminated.

From the saturation diagram and from experimental results it was calculated that a mass of 3 g of $CaHPO_4.2H_2O$ needs approximately 5 ml of 98 % sulphuric acid to start spontaneous nucleation of gypsum in 250 g of 27 % P_2O_5 solution. Unfortunately, Method A did not give a good crystal size distribution, which would be discussed in Chapter 4.3.3, *Results and Discussion*". This is required for the surfactant experiments where the crystals of different experiments using different surfactants would be compared visually.

Method B comprises of basically the same experimental set-up of Method A. A total of 250 g of 27 % P_2O_5 is again made up for each experiment, but it is split into three. Part one consists of 100g of 27 % P_2O_5 solution saturated with calcium sulphate dihydrate in which 1 g of seed crystals is added. This solution was placed in the Erlenmeyer flask clamped in the water bath at 80°C. Three different calcium sulphate dihydrates from different suppliers were analysed using SEM to select the best seed crystal with the right crystal structure. The suppliers were Unilab, Analar and ACE.

The second part consists of 75 g of 27 % P_2O_5 in which 3 g of $CaHPO_4.2H_2O$ is dissolved. This is poured into one of the burettes. The third part consists of the remaining 75 g of 27 % P_2O_5 in which 2 ml (3.68 g) of 98 % sulphuric acid is diluted and poured into the other burette. Less sulphuric acid is needed because the solution is already saturated.

When the solution in the waterbath reached 80 ^{o}C, the solutions in the burettes were added drop by drop to give the calcium ions and sulphate ions time to react and for proper mixing to take place. The sulphuric acid was diluted with the 27 % P_2O_5 so that there is not such a high sulphate concentration in the drop added to the solution. From the saturation diagram (Figure 13), it can be seen that a sudden high concentration of sulphates with a small amount of calcium, would push the system beyond the spontaneous nucleation point with high nucleation rates and smaller crystals. When this drop has been mixed in, the nucleation rate would decrease allowing better crystal growth.

After addition, the mixture was stirred for 30 minutes at 80°C and then allowed to cool down. It was filtered 24 hours later and the precipitate was washed with 99.9 % ethanol. An experiment was also done where the mixture was stirred for 30 minutes at 80°C and then removed where it was stirred further for a total of 24 hours to see the comparison. After this time the mixture was filtered and the precipitate again washed with 99.9 % ethanol. Both the above-mentioned experiments were repeated to determine reproducibility and the precipitate was analysed using XRD and SEM.

4.3.3 Results and Discussion

The super saturation curve with experimental and mathematical values obtained using Method A, is shown in Figure 16.
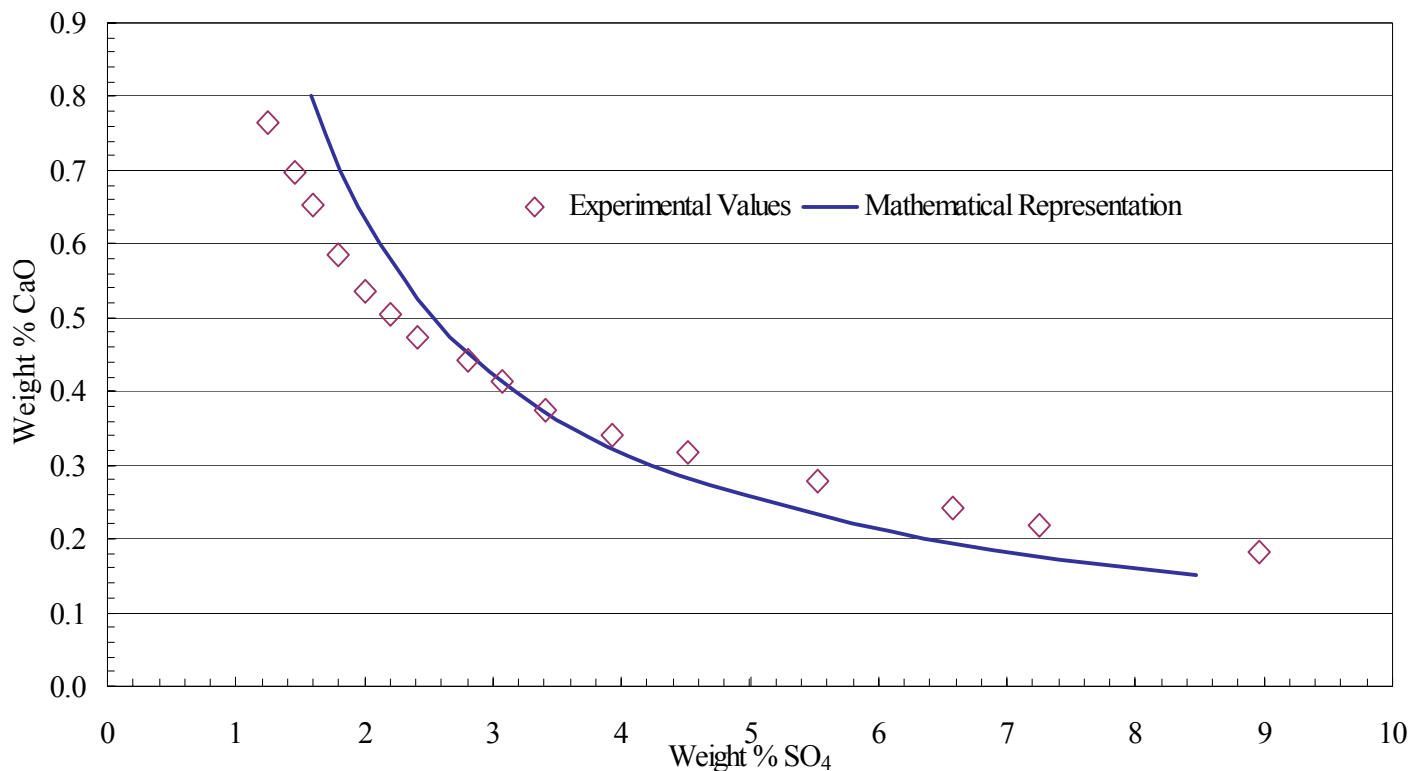
Figure 16: Super saturation diagram for 27 % P_2O_5 at 80 ^{o}C

Lower calcium concentrations were investigated, but the amount of sulphuric acid needed for spontaneous nucleation starts getting too high. This leads to dilution of the phosphoric acid concentrations and then the diagram becomes invalid. For a weight percentage of CaO of 0.03%, the phosphoric acid concentration dropped to 16.99 % P_2O_5 due to the addition of 80 ml (147.20 g) of 98 % sulphuric acid. For that reason the diagram only shows weight percentage CaO of 0.18 % to 0.76 %, where the phosphoric acid concentration varies between 24.48 % to 26.62 % respectively. The K_{SSL} was experimentally found to be 1.27 in 27% P_2O_5 phosphoric acid at 80°C. The solid line in Figure 16 mathematically represents this value. The diagram was only used to obtain an indication of how much of the reagents are needed.

The SEM analysis for precipitate obtained using Method A, showed a wide crystal size distribution (Figure 17). This is unsatisfactory for the surfactant experiments planned. The different surfactant's effect on the crystal habit modification will be analysed visually through SEM analysis and a wide crystal size distribution as shown, would make that this very difficult. The reference experiment's crystal size distribution should be very narrow, so that the effect that the surfactants would have could easily be identified.
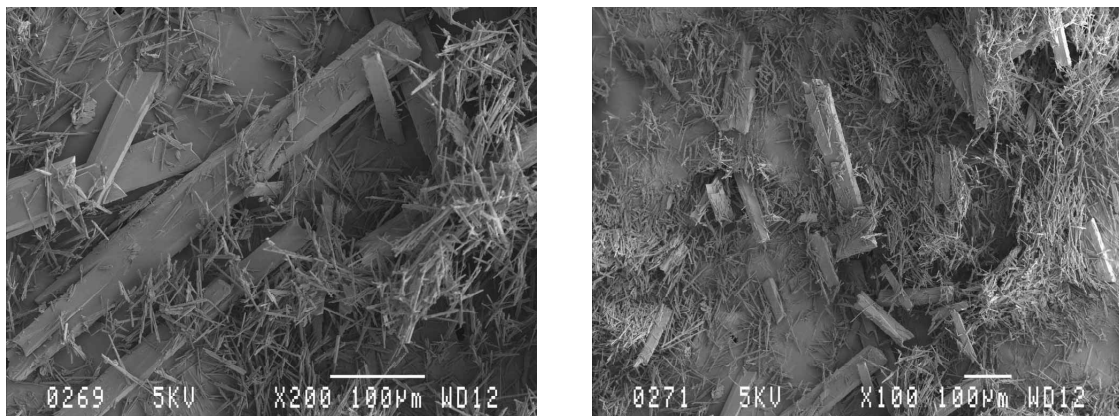
Figure 17: SEM of gypsum prepared through Method A

The three different seed crystals from different suppliers that were investigated using SEM are shown in Figure 18. From these pictures it is clear that only one of the three could possibly be used as seed crystals namely the calcium sulphate dihydrate supplied by Analar. It is the only sample that has a narrow crystal size distribution and that resembles the well-known needle-like shape although broader. The other samples don't resemble calcium sulphate dihydrate at all and this could possibly be due to the preparation method used by the companies mentioned. The crystal size distribution of the other samples is also too broad to be considered.
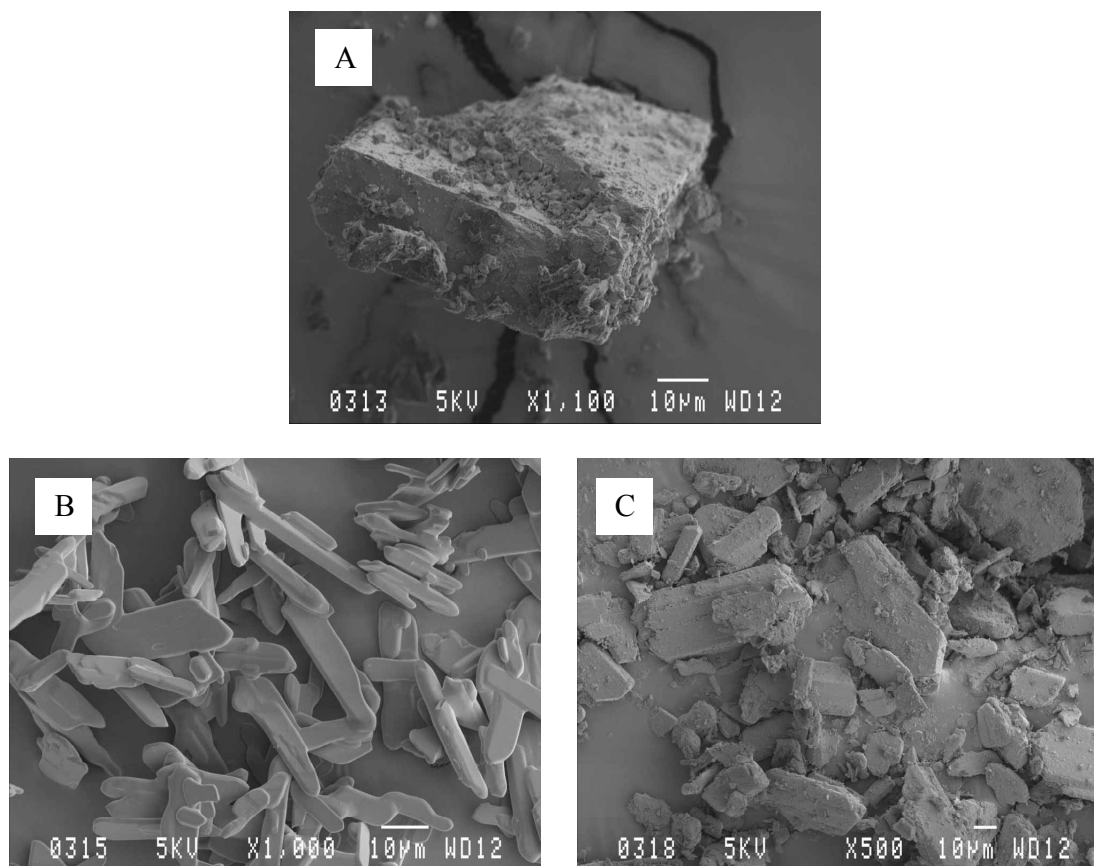
Figure 18: Calcium sulphate dihydrate supplied by A) ACE, B) Analar and C) Unilab

Using Method B and the seed crystals supplied by Analar, good results were obtained with regard to the crystal size distribution and the general shape of the crystals. Good reproducibility of the experiments was also obtained with an average crystal mass of 4.0 g for 30 minute stirring and 4.32 g for the 24 hour stirring that equals yields of 100 % depending on the experiment. XRD results are shown in Appendix E and from these results only calcium sulphate dihydrate was precipitated.

The difference in the crystal masses obtained can be explained through mass transfer restrictions. For the 30 minute stirring, mass transfer becomes a problem because the calcium and the sulphate in the system that are in contact with each other will react first to form gypsum. These crystals will settle to the bottom. Without further mixing, mass transfer becomes a problem as the ions in solution and the crystals are not in constant contact with each other. If enough time is allowed, the ions will diffuse through the solution and the reaction will continue until equilibrium is reached. As there is not such a large difference in the masses obtained between

the two experiments, it is clear that for 30 minute stirring, equilibrium conditions were almost reached. The reference experiment's SEM analysis for 30 minute stirring and 24 hour stirring is shown in Figure 19 and in Figure 20 respectively.
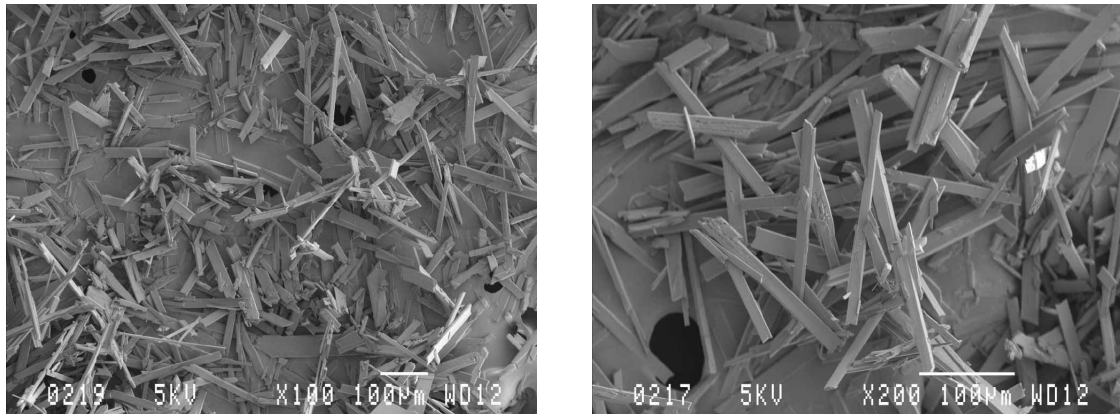
Figure 19: Gypsum prepared using Method B with 30 minute stirring

Comparing the crystals obtained from the two different experiments, it can be seen that stirring for 24 hours, possibly breaks down the crystals. The crystals from the 30 minute stirring experiments, have an average crystal size of approximately 200 µm, compared to the average crystal size of the 24 hour experiments of approximately 30 µm. Rough edges can also be seen on the crystals from the 24 hour stirring experiments which indicates breakage. Overall good crystal size distributions were obtained for both experiments.
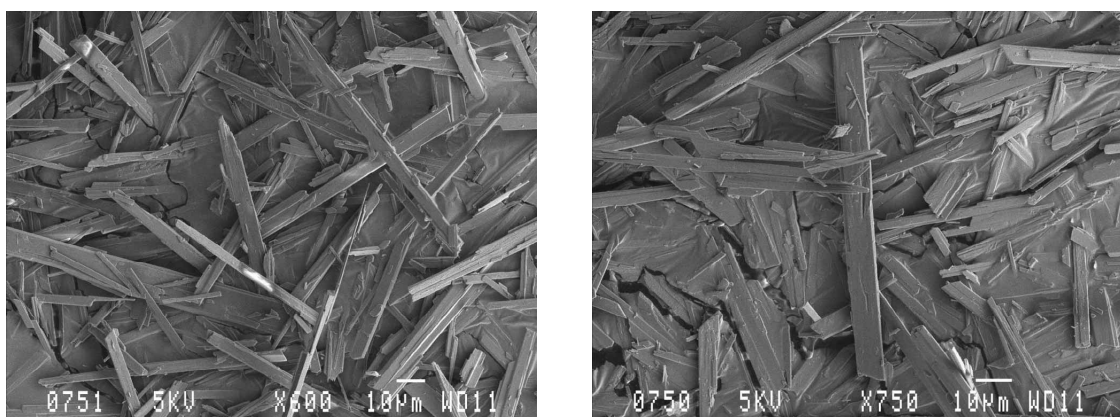
Figure 20: Gypsum prepared using Method B with 24 hour stirring

4.4   Experiments for the Production of Calcium Sulphate Dihydrate with Surfactants

4.4.1 Surfactants Used

In total, 12 different potential crystal habit modifiers were investigated using Method B.

Atphos E3205, Atpol E3202 and Atpol E1231 are polyethoxylated alkyl phenol phosphates esters and have the same basic structure shown in Figure 21 where only n and m differs. For Atpol E3202 and Atphos E3205, n equals 9 for both and m equals 6 and 9 respectively. All three these surfactants have an active ingredient percentage of 99 %.
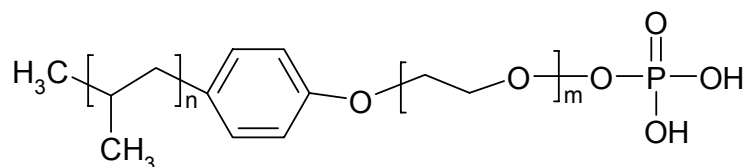
Figure 21: Basic molecular structure of Atphos E3205, Atpol E3202 and Atpol E1231

Dowfax 3B2 and Dowfax Hydrotrope are alkylated diphenyl oxide disulphonates.   Their basic molecular structure is shown in Figure 22. They were obtained as 45 % solutions.
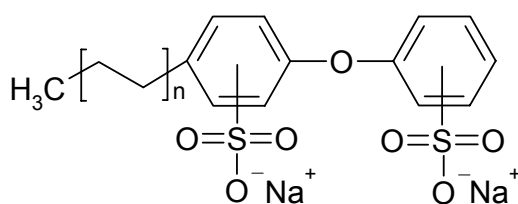
Figure 22: Basic molecular structure of Dowfax 3B2 and Dowfax Hydrotrope

Empicol LZ/D is a neat sodium alkyl sulphate. The structure is shown in Figure 23.
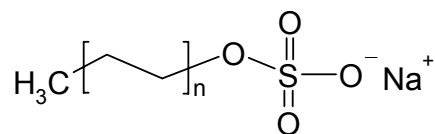
Figure 23: Basic molecular structure of Empicol LZ/D

Empimin KSN70 is a sodium alkyl ether (3EO) sulphate. This surfactant was 100 % active and is shown in Figure 24.
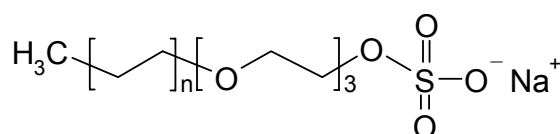
Figure 24: Basic molecular structure of Empimin KSN70

Nansa SS30 is a 30% solution of sodium dodecylbenzene sulphonic acid. The molecular structure is shown in Figure 25.
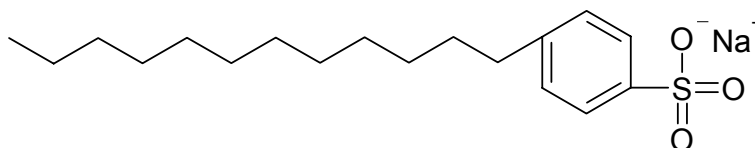
Figure 25: Molecular structure of Nansa SS30

Calcium gluconate monohydrate was also tested for its crystal habit modifier properties and its chemical structure is shown in Figure 26.
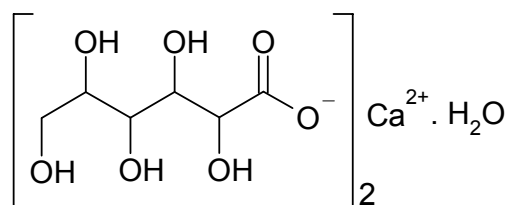
Figure 26: Molecular structure of calcium gluconate monohydrate

The other surfactants chosen were Arlatone 1489 (decylpolyglucoside and sodium cocoylisethionate) with an activity of 55 %, Calsoline oil (aqueous solution of sodium salt of a highly sulphate oil) with an activity of 49 % and Tamol NN 8906 (naphthalene sulphonic acid) with an activity of 100 %.

4.4.2 Planning and Procedure

Method B was used for the basis of the surfactant experiments as better crystal size distribution was achieved. More detailed information on Method B can be found in Chapter 4.3.2, *Planning and Procedure.*

Concentrations of surfactants used varied between 0.10 % to 5.00 % on the mass of crystals obtained from the experiments without surfactant. These masses obtained without surfactants were 4.0 g for the 30 minute stirring and 4.32 g for the 24 hour stirring experiments. The surfactants were added to the 100.00 g of 27 % P_2O_5 solution saturated with calcium sulphate dihydrate with added seed crystals. The solutions were then heated in a water bath to a controlled temperature of 80 ^{o}C before the solutions in the burettes (Method B) were added drop by drop. After addition, the experiments were stirred for 30 minutes and some experiments showing crystal habit modification potential were stirred for 24 hours. This was done so that the experiments with different stirring times could be compared to see the effect.

Precipitates obtained from the experiments were washed with 99.9 % ethanol. Powder X-Ray Diffraction (XRD) data of solid samples were recorded on a Siemens D501 automated diffractometer equipped with a secondary graphite monochromator, while electron micrographs were recorded on a JEOL JSM-840 scanning electron microscope (SEM).

4.4.3 Results and Discussion

The mass of the gypsum that precipitated from the 30 minute stirring reference experiment was 4.00 g which equals a yield of 100 %. For the 24 hour stirring experiment, the mass obtained was 4.32 g that also gives a yield of 100 %. Yield percentage is thus dependent on the stirring time of the experiment. For all the experiments, XRD results are shown in Appendix E. The surfactants that did not have any significant effect on the crystal structure will be discussed first.

Atphos E3205, Atpol E3202 and Atpol E1231

The concentration of polyethoxylated alkyl phenol phosphate esters added were 0.20 % based on the 4.00 g of crystals obtained from the reference experiment (0.008 g). None of these surfactants had any visible effect on the crystal structure of the precipitated gypsum. Small mass differences compared to the reference experiment for 30 minute stirring was found which could be attributed to experimental variance. From the XRD results (Appendix E) for all three surfactants, calcium sulphate dihydrate ($CaSO_4.2H_2O$) and smaller amounts of calcium sulphate hemihydrate ($CaSO_4.0.5H_2O$) was precipitated as the dihydrate peak is more intense than the hydrate peak. This shows that although there was so visible effect on the crystal structure, the surfactant did have an effect on the phases that formed.

Atpol E3202 gave a precipitated crystal mass of 3.81 g (95.25 % yield), which with the active ingredient percentage taken into account and the actual amount of crystals formed at the end of the experimental time frame, gives a final surfactant concentration of 0.22 %. The SEM analysis of this experiment is shown in Figure 27. From these images it is clear that there was no visible change in the crystal structure, but the average crystal size changed from approximately 200 µm without surfactant, to 40 µm with Atpol E3202 as surfactant. This is an indication of growth inhibitor and nucleation promoter as the total crystal mass does not differ that much from the reference experiment.
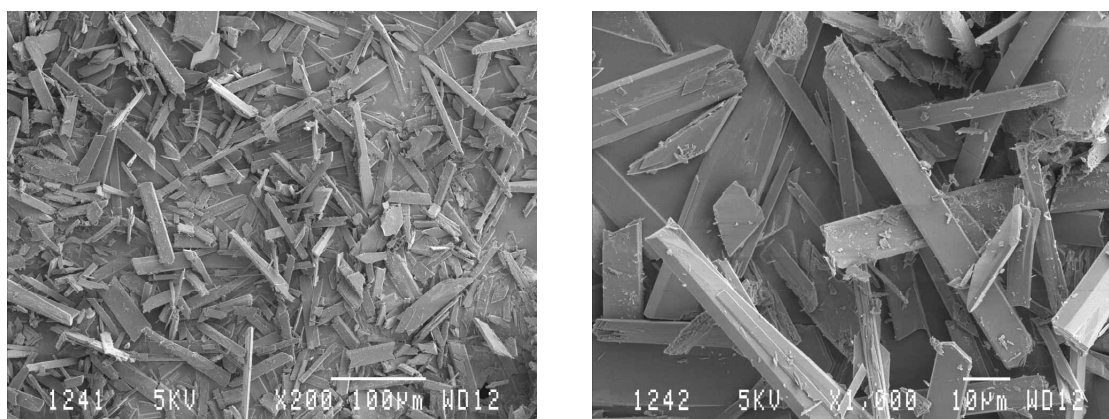
Figure 27: SEM analysis of experiment using Atpol E3202

Atphos E3205 gave virtually identical results to Atpol E3202. A crystal mass of 4.06 g (101.50 % yield) was obtained, which gives a final surfactant concentration of 0.20 % at the end of the experimental time frame on the actual amount of crystals formed. The SEM analysis of this

experiment is shown in Figure 28. Again no visible change in the crystal structure can be seen, but the crystals are smaller compared to the reference experiment with an average crystal size of approximately 80 μm. This again indicates a growth inhibitor and a nucleation promoter.
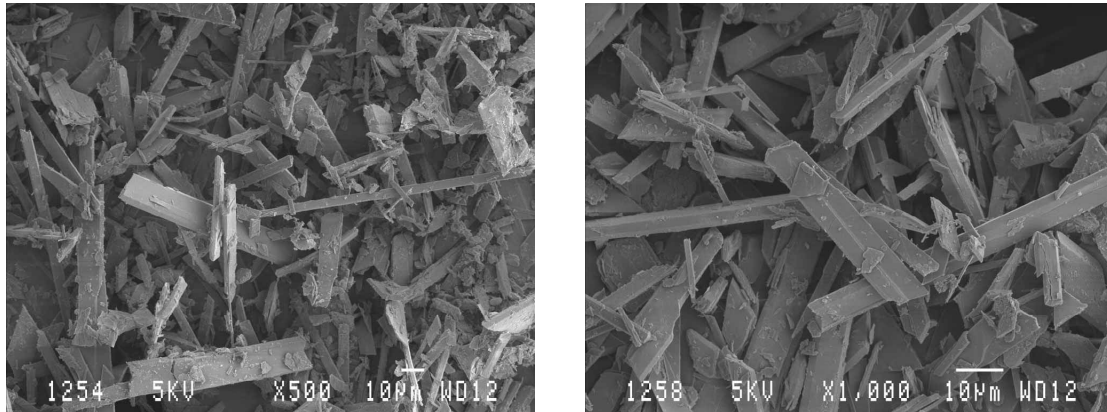
Figure 28: SEM analysis of experiment using Atphos E3205

Using Atpol E1231 as surfactant, a crystal mass of 3.71 g (92.75 % yield) was obtained that equals an actual surfactant concentration of 0.21 %. This mass obtained is not drastically lower than the other esters used, but it does show some inhibition of crystal formation. The SEM analysis of the experiments using this surfactant (Figure 29) shows crystal structure almost identical to the reference experiment with an average crystal size of approximately 250 μm. Due to the smaller mass of crystals and the increase in crystal size, it is concluded that this surfactant acts as a nucleation and not a growth inhibitor.
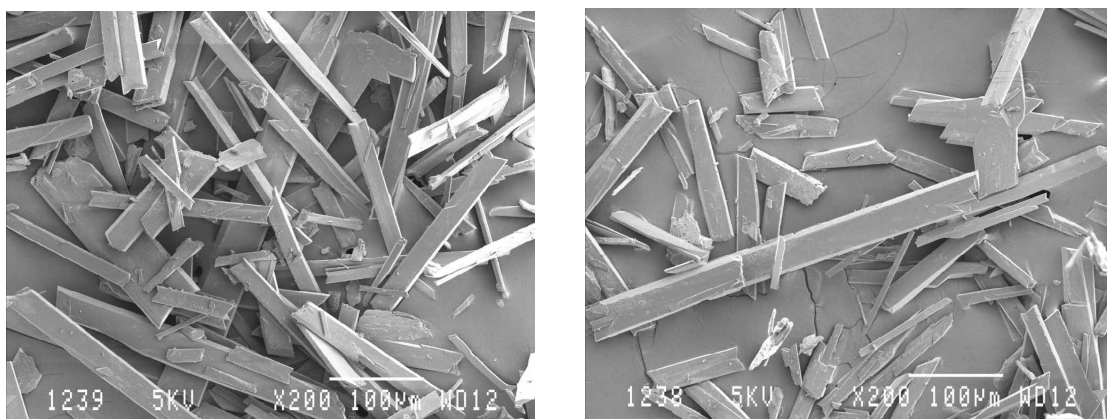
Figure 29: SEM analysis of experiment using Atpol E1231

Calsoline oil

The amount of Calsoline oil added to the reaction mixture was 0.20 % based on the 4.00 g of crystals obtained from the 30 minute reference experiment (0.008 g). The mass of crystals, formed at the end of the experimental time was 3.93 g that gives a yield of 98.25 %. Taking the percentage active ingredient of 49 % into account and the amount of crystals formed, the actual surfactant concentration was 0.10 %. The small difference in mass compared to the reference experiment for 30 minute stirring could again be attributed to experimental variance. From the XRD results shown in Appendix E, calcium sulphate dihydrate and calcium sulphate hemihydrate was precipitated. Looking at the intensities of the XRD peaks for the two species present, the calcium sulphate hemihydrate is found in smaller quantities compared to the calcium sulphate dihydrate.

From the SEM analysis (Figure 30) it is clear that the use of this surfactant causes a broader crystal size distribution. Thinner crystals and broader crystals with approximately the same length (~150 μm) are shown in Figure 30. The mass and the crystal length obtained from this experiment closely resemble the reference experiment. From the analysis it can thus be concluded that the surfactant effects the growth of the crystals and not the nucleation, because the crystal mass is approximately the same as the reference experiment, but with a different crystal size distribution.
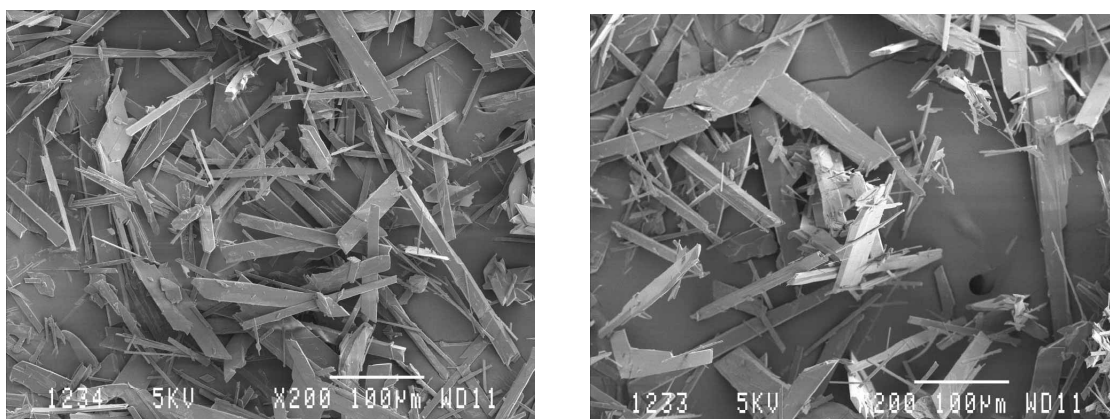
Figure 30: SEM analysis of experiment using Calsoline oil

Arlatone 1489

The Arlatone 1489 concentration added to the reaction mixture was 0.20 % based on the 4.00 g of crystals obtained from the 30 minute reference experiment (0.008 g). The mass of crystals formed at the end of the experimental time was 4.10 g that gives a yield of 102.50 %. Taking the percentage active ingredient concentration of 55 % into account and the amount of crystals formed, the actual surfactant concentration was 0.11 %. The slight increase in mass compared to the reference experiment for 30 minute stirring is again too small to conclude that the surfactant might have had an effect on nucleation. The fact that the size of the crystals of approximately 150 µm closely resembles the reference experiment indicates that it did not effect growth.

Figure 31 show that Arlatone 1489 did not have any visible effect on the crystal size and form. From the XRD results shown in Appendix E, calcium sulphate dihydrate and calcium sulphate hemihydrate was precipitated.   As with the previous experiment, the calcium sulphate hemihydrate is present in smaller quantities.
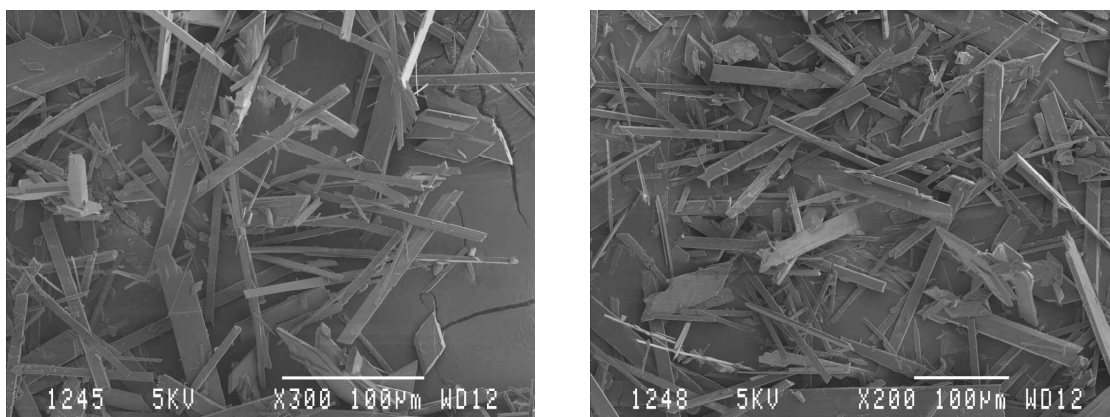
Figure 31: SEM analysis of experiment using Arlatone 1489

Tamol NN 8906

This surfactant had no effect on the structure or size of the precipitated crystals as shown in Figure 32. The same concentration was used as with the previous discussed surfactants namely 0.20 % based on the mass of crystals of the reference experiment for 30 minute stirring. As the

surfactant comprises of 100 % active ingredient, the final concentration on the actual amount of crystals formed was 0.21 % as 3.90 g of crystals were precipitated. This gives a yield of 97.50%. The XRD results (Appendix E) show the formation of calcium sulphate dihydrate and calcium sulphate hemihydrate ($CaSO_4.0.5H_2O$) or bassanite as it is known during the experiment. From these results it can be concluded that this surfactant has no effect on nucleation or growth of the precipitated gypsum crystals.
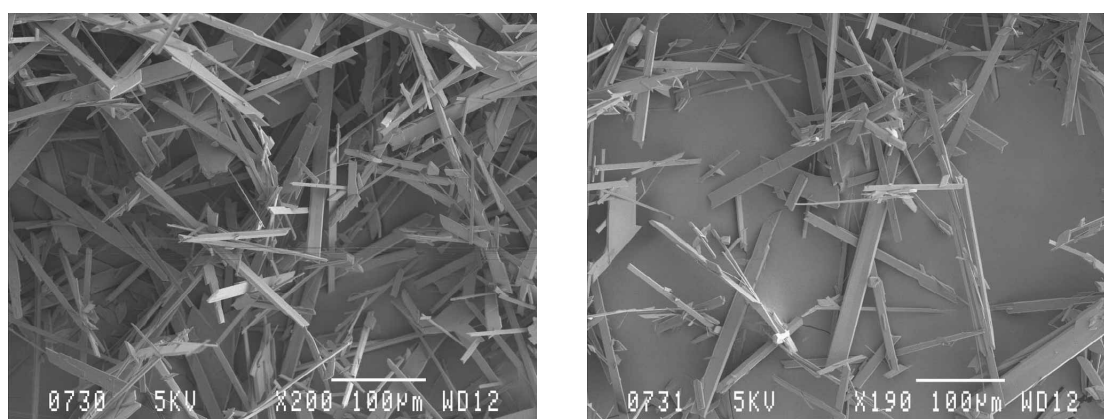
Figure 32: SEM analysis of experiment using Tamol NN 8906

Calcium gluconate monohydrate

The same concentration of calcium gluconate monohydrate was used as for the previous experiments namely 0.20 % based on the mass of the crystals collected from the reference experiment and similar results were obtained. The mass of crystals obtained was 3.92 g that equals a yield of 98.00 %. This mass difference compared to the reference experiment was too small to conclude that this surfactant had any effect. Examining the SEM analysis (Figure 33), it is clear that this compound again had no visible effect on the crystal structure and the average crystal size was 200 μm.

The XRD results (Appendix E) only indicate the formation of calcium sulphate dihydrate ($CaSO_4.2H_2O$) and this means that these results with the SEM results show that this compound had no effect on the crystal structure or the phases that formed.
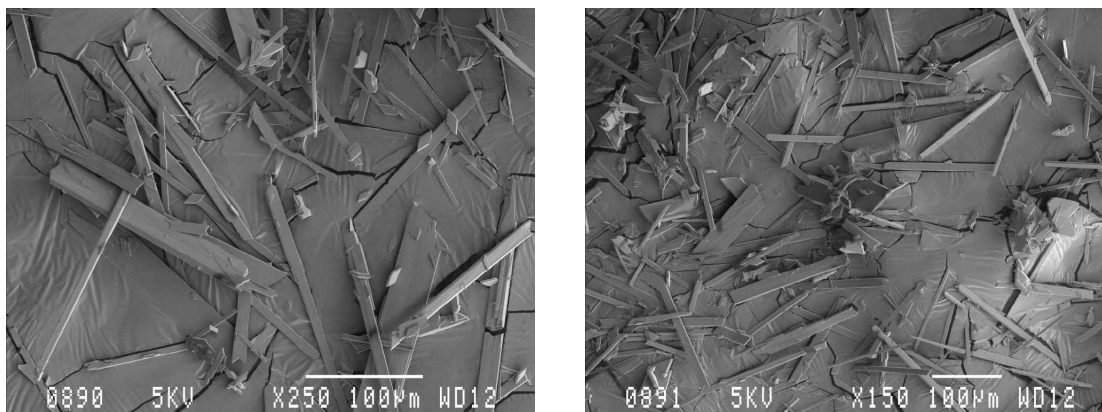
Figure 33: SEM analysis of experiment using calcium gluconate monohydrate

Nansa SS30

The most interesting results were found using this surfactant and this lead to more detailed experiments concerning a range of concentrations and different conditions. From these results, surfactants that were similar in structure were thus also investigated in more detail.

As with the previously discussed surfactants, the concentration of Nansa SS30 was firstly also used as 0.20 % based on the mass of the reference experiment for 30 minute stirring. From the SEM analyses of the precipitate obtained from this experiment, it was clear that this surfactant had drastic effects on crystallisation. There is no characteristic gypsum crystal shape seen previously, but rather small hexagonal rods shown in Figure 34. The average crystal sized of the crystals shown is approximately 12 μm, but vary between 6 μm and 14 μm as can be seen in the SEM images. Some larger crystals that are not shown in these images were present, but were not taken into account for the crystals size calculation, as they resembled seed crystals.

This experiment was repeated to investigate the reproducibility and the same results were obtained. The mass obtained from these two experiments were 1.96 g and 2.01 g respectively which gives an average mass obtained of 1.99 g (49.63 % yield). As the active ingredient percentage of this surfactant is only 30 %, the surfactant concentration on the actual mass of crystals obtained during the experimental time is 0.12 %.

Only one of these experiments XRD results is shown in Appendix E, but both gave the same results. Calcium sulphate dihydrate and calcium sulphate hemihydrate were formed, but now the calcium sulphate hemihydrate is more prominent as those XRD peaks increased in intensity.
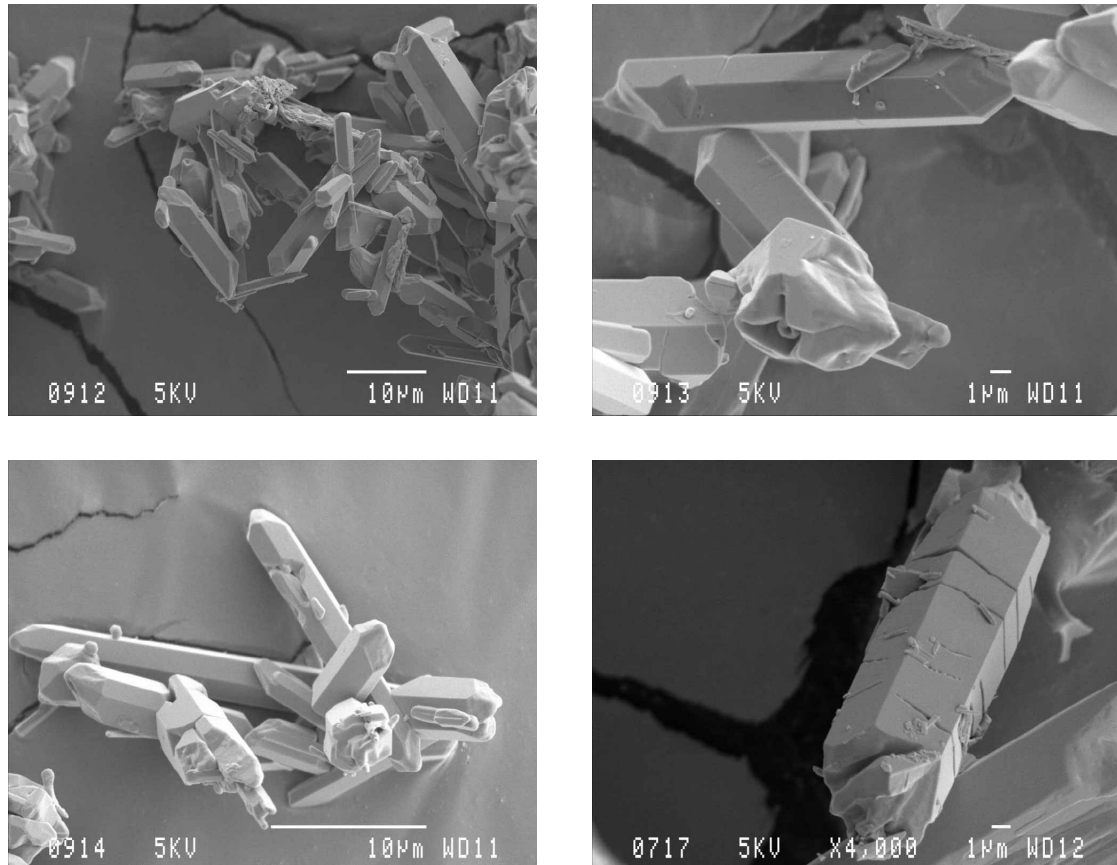

Figure 34: SEM analysis of experiments using 0.20 % Nansa SS30 (30 minute stirring)

As mentioned previously, the change in crystal structure could be due to the surfactant absorbing on one crystal face blocking growth in one direction, while permitting growth in another. Less crystal mass was obtained, but the crystals were much smaller than in any of the previously discussed experiments. The crystals are approximately 14 times smaller than the reference experiment, but the mass obtained is only approximately half of what was collected previously. From these results, it can be concluded that this surfactant can be classified as a growth inhibitor, but a nucleation promoter. It acts as nucleation promoter as there are a large number of small crystals present.

From the good results obtained with the 0.20 %, further experiments using different concentrations were investigated. The extra concentrations used were 0.10 %, 0.30 %, 0.50 %, 0.75 %, 1.00 %, 1.50 %, 2.00 %, 2.50 %, 3.00 % and 5.00 % based on the mass of reference experiment for the 30 minute stirring. The results of these experiments are presented graphically in Figure 35, where the x-axis represents the actual surfactant concentration on the mass of crystals precipitated during the experimental time frame.
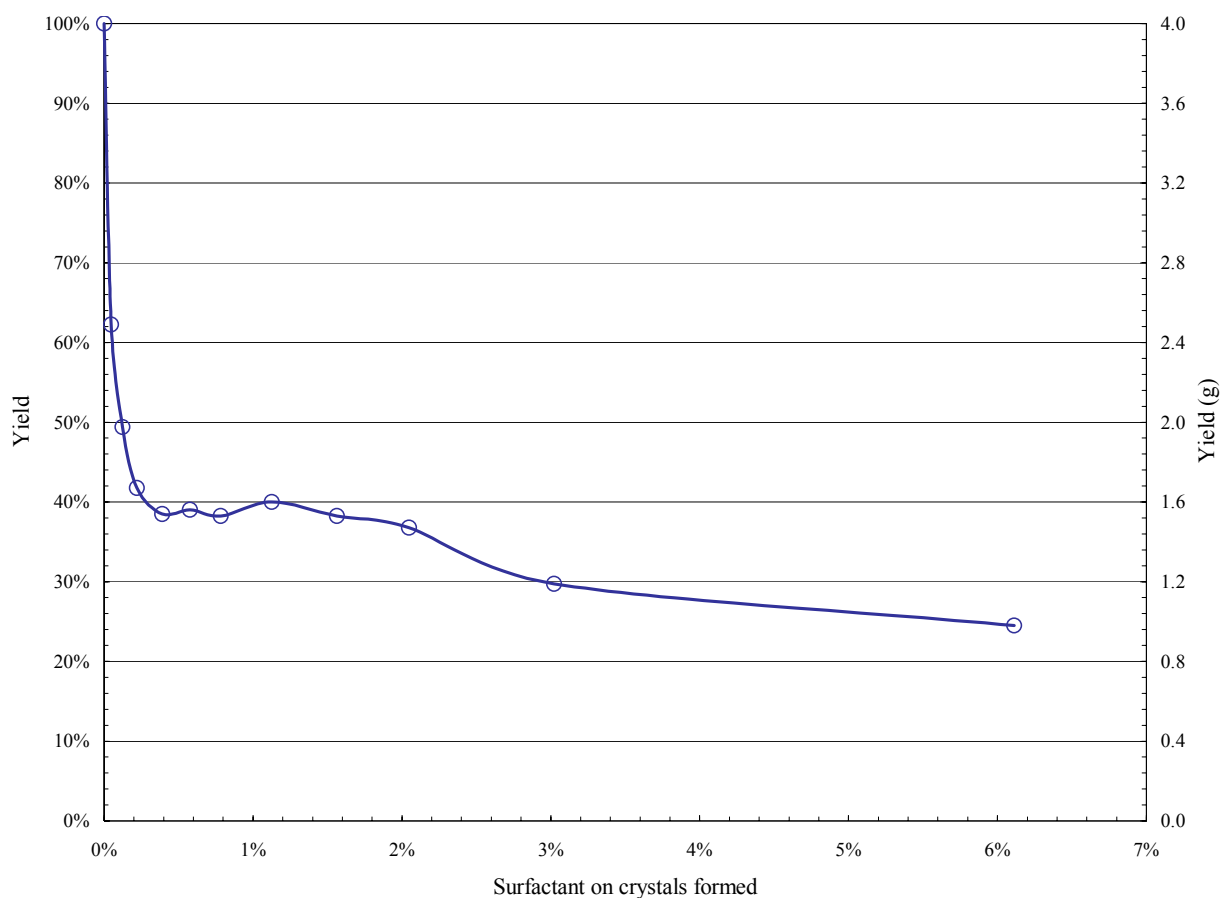
Figure 35: Yield results using different concentrations of the active ingredient in Nansa SS30 for 30 minute stirring

From this graph, it is clear that with an increase in Nansa SS30, there is decrease in mass of crystals obtained. There is a slight increase in mass at approximately 1.00 % actual surfactant concentration, but this is attributed to experimental variance. It was also noticed that with an increase in the surfactant concentration, filtration became increasingly difficult.   This

observation could possibly be explained through the SEM analysis of the samples. Due to the different crystal structures, crystal sizes and distributions at the different concentrations, experiments will be discussed separately.

Some crystal structure changes can already be seen at 0.10 % surfactant concentration taken on the reference experiment (actual concentration of 0.05 %). A narrow crystal size distribution exists, but the crystals are much broader than compared to the reference experiment with a aspect ratio of approximately 1:2.3. The average crystal size is approximately 100 μm, but some larger crystals are present as shown in the SEM analysis of Figure 36.
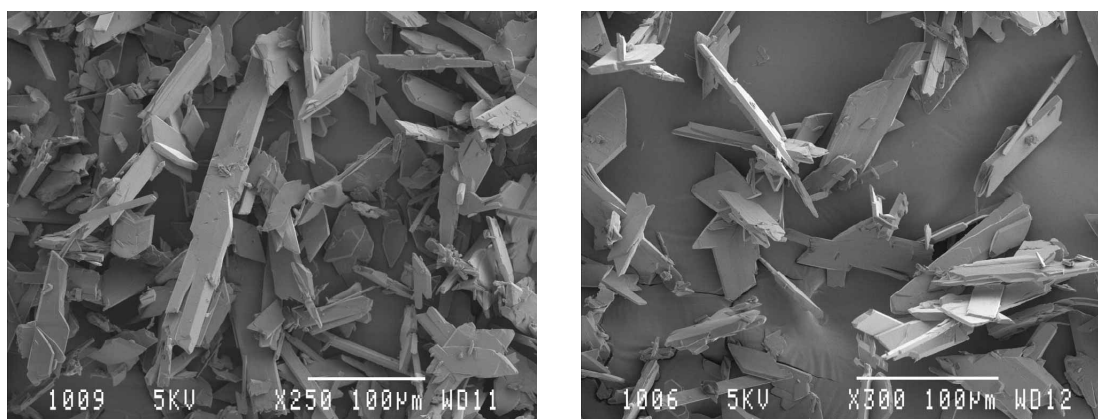
Figure 36: SEM analysis of experiment using 0.10 % Nansa SS30 (30 minute stirring)

Calcium sulphate dihydrate and smaller amounts of calcium sulphate hemihydrate were identified using XRD analysis. There is also a slight hint that minute quantities of calcium sulphate anhydrite ($CaSO_4$) are present

Using 0.30 % surfactant based on the crystal mass of the reference experiment (actual concentration of 0.22 %), similar results were found as with the 0.20 %. Clear differences in the crystal structure compared to the reference experiment are shown in Figure 37. The hexagonal type crystals can still be seen, but these crystals are more deformed. The larger crystal also shows deformity. This indicates that the surfactant possibly absorbs on the crystal faces of the newly nucleated crystals and on the seed crystals and this causes growth variations. It is difficult to say what the average crystal size is due to these deformities, but this explains difficulties in

filtration. Small and large crystals are present. The smaller crystals can closely pack between the larger crystals to form a dense cake that slows filtration. The larger the crystal size distribution, the more difficult filtration will be.
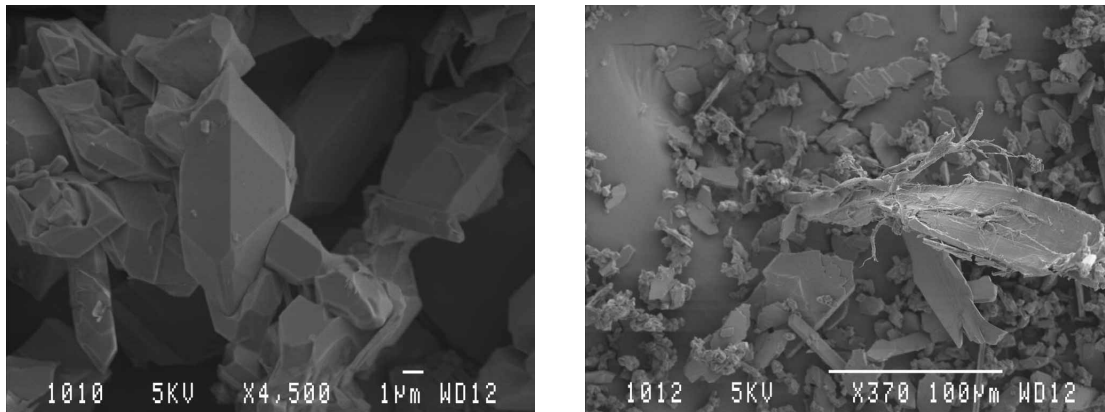

Figure 37: SEM analysis of experiment using 0.30 % Nansa SS30 (30 minute stirring)

Calcium sulphate dihydrate and larger amounts of calcium sulphate hemihydrate were identified using XRD analysis. The amount of hemihydrate seems to increase from 0.10 % surfactant concentration to 0.20 % surfactant concentration and now to the maximum at 0.30 % surfactant concentration when compared to the other XRD analyses. This increase in the hemihydrate phase with an increase in the surfactant concentration indicates that not only does the surfactant affect the crystal size (continuous decrease) and the crystal size distribution (continuous increase), but it also affects the crystal phases that form.

The other surfactant concentrations namely 0.50 %, 0.75 %, %, 1.00 %, 1.50 %, 2.00 %, 2.50 %, 3.00 % and 5.00 %, based on the mass of reference experiment for the 30 minute stirring, can be discussed as a whole due to their similar crystal structure results. These experiments SEM analysis is shown in Figure 38 to Figure 45. With an increase in surfactant concentration, there is an increase in the crystal size distribution with the amount of smaller crystals increasing. On average, the larger crystals become larger, with the smaller ones becoming smaller with an increase in the surfactant concentration. There is also an increase in crystal deformation

especially with the crystals with average crystal size of ~1 μm, where no specific crystal structure can be identified. These results lead to increasing filtration difficulties.
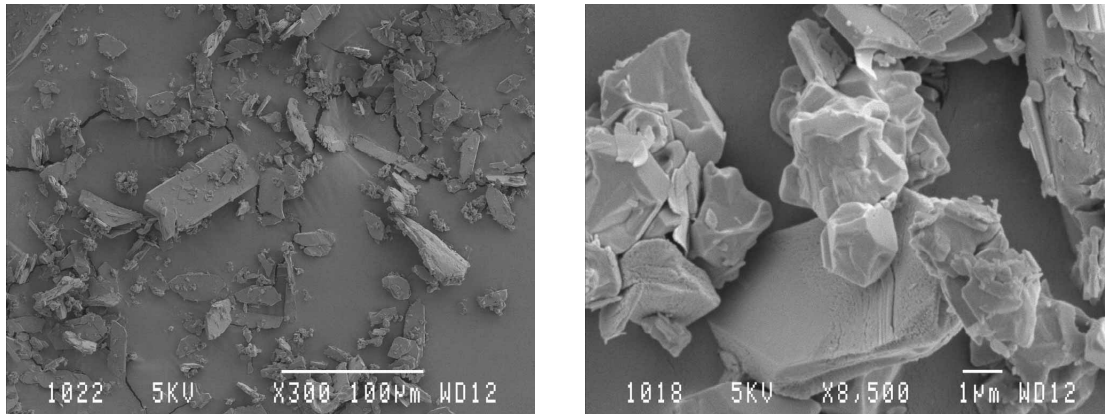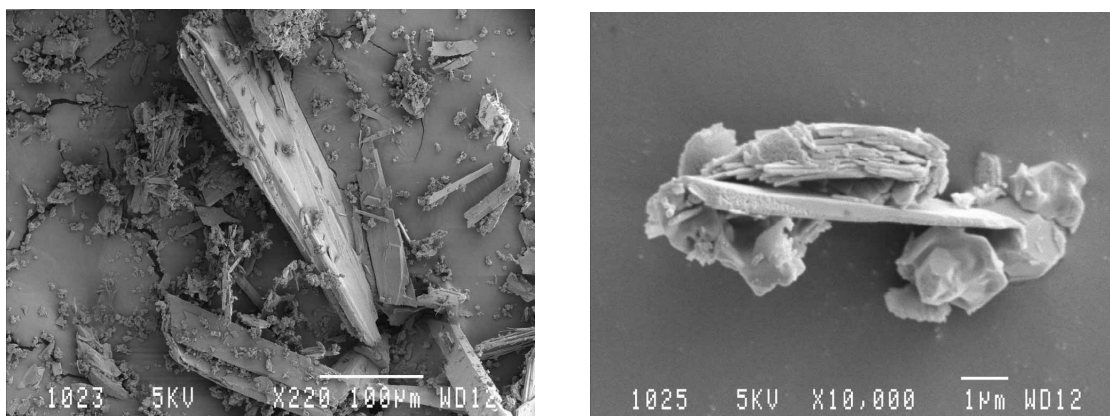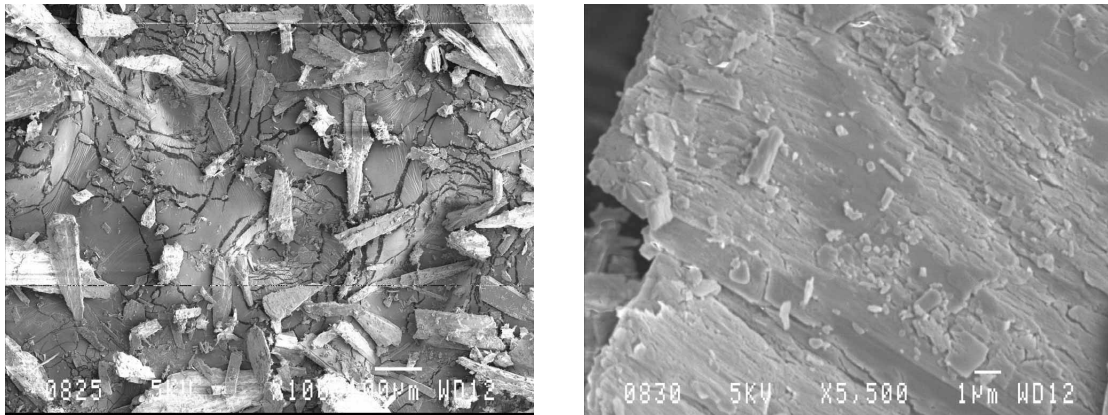

Figure 38: SEM analysis of experiment using 0.50 % Nansa SS30 (30 minute stirring)

XRD result for 0.50 % of surfactant (actual concentration of 0.39 %) indicates the presence of calcium sulphate dihydrate, smaller amounts of calcium sulphate hemihydrate and calcium sulphate anhydrite. As explained earlier and looking at this XRD analysis, the presence of anhydrite is possible, but unlikely and not conclusive.

Figure 39: SEM analysis of experiment using 0.75 % Nansa SS30 (30 minute stirring

XRD result for 0.75 % of surfactant (actual concentration of 0.58 %) indicates the presence of calcium sulphate dihydrate, smaller amounts of calcium sulphate hemihydrate and possibly calcium sulphate anhydrite in the sample. The peaks indicating the anhydrite are more prominent in this diagram. This means that the anhydrite phase is more likely present in this sample compared to the previous samples.

Figure 40: SEM analysis of experiment using 1.00 % Nansa SS30 (30 minute stirring)

XRD result for 1.00 % of surfactant (actual concentration of 0.78 %) indicates the presence of calcium sulphate dihydrate, smaller amounts of calcium sulphate hemihydrate and calcium sulphate anhydrite. In this sample the anhydrite phase is indicated more clearly with higher peak intensities. It can therefore be concluded that this phase does exist in this sample and that the previous samples might have shown a very small, but increasing amount of the anhydrite phase.
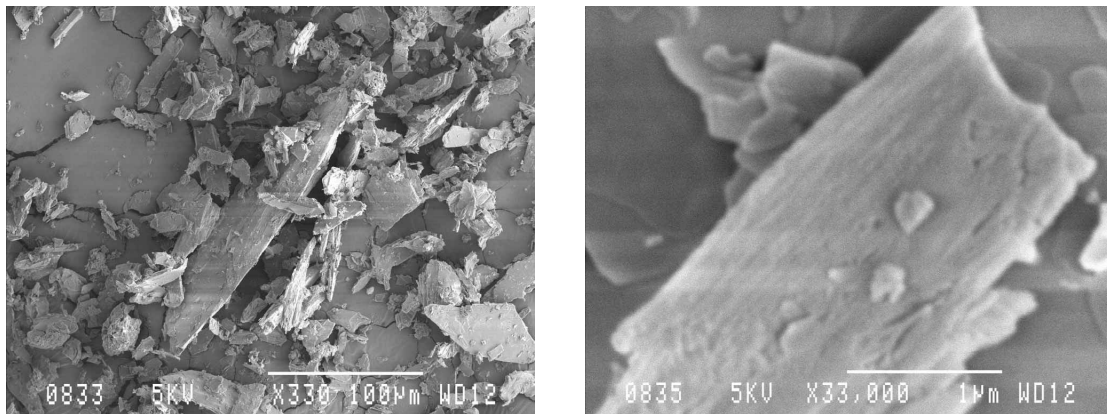
Figure 41: SEM analysis of experiment using 1.50 % Nansa SS30 (30 minute stirring)

Calcium sulphate dihydrate, smaller amounts of calcium sulphate hemihydrate and calcium sulphate anhydrite are present in the sample where 1.50 % surfactant was used (actual concentration of 1.13 %). The presence of the anhydrite phase is definitely becoming more prominent and has slowly been increasing with an increase in concentration of surfactant used.
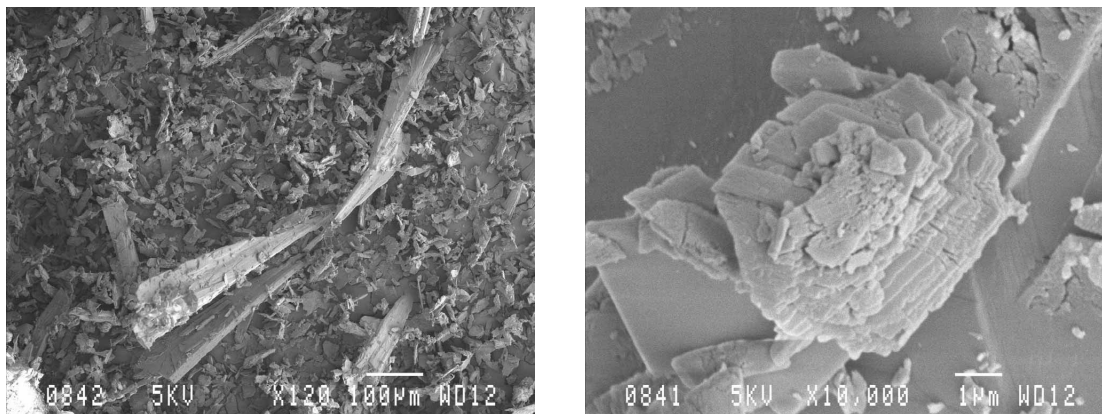
Figure 42: SEM analysis of experiment using 2.00 % Nansa SS30 (30 minute stirring)

Again calcium sulphate dihydrate, calcium sulphate hemihydrate and calcium sulphate anhydrite is present in the sample. The amount of the anhydrite phase is still increasing with an increase in concentration of surfactant used in the precipitated crystals where 2.00 % surfactant was used (actual concentration of 1.56 %). The anhydrite phase and the dihydrate phase amounts are approximately equal if the intensities of the XRD peaks are used as an indicator.
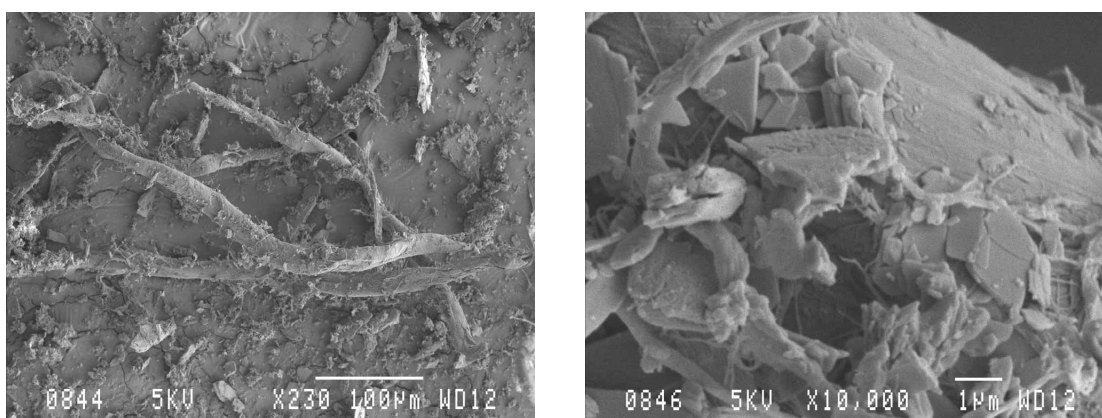
Figure 43: SEM analysis of experiment using 2.50 % Nansa SS30 (30 minute stirring)

The most interesting crystal structure is shown in Figure 43 for the use of 2.50 % surfactant (actual concentration of 2.05 %). The larger crystals grew to form bend hair-like structures on which much smaller crystals with no particular crystal structure can be seen. The sharp corners of the large crystals seen in the previous images are gone. From the XRD results, calcium sulphate dihydrate, calcium sulphate hemihydrate and calcium sulphate anhydrite is present in the sample. The maximum amount of the anhydrite phase is present in this sample compared to

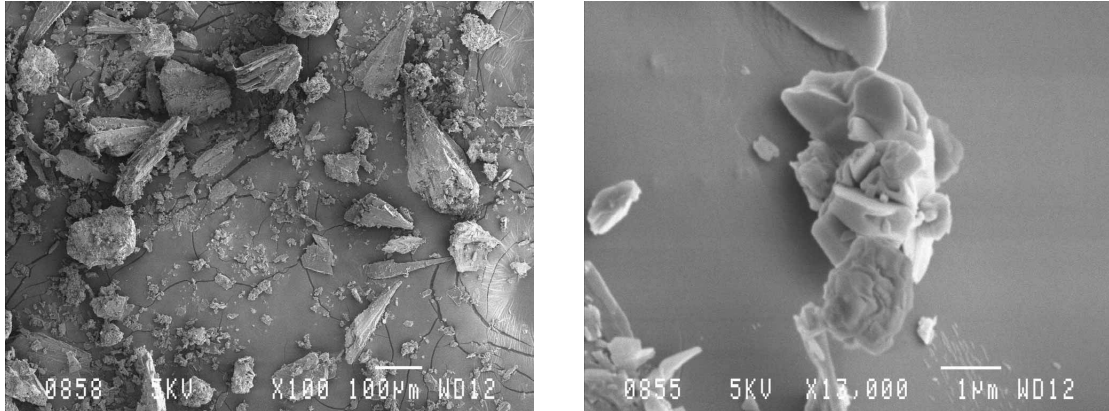other experiments using Nansa SS30 and now the anhydrite phase is more prominent than the dihydrate phase.

Figure 44: SEM analysis of experiment using 3.00 % Nansa SS30 (30 minute stirring)

The XRD results for the 3.00 % surfactant concentration experiments (actual concentration of 3.02 %) only show the presence of calcium sulphate dihydrate and calcium sulphate hemihydrate. No anhydrite phase is indicated.
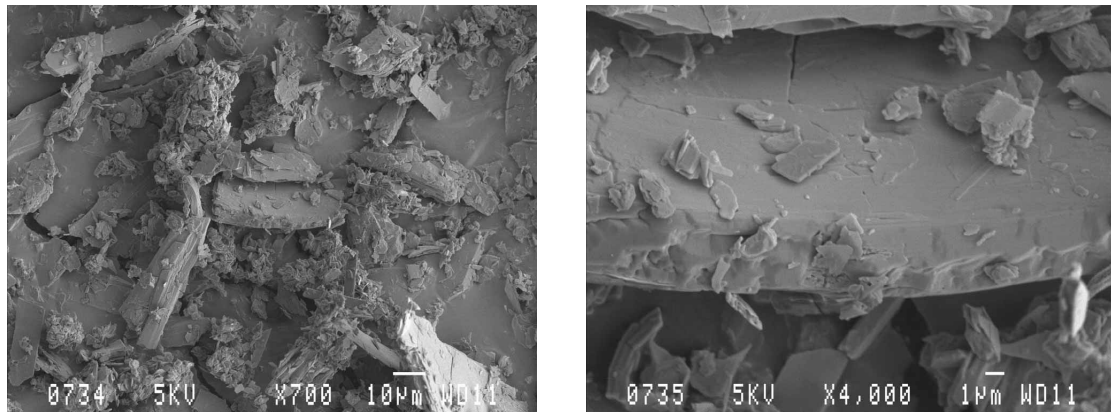

Figure 45: SEM analysis of experiment using 5.00 % Nansa SS30 (30 minute stirring)

The maximum concentration of Nansa SS30 that was used was 5.00 % (actual concentration of 6.11 %). The XRD results indicate mostly calcium sulphate dihydrate with very small amount of calcium sulphate hemihydrate and calcium sulphate anhydrite.

The increase in the crystal size distribution with larger crystals becoming larger and the smaller crystals becoming smaller with an increase in the surfactant concentration can possibly be explained. It is possible that the surfactant absorbs on the crystal faces of the newly nucleated

crystals, covering them. The crystals remain small, as growth does not take place on the covered surfaces. As the surfactant inhibits growth on the covered crystals, growth continues on crystals that have not been in contact with surfactant. With an increase in surfactant concentration, the possible contact between surfactant and newly nucleated crystals increases. The time until contact also decreases thereby covering newly nucleated crystals quicker. This increases the amount of smaller crystals. Less and less crystals are left uncovered as the surfactant is used up. Growth thus continues on the few untouched crystals growing them bigger and bigger with an increase in the surfactant concentration.

To eliminate any mass transfer problems and for comparison, experiments were carried out where they were stirred for 24 hours as explained in Chapter 4.4.2, *Planning and Procedure*". The surfactant concentrations were used based on the mass of the reference experiment for 24 hour stirring. These experiments showed the same trend as the previous experiments using 30 minute stirring, where there is a decrease in yield with an increase in surfactant concentration. The graph shown in Figure 46, shows the yield obtained using the surfactant concentrations on the actual amount of crystals obtained where the active ingredient percentage is taken into account. The results from these experiments again indicate that the surfactant affects crystal growth and nucleation.

Higher yields were obtained compared to the previous Nansa SS30 experiments only going down to a minimum of 79.17 % for the concentrations used. This proves that the mass transfer barriers were overcome and that this surfactant acts as less of a nucleation inhibitor when the experiments are stirred for longer periods of time. With an increase in surfactant concentration, filtration became even more difficult than compared to the experiment stirred for 30 minutes.
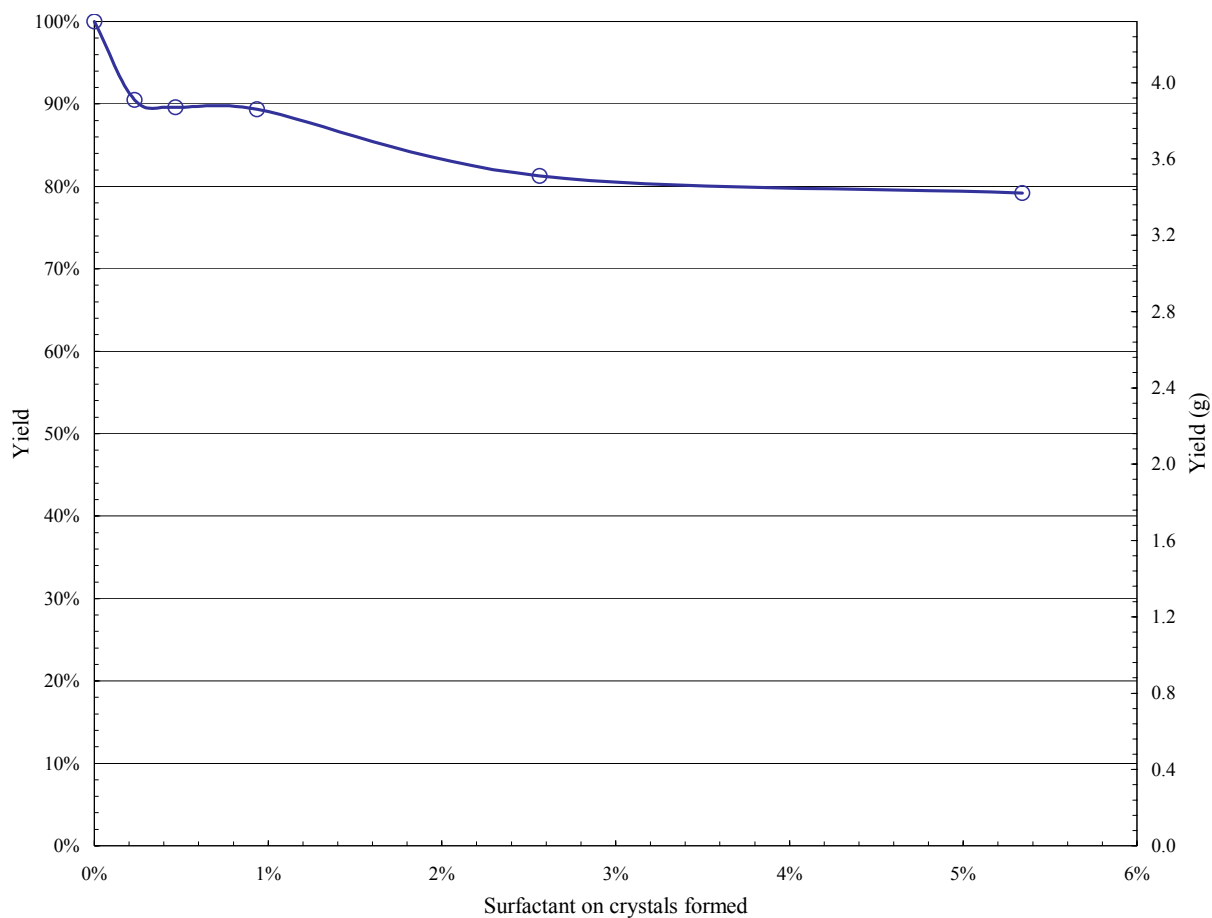
Figure 46: Yield results using different concentrations of the active ingredient in Nansa SS30 for 24 hour stirring

As with the reference experiment for 24 hour stirring, the crystal sizes are smaller than when the experiments are stirred for shorter periods of time, but with the addition of Nansa SS30 as surfactant the crystals became even smaller. All of the experiments have average crystal sizes of approximately 3 μm and are more irregular with increasing surfactant concentration. This explains the increasing filtration difficulties as irregular small crystals can pack more closely.

The surfactant is a growth, but not a nucleation inhibitor and this is indicated by the large amount of small crystals. The crystal sizes are approximately 67 times smaller, but the mass obtained is only approximately 1.26 times less. This surfactant is thus a strong nucleation promoter. It does seem that the crystals are broken down through stirring, but the surfactant added is also mixed thoroughly. This means that covering of newly nucleated crystals with surfactant occurs faster

and more uniformly and due to no mass transfer barriers, growth does not just take place on non-coated crystal faces as they are coated with surfactant. This means, that if growth can not take place, nucleation will.

The hexagonal type crystal structure found in the previous experiment at 0.12 % and 0.22 % actual surfactant concentration with 30 minute stirring can again be seen at 0.69 % surfactant concentration based on the mass of the reference experiment for 24 hour stirring (0.23 % actual surfactant concentration). These crystals are shown in Figure 47, but other misshapen crystals are also present and more prominent. The XRD analysis of this experiment indicates the presence of calcium sulphate dihydrate, calcium sulphate hemihydrate and calcium sulphate anhydrite in the order of dominance. A very small amount of the anhydrite phase is present.
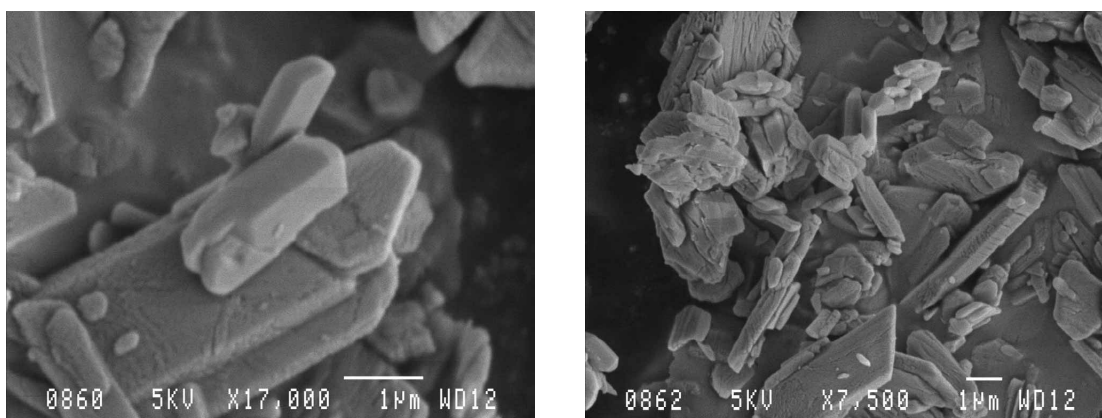

Figure 47: SEM analysis of experiment using 0.69 % Nansa SS30 (24 hour stirring)

The other experiments namely 1.40 %, 2.78 %, 6.94 % and 14.09 % show the same deformed, misshapen crystal structure shown in Figure 48 and therefore the SEM analysis for these experiments will not be shown separately. As the surfactant concentration is increased, the nucleated crystals are coated better and growth is stopped faster and this with breaking of the crystals due to stirring explains the deformities.

The XRD results for 1.40 %, 6.94 % and 14.09 % surfactant (actual concentration of 0.47 %, 2.56 % and 5.34 % respectively) indicate the presence of calcium sulphate dihydrate and calcium sulphate hemihydrate. The hemihydrate phase is more prominent than the dihydrate phase with

the use of 6.94 % and 14.09 % surfactant.   The XRD results of 2.78 % surfactant (actual concentration of 0.93 %) indicate the presence of calcium sulphate dihydrate, calcium sulphate hemihydrate and calcium sulphate anhydrite.   There does not seem to be a trend with these experiments like there was with the experiments that were stirred for 30 minutes where there was an increase in the anhydrite phase up to a maximum.
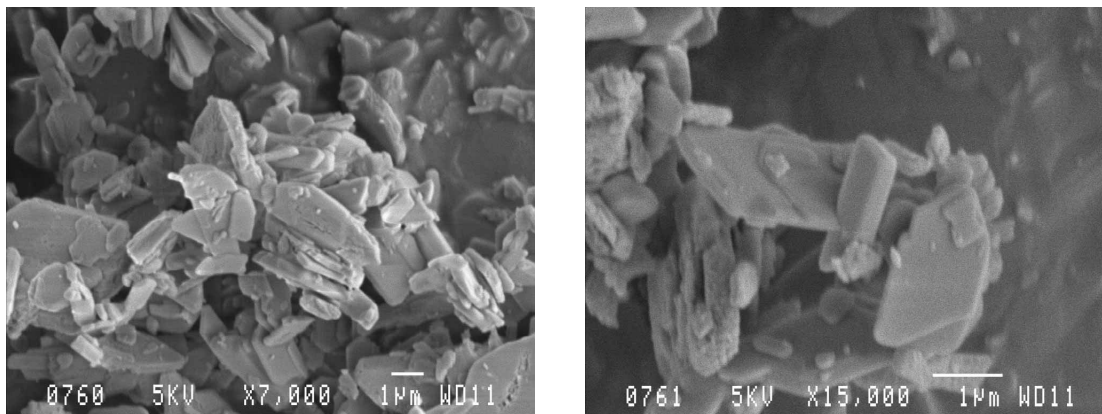

Figure 48: SEM analysis of experiments using 1.40 %, 2.78 %, 6.94 %, 14.09 % Nansa SS30 (24 hour stirring)

Finally, to compare the experiments using 30 minute and 24 hour stirring effect on yield directly, a graph was compiled shown in Figure 49.   The x-axis represents the actual surfactant concentration on the mass of crystals formed and the y-axis represents yield for both experiments starting at 100 % where no surfactant was used.   This 100 % yield does not indicate the same mass, but equals 4.00 g for 30 minute stirring and 4.32 g for 24 hour stirring and is represented in this way to make direct comparison possible.

From Figure 49 it is clear that the different stirring times does affect the yields obtained, but not the trends.   The two stirring methods show sudden decreases in yield and reach a minimum at virtually the same surfactant concentrations.   Even the same type of crystal structure was found at approximately the same surfactant concentration.   The difference in yields obtained can again be explained through mass transfer problems encountered when the experiments were stirred for shorter periods of time.   The mass obtained is influenced by nucleation and nucleation can not take place unless mass transfer barriers have been overcome.   With enough time before filtration,

the yields might have increased even with the short stirring times because the SO_4^{2-} and Ca^{2+} ions would have had more time to react.
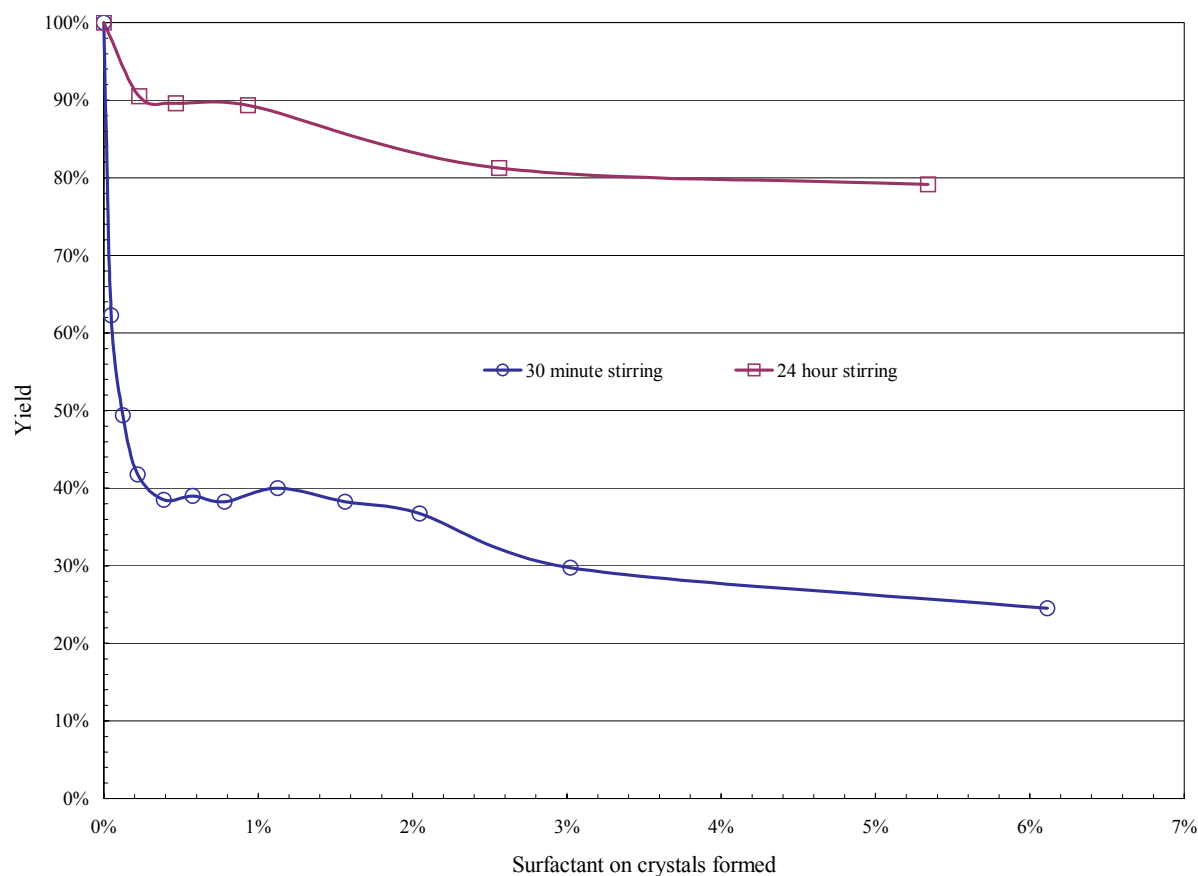

Figure 49: Yield comparison for 30 minute and 24 hour stirring using Nansa SS30

Dowfax 3B2 and Dowfax Hydrotrope

Good results were obtained with Nansa SS30 and thus it was decided to investigate Dowfax surfactants in more detail. This is due to the molecular structure of the alkylated diphenyl oxide disulphonates resembling the structure of the dodecylbenzene sulphonic acid (Nansa SS30) closely. Instead of the one benzene ring in the structure, there are now two.

The 0.20 % Dowfax Hydrotrope used based on the mass of the reference experiment for 30 minute stirring did not have much effect on the mass of the crystals obtained. The yield of

crystals was 94.75 % that equals an actual surfactant concentration of 0.09 % when the active ingredient percentage is taken into account. The XRD analysis indicated the presence of calcium sulphate dihydrate and calcium sulphate hemihydrate where the dihydrate phase dominates. From the SEM analysis shown in Figure 50 it does not seem as if any surfactant was added. The crystal structure did not change at all compared to the reference experiment where no surfactant was used. The average crystal size is still approximately 200 μm. Due to poor crystal habit modification results, no further experiments were done using this surfactant.
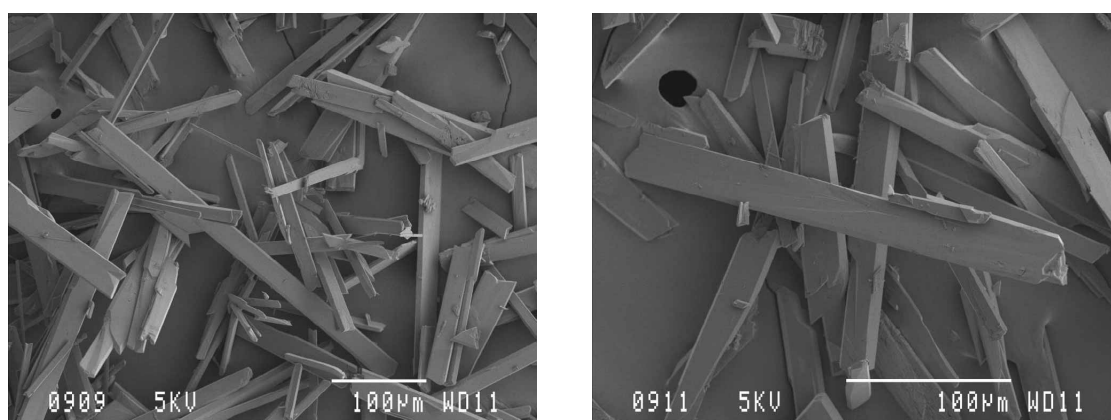

Figure 50: SEM analysis of experiment using 0.20 % Dowfax Hydrotrope

Using Dowfax 3B2, better results were achieved. A concentration of 0.20 % surfactant based on the mass of the reference experiment for 30 minute stirring gave a yield of 81.75 % and thus 1.00 %, 3.00 % and 5.00 % surfactant concentrations were also investigated. The yield results of these experiments are graphically presented in a graph (Figure 51).

From this graph it is clear that a minimum is reached at approximately 70.00 % yield and then it increases again to just below the 100.00 % yield mark where it remained constant. It is not clear what kind of interaction this surfactant has with the SO_4^{2-} and Ca^{2+} ions in the phosphoric acid medium at the experimental conditions to produce these results. At the highest surfactant concentration tested, the yield obtained almost equals the yield obtained without surfactant and could be attributed to experimental variance. This means that above an actual surfactant concentration of 1.70 %, the surfactant possibly has no effect on the yield. The effect of the

different surfactant concentrations on the crystal structures as well as their XRD results will be discussed separately.
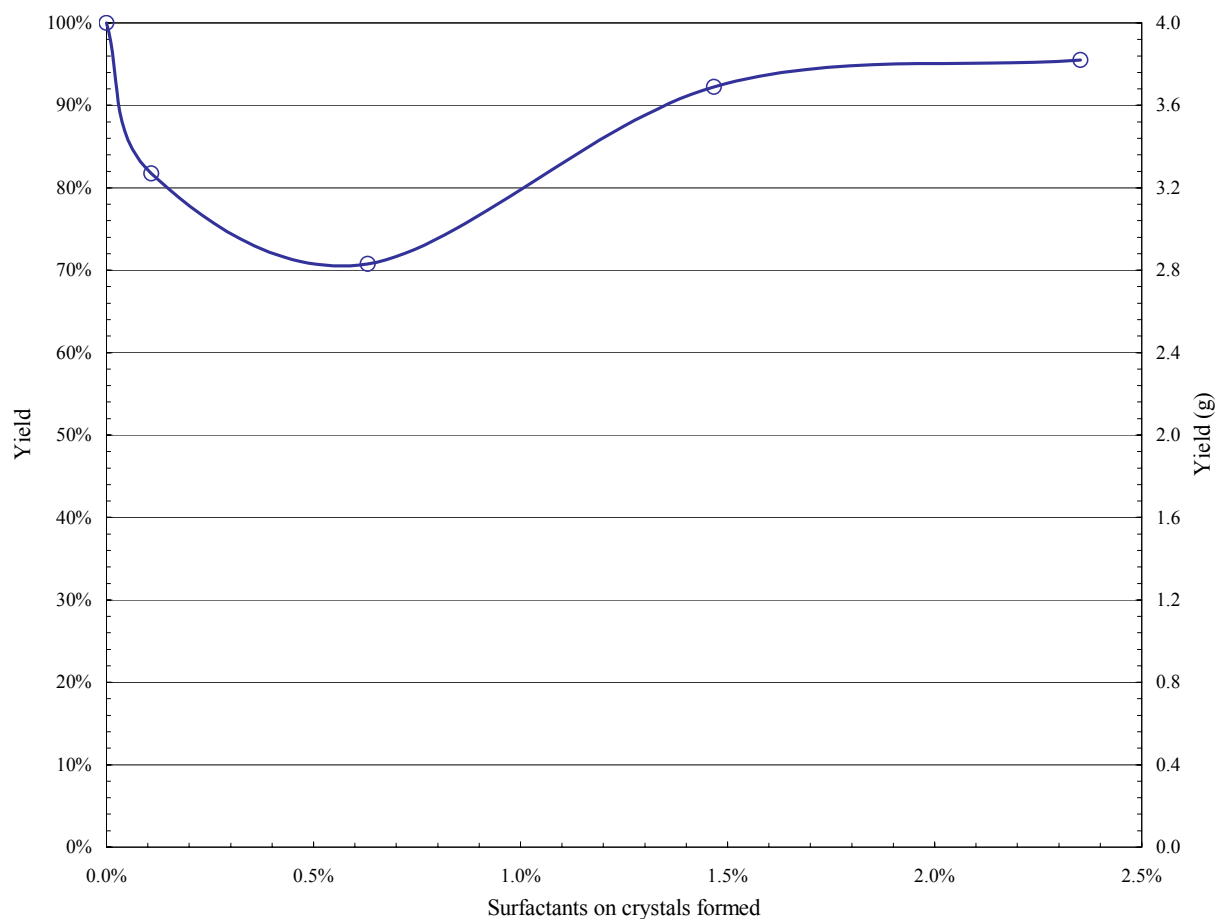

Figure 51: Yield results using different concentrations of active ingredient in Dowfax 3B2

The use of 0.20 % (actual concentration of 0.11 %) and 1.00 % (actual concentration of 0.63 %) Dowfax 3B2 had the same effect on the crystal structure as shown in Figure 52 although different yields were obtained. The crystal size distribution is relatively broad. Longer, thinner crystals with an average crystal size of approximately 130 μm and broader shorter crystals of varying sizes are present. There are also a few very thin needle-like crystals with an average size of approximately 40 μm present in the sample. These varying sizes and shapes lead to filtration difficulties as explained earlier.

The XRD analysis of both samples indicated the presence of calcium sulphate dihydrate and smaller amounts of calcium sulphate hemihydrate. No other phases are present.
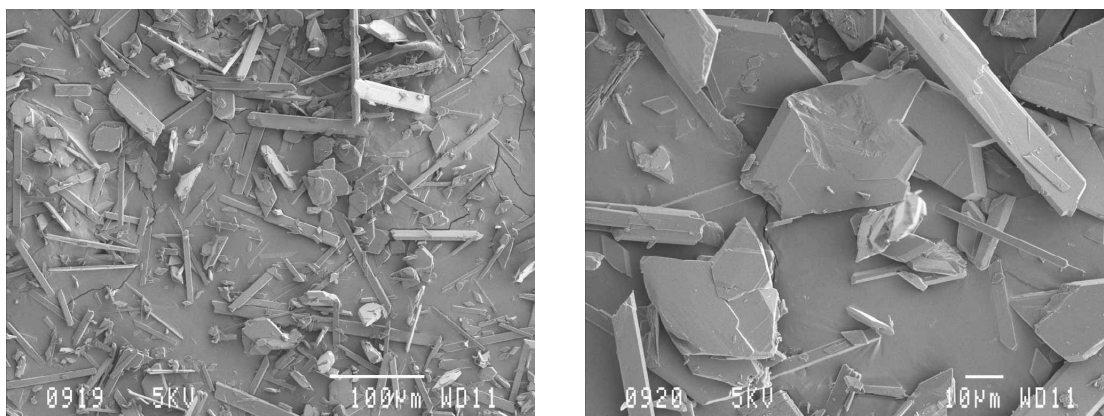

Figure 52: SEM analysis of experiment using 0.20 % and 1.00 % Dowfax 3B2

With the use of 3.00 % Dowfax 3B2 (actual concentration of 1.47 %), there was an increase in the yield obtained and interesting results were found. Firstly looking at the SEM images of this sample in Figure 53, it seems as if there was no visible effect. The crystal size distribution is not as broad as with the previous experiment and this explains the better filtration. With a closer look, twinning of crystals can be seen indicated by the white arrows on the picture.
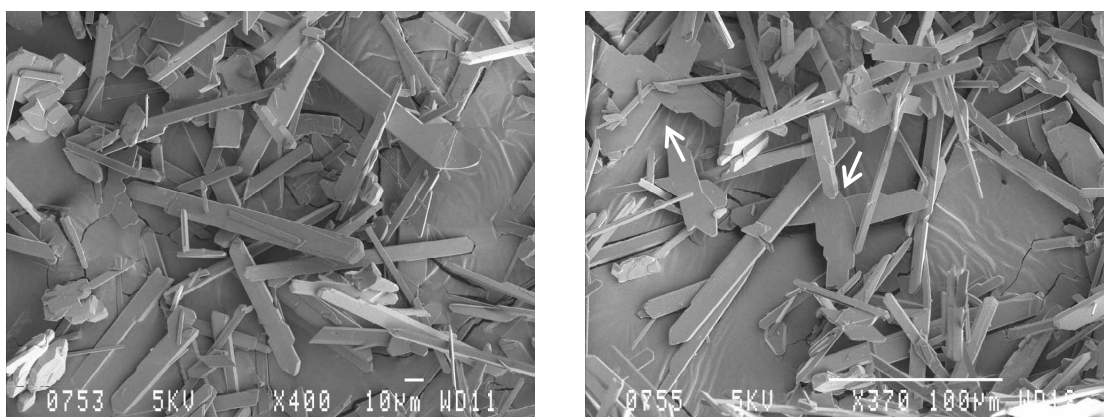

Figure 53: SEM analysis of experiment using 3.00 % Dowfax 3B2

Twinning is when the crystals grow from four instead of the usual two directions and forms a cross. This indicates that the surfactant possibly absorbs on the crystal faces and promotes and not inhibits growth on that face.

The XRD analysis of this sample indicates the presence of calcium sulphate dihydrate, calcium sulphate hemihydrate and calcium sulphate anhydrite. Studying the XRD analysis and the peaks more carefully, it actually seems as if the hemihydrate phase might not be present. The characteristic first hemihydrate peak located right next to the first dihydrate peak on the graph does not seem to be present and the other peaks don't correlate well. It is therefore doubtful if any hemihydrate is present in this sample.

Crystals that almost resemble the crystal structure encountered with the use of Nansa SS30, can be seen with the use of 5.00 % Dowfax 3B2 (actual concentration of 2.35 %). The SEM analysis (Figure 54) shows the presence of smaller crystals with varying crystal sizes that looks different from the larger (~100 µm) needle-like crystals. Due to these variations in sizes, this sample does not have a good crystal size distribution needed for fast efficient filtration.
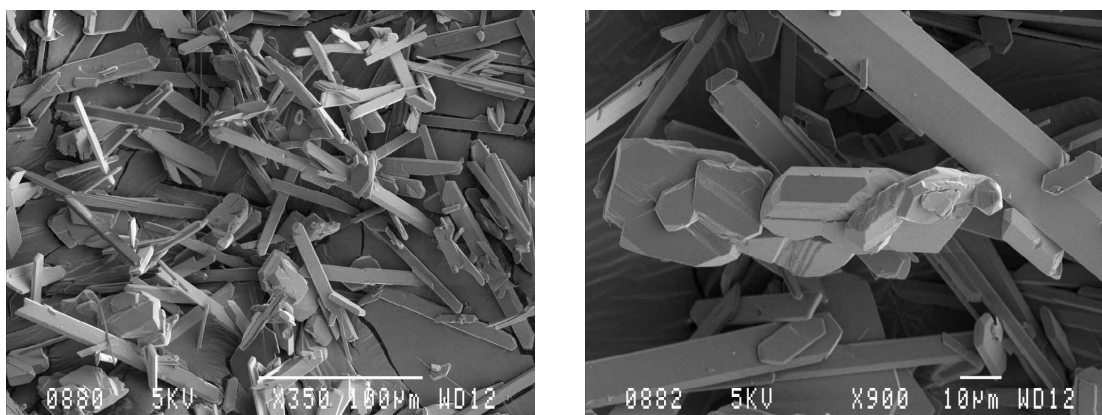

Figure 54: SEM analysis of experiment using 5.00 % Dowfax 3B2

The XRD analysis of this sample indicates the presence of calcium sulphate dihydrate and smaller amounts of calcium sulphate hemihydrate. None of these experiments were repeated with 24 hour stirring. The crystal habit modification properties of this surfactant were not as drastic as with Nansa SS30, although it produced yield differences. Due to the presence of large amounts of smaller crystals and the almost constant yield obtained compared to the reference experiment, it can be concluded that this surfactant is a growth and not a nucleation inhibitor.

Empicol LZ/D

Empicol LZ/D is a sodium alkyl sulphate and this molecular structure resembles the structure of Nansa SS30, but no benzene ring is present. Only three different surfactant concentrations were investigated namely 0.20 %, 1.00 % and 3.00 % and the yield obtained versus the actual surfactant concentration is shown in Figure 55.
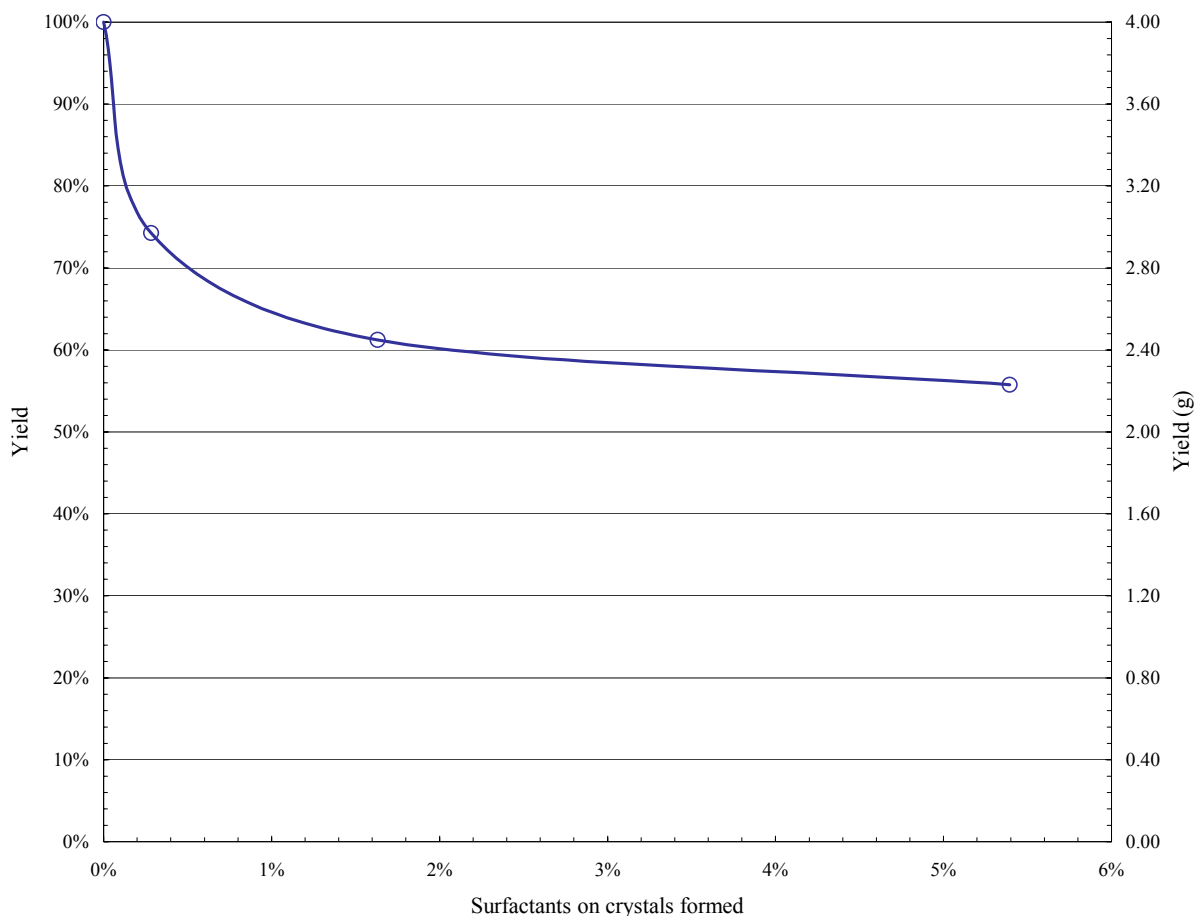
Figure 55: Yield results using different concentrations of active ingredient in Empicol LZ/D

This graph follows the same trend as with the experiments where Nansa SS30 was used as surfactant. There is a continuous decrease in the yield obtained with an increase in the surfactant concentration. To determine what effect it has on the growth and nucleation of the crystals, the SEM images have to be analysed.

With the use of 0.20 % surfactant based on the mass of crystals obtained from the reference experiment for 30 minute stirring, a yield of 74.25 % was obtained. This equals an actual surfactant concentration of 0.28 %. The SEM analysis is shown in Figure 56.
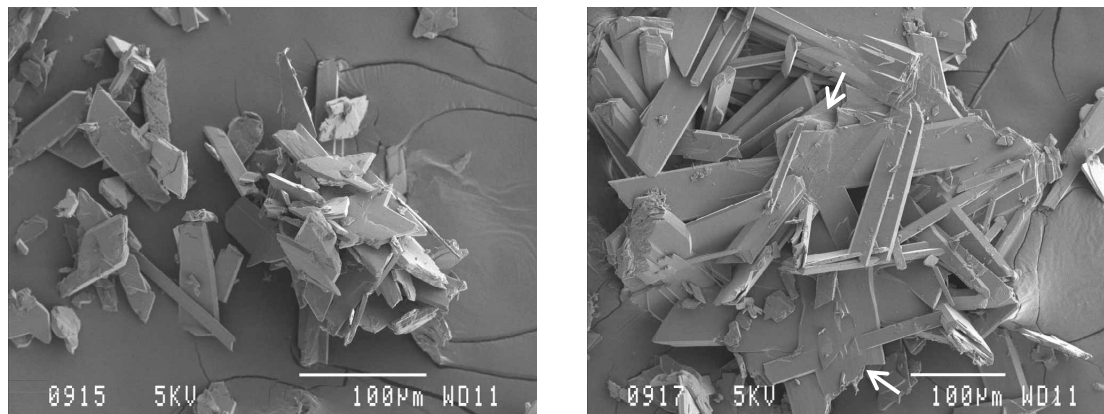

Figure 56: SEM analysis of experiment using 0.20 % Empicol LZ/D

The average crystal size of the crystals did not change much compared to the reference experiment, but the crystals are broader and some type of twinning can be seen on the images indicated by the arrows. The twinning isn't complete, but the crystals could have been broken. The crystals indicating twinnings are also not symmetrical especially the crystal indicated with the bottom arrow on the image. The crystals growing on one side is not as broad as the crystal growing in the other direction.

This growth was possibly influenced by concentration differences of the surfactant on the crystal faces. It seems as if this surfactant promotes growth of crystals on the opposite face than usual making them broader, so it is possible that less surfactant was absorbed on the crystal face where the thinner crystals grew from. It can therefore be concluded that for 0.20 % surfactant used, Empicol LZ/D promotes growth on some faces. It is very difficult to determine what effect the surfactant had on nucleation. The XRD results for the 0.20 % surfactant used, indicates the formation of calcium sulphate dihydrate and very little amounts of calcium sulphate hemihydrate.

A yield of 61.25 % was obtained with the use of 1.00 % surfactant based on the mass of crystals obtained from the reference experiment for 30 minute stirring (actual concentration of 1.63 %). The XRD results for this experiment was the same as the previous experiment where only calcium sulphate dihydrate and calcium sulphate hemihydrate were formed, but the amount of hemihydrate increased. The SEM analysis of the sample indicates that some kind of crystal modification is starting to take place (Figure 57). The crystal size distribution broadened considerably, with large broad crystals of approximately 200 μm and smaller crystals of approximately 3 μm present in the sample. It is the smaller crystals that have a rounder, slightly misshapen crystal structure that almost resembles the hexagonal type crystals formed when Nansa SS30 was used.
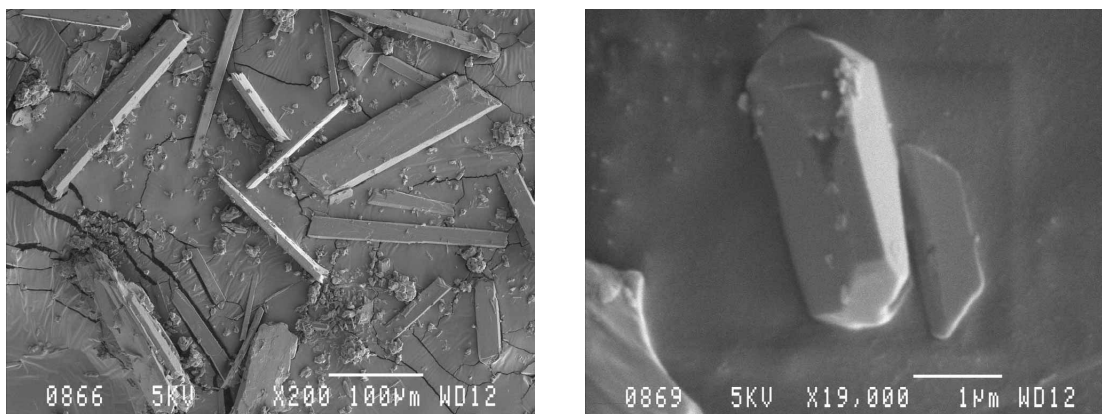

Figure 57: SEM analysis of experiment using 1.00 % Empicol LZ/D

With a higher concentration of Empicol LZ/D used, it seems as if this surfactant changed from a growth promoter to a growth inhibitor because although broad longer crystals are present, there are now also much smaller crystals formed. Due to the presence of a large amount of crystals present that are approximately 66.67 times smaller , but the mass being only 1.63 times less, the surfactant can be classified as a nucleation promoter.

The last Empicol LZ/D concentration used was 3.00 % with a yield of 55.75 % (actual surfactant concentration of 1.63 %). The SEM analysis in Figure 58 shows bend crystals of approximately 30 μm and smaller crystals of 2 μm to 4 μm with no specific crystal structure. Straight, broad

crystals seen with the previous experiments of approximately 30 μm are also present in the sample, but are not shown. The crystal size distribution is very broad and this explains filtration difficulties that were encountered with increasing surfactant concentration.

The XRD results indicate the presence of calcium sulphate dihydrate, calcium sulphate hemihydrate and some calcium sulphate anhydrite. It is not clear what kind of interaction Empicol LZ/D has with the SO_4^{2-} and Ca^{2+} ions in the phosphoric acid medium at the experimental conditions to produce these results. It is however clear that this surfactant acts as a nucleation promoter as there is a definite decrease in crystal size although the yield obtained does not decrease by the same amount. It is however not clear whether it acts as a growth inhibitor or promoter as broader crystals are obtained, but also smaller deformed crystals.
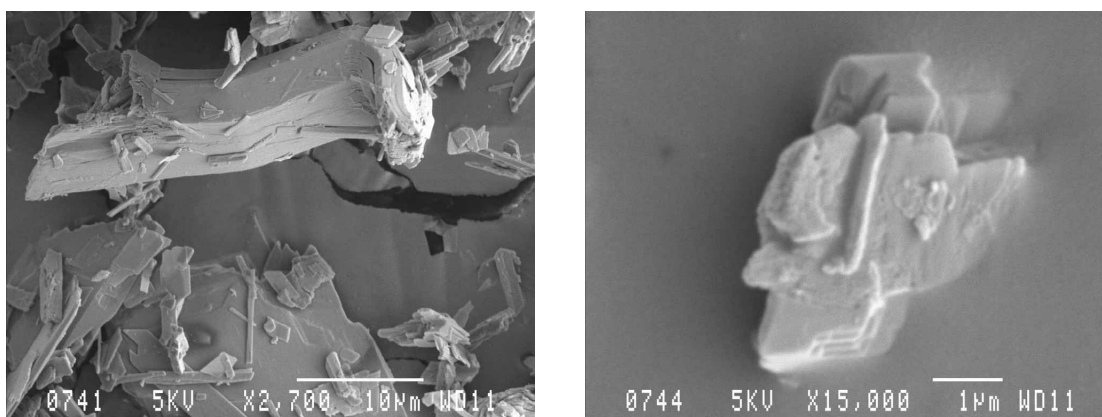
Figure 58: SEM analysis of experiment using 3.00 % Empicol LZ/D

Further experiments using more concentrations and investigating 24 hour stirring was not considered as even though there were crystal and size changes, it was not as specific and drastic as was found with the use of Nansa SS30 as additive.

Empimin KSN70

Empimin KSN70 is a sodium alkyl ether (3EO) sulphate and the chemical structure looks similar to Empicol LZ/D with an extra ether molecular section and Nansa SS30 without the benzene ring.

The yield obtained for the three different concentrations investigated are graphically presented in Figure 59, where 0.20 %, 1.00 % and 3.00 % surfactant based on the mass of the reference experiment for 30 minute stirring were used. All these experiments were repeated due to the variation in the yields obtained where a minimum and a maximum was achieved with the concentrations used. Due to the minimum (96.25 %) and the maximum (107.00 %) yield obtained being so close to the 100.00 % yield obtained without surfactant, these variations can be due to experimental variance, but each time the same results were obtained. Overall, very high yields were obtained.
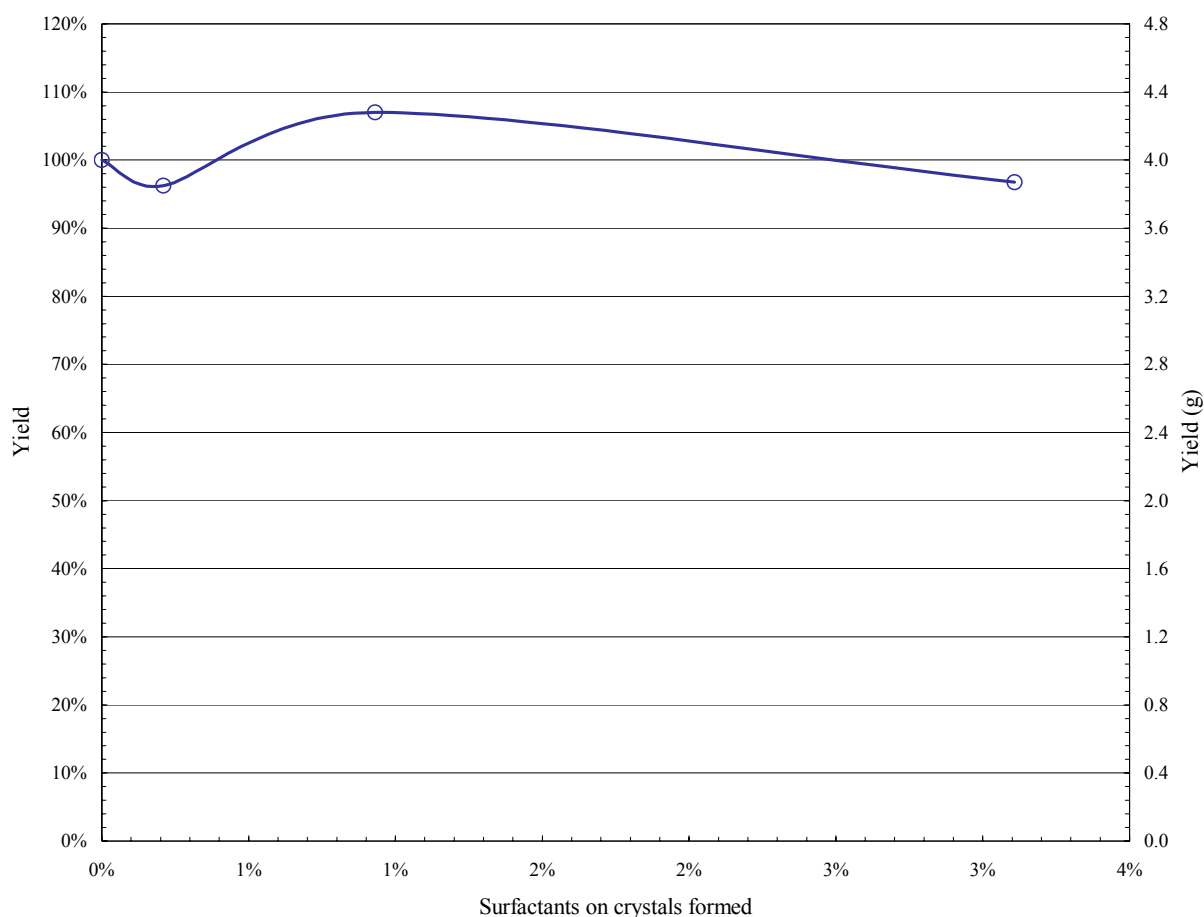

Figure 59: Yield results using different concentrations of active ingredient in Empimin KSN70

When the SEM analyses of these three experiments are compared, the same results were achieved. The crystal size distributions of all three experiments and their repeats are very narrow with the crystal structure resembling the reference experiment with the average crystal size being slightly larger at 250 μm. The only difference being that the crystals seems to be more porous or fibrous shown in Figure 60.

The XRD results indicate the presence of calcium sulphate dihydrate and calcium sulphate hemihydrate for the use of 0.20 % surfactant (actual concentration of 0.21 %). For the use of the 1.00 % (actual concentration of 0.93 %) and 3.00 % (actual concentration of 3.11 %) surfactant, calcium sulphate dihydrate, calcium sulphate hemihydrate and calcium sulphate anhydrite is present.

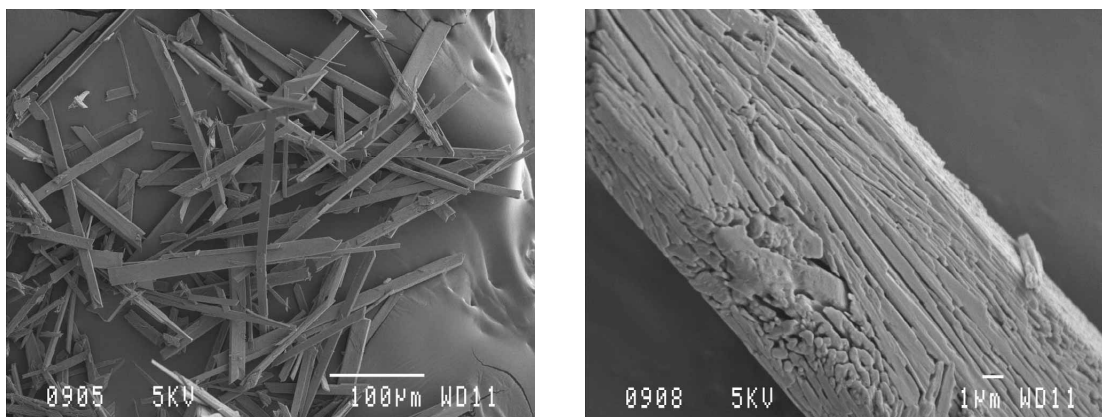**Figure 60: SEM analysis of experiment using 0.20 %, 1.00 % and 3.00 % Empimin KSN70**

To conclude, Empimin KSN70 can not be classified as a crystal nucleation inhibitor as yield results of almost 100 % was achieved where the average crystal size achieved was also close to the crystal size of the reference experiment. Due to these results, no further experiments were done using this surfactant.

4.5   Conclusions and Recommendations

Experiments for the production of calcium sulphate dihydrate without surfactants

- Method A was used to draw up a super saturation diagram for 27 % P_2O_5 at 80 ^{o}C needed for the surfactant experiments. The diagram was only used to get an indication of how much of the reagents are needed so that experimental parameters can be kept constant. Unfortunately, the lower the calcium concentration, the more sulphates (sulphuric acid) is needed for nucleation to take place. This causes a dilution of the phosphoric acid solution, making the diagram invalid at low calcium concentrations.

- An unsatisfactory crystal size distribution was obtained using Method A. The reference experiment's crystal size distribution needs be very narrow, so that the effect that surfactants would have could easily be identified.

- Method B produced crystals with a narrow crystal size distribution with the use of seed crystals and the experiments were reproducible. An average crystal mass of 4.0 g for the 30 minute stirring and 4.32 g for the 24 hour stirring were obtained. The average crystal sizes were approximately 200 μm and 30 μm respectively. Comparing the crystals obtained, it can be seen that stirring for 24 hours possibly breaks down the crystals as they contain sharp edges. The difference in crystal masses obtained can be explained through mass transfer restrictions.

Experiments for the production of calcium sulphate dihydrate with surfactants

- Method B was used for the basis of the surfactant experiments as better crystal size distributions were achieved.

- The concentrations of Atphos E3205, Atpol E3202 and Atpol E1231 added were 0.20 % based on the 4.00 g of crystals obtained from the 30 minute reference experiment. The following results were found using these surfactants:
  − No visible effect on the crystal structure of the precipitated gypsum was observed, but differences in the crystal sizes were seen.
  − Smaller crystal sizes were obtained using Atphos E3205 and Atpol E3202 with approximately 80 μm and 40 μm respectively. Smaller crystal structures with relatively

equal masses compared to reference experiments are an indication of a growth inhibitor and nucleation promoter.

− The average crystal sizes using Atpol E1231 were approximately 250 μm. Due to the smaller mass of crystals obtained and the increase in crystal size, it is concluded that this surfactant acts as a nucleation inhibitor.

− From the XRD results it was found that small quantities of calcium sulphate hemihydrate is present compared to calcium sulphate dihydrate.

• The concentration of Calsoline oil added was 0.20 % based on the 4.00 g of crystals obtained from the 30 minute reference experiment. Results using this surfactant are as follows:

− The use of Calsoline Oil causes a larger crystal size distribution in the precipitated crystals as thin and broad crystals with approximately the same length are found (~150 μm). This has a negative effect on the filterability, because smaller thinner crystals could pack between the broader crystals and so cause packing to be too tight for fast effective filtration.

− As the crystal mass obtained is approximately the same as the reference experiment it can be concluded that the surfactant affects the growth of the crystals and not the nucleation.

− Small quantities of calcium sulphate hemihydrate are present compared to calcium sulphate dihydrate.

• The concentration of Arlatone 1489 added was 0.20 % based on the 4.00 g of crystals obtained from the 30 minute reference experiment. Results obtained are:

− This surfactant did not have any significant effect on the crystal size and form.

− The slight increase in mass compared to the reference experiment for 30 minute stirring is too small to conclude that the surfactant might have enhanced nucleation.

− Small quantities of calcium sulphate hemihydrate are present.

• The concentration of Tamol NN 8906 added was 0.20 % based on the 4.00 g of crystals obtained from the 30 minute reference experiment. The following results were found using this surfactant:

− No effect on the structure or size of the precipitated gypsum was seen.   The surfactant thus has no effect on nucleation or growth of the precipitated gypsum crystals.

- The XRD results prove the formation of calcium sulphate dihydrate and calcium sulphate hemihydrate.

- The use of calcium gluconate monohydrate (concentration of 0.20 % based on the 4.00 g of crystals obtained from the 30 minute reference experiment) had no effect on the crystal structure or the phases that formed.

- Various concentration of Nansa SS30 was used with 30 minute and 24 hour stirring experiments as this surfactant had drastic effects on crystallisation. Reproducible results were obtained and are as follows:

  - At a surfactant concentration of concentration of 0.20 % based on the 4.00 g of crystals obtained from the 30 minute reference experiment, there is no characteristic gypsum crystal shape, but rather small hexagonal rods. The average crystal sizes of the crystals are approximately 12 μm, but vary between 6 μm and 14 μm. The crystals are approximately 14 times smaller than the reference experiment, but the mass obtained is only approximately half of what was collected previously. From these results, it can be concluded that this surfactant can be classified as a growth inhibitor, but a nucleation promoter. XRD confirmed the presence of calcium sulphate dihydrate and calcium sulphate hemihydrate with the hemihydrate being more prominent.

  - With an increase in surfactant concentration, there is a clear decrease in the mass of crystals obtained.

  - With an increase in the surfactant concentration, filtration became increasingly difficult as the crystal size distribution broadened. With a broadening of the crystal size distribution, tighter packing is possible.

  - 24 Hour experiments showed the same trends as previous experiments based on 30 minute stirring. There is a decrease in yield with an increase in surfactant concentration, but higher yields were obtained showing that mass transfer problems were thus overcome. The results from these experiments again indicate that the surfactant affects crystal growth and nucleation.

- Dowfax surfactants were investigated in more detail as their molecular structures resembles Nansa SS30. The following results were obtained:

- Poor crystal habit modification results were achieved using Dowfax Hydrotrope as it did not have any effect on the crystal structure or crystal size distribution. The XRD analysis indicated the presence of calcium sulphate dihydrate and calcium sulphate hemihydrate where the dihydrate phase dominates.

- With the use of Dowfax 3B2 there is definite reduction in yield with an increase in surfactant concentration but reaches a minimum at approximately 0.7 % actual surfactant concentration. Some twinning of gypsum crystals could also be seen (actual concentration of 1.47 %), which indicates that the surfactant possibly absorbs on the crystal faces and promotes and not inhibits growth on that face. Above an actual surfactant concentration of 1.70 %, there is no effect on the yield obtained compared to the 30 minute reference experiment. Due to the presence of large amounts of smaller crystals and the almost constant yield obtained compared to the reference experiment, it can be concluded that this surfactant is a growth and not a nucleation inhibitor.

- Various concentrations of Empicol LZ/D were investigated. Results obtained were:
  - A decrease in the yield with an increase in surfactant concentration was observed.
  - At higher concentration of Empicol LZ/D, it seems as if this surfactant changed from a growth promoter to a growth inhibitor because although broad longer crystals are present, there are now also much smaller crystals formed. The crystal size distribution broadens considerably, with large broad crystals of approximately 200 μm and smaller crystals of approximately 3 μm present in the sample.
  - The smaller crystals have a rounder slightly misshapen crystal structure that almost resembles the hexagonal type crystals formed with the use of Nansa SS30.
  - Twinning of crystals were also observed.

- High yields were obtained with the use of Empimin KSN70. The crystal size distributions of the experiments and their repeats were very narrow. The only difference compared to the reference experiments being that the crystals seem to be more porous or fibrous.

It is recommended that the experiments showing promise as crystal habit modifiers like Nansa SS30 and Empicol LZ/D be investigated in more detail as well as combinations of surfactants.

5.   References

Agnihotri, R., Mahuli, S.K., Chauk, S.S. and Fan, L. (1999) "Influence of surface modifiers on the structure of precipitated calcium carbonate." *Industrial and Engineering Chemistry Research,* 38, p 2283-2291.

Al-Sabbagh, A, Widua, J. and Offermann, H. (1996) "Influence of different admixtures on the crystallisation of calcium sulphate crystals", *Chemical Engineering Communications*, 154, p 133-145.

Anon (1997) *"Automation aids sulphate control - Phosphoric acid processing "*, *Phosphorus and Potassium,* No 210, July - August, p 30 - 35.

Becker, P. (1989) *Phosphates and Phosphoric Acid: Raw materials - Technology, and Economics of the Wet-Process*, 2nd edition, Marcel Dekker Inc., New York.

Brandse, W.P., Rosmalen, G.M. and Brouwer, G. (1977) "The influence of sodium chloride on the crystallisation rate of gypsum" *Journal of inorganic and nucleation chemistry*, 39, p 2007-2010.

Budz, J, Jones, A.J. and Mullin, J.W. (1986) "Effect of selected impurities on the continuos precipitation of calcium sulphate (gypsum)", *Journal of chemical technology and biotechnology*, 36, p 153-161.

Caminiti, R. (1982) "Nickel and cadmium phosphates in aqueous solution. Cation-anion complex formation and phosphate-H_2O interactions", *Journal of Chemistry Physics*, 77 (11), p 5682-5686.

Caminiti, R., Cucca, P. and Atzei, D. (1985) "Phosphate-H_2O Interactions in Concentrated Aqueous H_3PO_4 Solutions", *Journal of Physical Chemistry*, 89, p 1457-1460.

Farmer, V.C. (1974) *Mineralogical Society Monograph 4. The Infrared Spectra of Minerals*, Adlard & Son Ltd., Surrey, p 384.

Feki, M and Ayedi, H.F. (1998) "Purification of wet process phosphoric acid by solvent extraction with methyl isobutyl ketone: Systematic study of impurity distribution", *Separation cience and technology*, 33 (16), p 2609-2622.

Franchini-Angela, M. and Rinaudo, C. (1989) "Influence of sodium and magnesium on the growth morphology of gypsum, $CaSO_4.2H_2O$", *Neues Jahrbuch Miner. Abh.*, 160 (1), p 105-115.

Frazier, A.W. and Kim, Y.K. (1989) "Redistribution of impurities in commercial wet-process acid", *Fertiliser Research,* 21, p 45-60.

Frazier, A.W., Waerstad, K.R., Kim, Y.K., Crim, B.G. (1989)"Phase System Fe_2O_3-K_2O-P_2O_5-H_2O at 25°C*", Industrial and Engineering Chemistry Research*, 28, p 225-230.

Glazyrina, L.N., Savinkova, E.I. and Grinevich, A.W. (1981) "Solubility of calcium sulphate hemihydrate and dihydrate in phosphoric acid containing Al^{3+}, F^- and SiF_6^{2-}", *Zhurnal Prikladnoi Khimii*, 53 (11) p 2524-2527.

Górecki, H., Górecka, H. and Sielicki,A. (1989) "Uranium extraction from wet-process phosphoric acid by kerosene solutions of nonylphenyl phosphoric acids and hexylphenyl phosphoric acids", *Nukleonika*, 34, p. 191-213.

Hasson, D., Addai-Mensah, J. and Metcalfe, J. (1990) "Filterability of gypsum crystallised in phosphoric acid solutions in the presence of ionic impurities", *Industrial engineering chemical research*, 29, p 867-875.

Hudson, R.B. and Dolan, M.J.(1982) "Phosphoric Acid and Phosphates", *Kirk Othmer*, Volume 17, 3rd edition, John Wiley & Sons, New York.

Hünger, K. and Henning, O. (1988) "On the crystallisation of gypsum from supersaturated solutions" *Crystallisation and Research Technology*, 23 (9), p 1135-1143.

Jun, L., JianHua, W. and YunXiang, Z. (1997) "Effects of the impurities on the habit of gypsum in wet-process phosphoric acid", *Industrial engineering chemical research*, 36, p 2657-2661.
Klima, W.F. and Nancollas, G.H. "The Growth of Gypsum", *AIChe Symposuim Series*, 253 (83), p 23-30.

Klima, W.F. and Nancollas, G.H. "The Growth of Gypsum", *AIChe Symposuim Series*, 253 (83), p 23-30.

Kosswig, K. (1994) "Surfactants" in *Ullman's Encyclopaedia of Industrial Chemistry*, Vol A25, B. Elvers, S. Hawkins and W. Russey (Editor-in-Chief), VCH Verlagsgesellschaft, Weinheim, p 751.

Kruger, A, Focke, W.W., Kwela, Z. and Fowles, R. (2001) "Effect of ionic impurities on the crystallization of gypsum in wet-process phosphoric acid", *Industrial and Engineering Chemistry Research,* 40, p 1364-1369.

Lehr, J.R., Frazier, A.W. and Smith, J.P. (1966) "Precipitated Impurities in wet-process phosphoric acid", *Journal of Agriculture and Food Chemistry*, 14 (1), p 27-33.

Liu, S. and Nancollas, G.H. (1973) "The Crystal Growth of Calcium Sulphate Dihydrate in the Presence of Additives" *Journal of Colloid and Interface Science*, 44 (3), p 422-429.

Lynn, J.L. and Bory, B.H. (1995) "Surfactants", in *Kirk Othmer's Encyclopaedia of Chemical Technology*, Vol. 23, Howe-Grant, M. (Editor-in-Chief), John Wiley & Sons, p 478.

Magini, M. (1979) "Solute structuring in aqueous iron(III) sulphate solutions. Evidence for the formation of iron(III)-sulphate complexes.", *Journal of Chemistry Physics*, 70 (1), p 317-324.

Marcilla, A., Ruiz, F., Campos, J. and Asensio, M. (1989) "Purification of wet process phosphoric acid by solvent extraction with dibutyl ether - Part I: Liquid-liquid equilibrium of the system water-phosphoric acid-dibutyl ether at 25 $^{\circ}$C", *Solvent extraction and ion exchange*, 7 (2), p 201-210.

Marcilla, A., Ruiz, F., Campos, J. and Asensio, M. (1989) "Purification of wet process phosphoric acid by solvent extraction with dibutyl ether - Part II: Study of the impurities distribution", *Solvent extraction and ion exchange*, 7 (2), p 211-221.

Martin, J.E., Boliva, J.P., Respaldiza, M.A., Garcia-Tenorio, R. and Da Silva, M.F. (1995) "Environmental impact of fertiliser industries evaluated by PIXE", *Nuclear Instruments and Methods in Physics Research B*, 103, p 477-481.

McCartney, E.R. and Alexander, A.E. quoted by Smith, B.R. and Alexander, A.E. (1958) "The effect of additives upon the process of crystallisation I - Crystallisation of calcium sulphate", *Journal of Colloid Science,*13, p 383-396.

Öner, M., Dogan, Ö. and Öner, G. (1998) "The influence of polyelectrolytes architecture on calcium sulfate dihydrate growth retardation" *Journal of Crystal Growth*, 186 (1998), p 427-437.

Petersen, J.D., Kaleta, N.W. and Kingston, L.W. (1995) "Calcium compounds (calcium sulphate)", in *Kirk Othmer's Encyclopaedia of Chemical Technology*, Vol. 4, Howe-Grant, M. (Editor-in-Chief), John Wiley & Sons, p 812-826.

Rickelton, W.A. (1988) "Uranium extraction form wet proces phosphoric acid using a liquid phophine oxide synergist", *Solvent extraction and ion exchange*, 6 (6), p 1137-1142.

Rinaudo, C and Franchini-Angela, M. (1989) "Curvature of gypsum crystals induced by growth in the presence of impurities", *Mineralogical Magazine*, 53, p 479-482.

Rinaudo, C., Robert, M.C. and Lefaucheux, F. (1985) "Growth and characterisation of gypsum crystals" *Journal of crystal growth*, 71, p 803-806.

Rosmalen, G.M., Daudey, P.J. and Marchee, W.G.J. (1981) "An analysis of growth experiments of gypsum crystals in suspension" *Journal of crystal growth*, 52, p 801-811.

Schorr, M and Lin, I.J. (1997) "Wet process phosphoric acid - Production problems and solutions", *Industrial Minerals*, 355, p 61-71.

Slack, A.V. (1968a) *Phosphoric acid*, Volume 1, Part I., Marcel Dekker Inc., New York.

Slack, A.V. (1968b) *Phosphoric acid*, Volume 1, Part II, Marcel Dekker Inc., New York.

Smith, B.R. and Alexander, A.E. (1970) "The Effect of Additives on the Process of Crystallisation II – Further studies on Calcium Sulphate" *Journal of Colloid and Interface Science*, 34 (1), p 81-90.

Smith, B.R. and Sweett, F. (1971) "The Crystallisation of Calcium Sulphate Dihydrate" *Journal of Colloid and Interface Science*, 37 (3), p 612-618.

Stenström, S. (1989) "Extraction of cadmium from phosphoric acid solutions with amines", *Hydrometallurgy*, 22, p 159-169.

Tjioe, T.T., Durville, P.F.M. and Van Rosmalen, G.M. (1989) "Extraction of cadmium from phosphoric acid with diorganyldithiophosphinic acid - Part I: Equilibrium data", *Solvent extraction and ion exchange*, 7 (3), p 435-459.

Tjioe, T.T., Durville, P.F.M. and Van Rosmalen, G.M. (1989) "Extraction of cadmium from phosphoric acid with diorganyldithiophosphinic acid - Part II: Rate of extraction and decomposition", *Solvent extraction and ion exchange*, 7 (3), p 461-487.

Tjioe, T.T., Weij, P., Wesselingh, J.A. and Van Rosmalen, G.M. (1988) "Removal of cadmium by anion exchange in a wet phosphoric process - Part I: Chemistry", *Solvent extraction and ion exchange*, 6 (2), p 335-360.

Tromp, H.R., Spieser, S.H. and Neilson, G.W. (1999) "A neutron diffraction and computer modelling study of the interatomic structure of phosphoric acid", *Journal of Chemical Physics*, 110 (4), p 2145-2150.

Van der Sluis, S., Schrijver, A.H.M., Baak, F.P.C. and Van Rosmalen, G.M. (1988) "Fluoride distribution coefficients in wet phosphoric acid processes", *Industrial engineering chemical research*, 27, p 527-536.

Waerstad, K.R., Frazier, A.W. (1987) "X-Ray Powder Diffraction and Single-Crystal Data for the Isomorphous Series $(Fe,Al)_3(K,NH_4,H_3O)H_{14}(PO_4)_8.4H_2O$", *Powder Diffraction*, 2(3), p 187-190.

Willis, H. A., van der Maas, J. H. and Miller, R. G. J. (1987), *Methods in Vibrational Spectroscopy*, 3rd edition, John Wiley & Sons Ltd.

Wirsching, F. (1985) "Calcium Sulphate", in *Ullmann's Encyclopaedia of Industrial Chemistry*, A4, Wolff, R. (Editor-in-Chief), VCR Vertrieb Publishers, Düsseldorf, p 555-583.

Witkamp, G.J., Van Der Eerden, J.P. and Rosmalen, G.M. (1990) "Growth of Gypsum – Kinetics" *Journal of Crystal Growth*, 102 (1990), p 281-289.

Zwick, A., Lakhdar-Ghazal, F. and Tocanne, J. (1989) "Characterization of the Ionization of Phosphoric Acid using Raman Spectroscopy", *Journal of the Chemical Society - Faraday Transactions 2*, 85 (7), p 783-788.